



This is to certify that the

dissertation entitled

Experimental and Analytical Development of A Poroelastic Finite Element Model for Tendon

presented by

Theresa Staton Atkinson

has been accepted towards fulfillment of the requirements for

Ph.D. degree in Mechanics

Roger C Hant Major professor

ite July 15, 1998

MSU is an Affirmative Action/Equal Opportunity Institution

O-12771

# LIBRARY Michigan State University

# PLACE IN RETURN BOX to remove this checkout from your record. TO AVOID FINES return on or before date due.

DATE DUE	DATE DUE	DATE DUE
11101/1 4 199	9	
· <del></del>		
		+=

1/98 c/CIRC/DateDue.p65-p.14

### EXPERIMENTAL AND ANALYTICAL DEVELOPMENT OF A POROELASTIC FINITE ELEMENT MODEL FOR TENDON

By

Theresa Staton Atkinson

### A Dissertation

Submitted to
Michigan State University
in partial fulfillment of the requirements
for the degree of

**DOCTOR OF PHILOSOPHY** 

Department of Materials Science and Mechanics

1998

#### ABSTRACT

### EXPERIMENTAL AND ANALYTICAL DEVELOPMENT OF A POROELASTIC FINITE ELEMENT MODEL FOR TENDON

By

### Theresa Staton Atkinson

Mechanical models which allow the mechanical response of tendon to be predicted and quantified are important in the development and assessment of orthopaedic reconstruction techniques. In the first study an autogenous patellar tendon ACL reconstruction was performed in a goat model in order to gain first hand insight into the assessment of reconstruction techniques. Extensive tendon and fat pad proliferation were observed along with significant reductions in the biomechanical properties of the host tendon. An existing mechanical model was used to obtain a description of the tensile response of the tissue. While these data helped explain some of the clinical complications documented in the reconstructed joint, they did not describe the role of the fluid within the healing tissue. Experimental evidence suggests that the tensile behavior of tendon is a function of the collagen structure of the tissue and the tissue hydration. The models currently available do not offer a means by which the hydration effects might be explicitly explored. In order to study potential influences of water content on tendon tensile response a finite element model of a subfascicle (a microstructural element of tendon) was constructed in the second study. The collagen fiber morphology reflected in the model

interacted with the interfibrillar matrix to produce behaviors similar to those seen in tendon and ligament during tensile, cyclic, and relaxation experiments conducted by others. Although this model exhibited mechanical responses which were similar to those observed in whole tendon and ligament, it was preliminary in nature and as such contained some undesirable compromises. In the third study a more detailed description of the subfascicular microstructure was incorporated into the model. This model was shown to exhibit reasonable relaxation and tensile responses as well as a realistic, positive pressure profile throughout the subfasicle. In the fourth study experiments were performed to support the development of the subfascicle model and its extension to whole tendon. The experimental data suggested that small portions of tendon exhibit a higher tensile modulus, a slower rate of relaxation and a lower amount of relaxation in comparison to larger specimens from the same location in the same tendon. In the fifth study the subfascicle model was able to match subfascicle relaxation and constant strain rate tensile responses as described in the previous experimental study. In addition, a fascicle model, consisting of two subfascicles surrounded by epitenon, was created to investigate potential interactions between subfascicles and the connective tissue membrane. This analysis suggested that the presence of connective tissues in tendon may play an important role in defining the whole tendon relaxation response. In the final study the subfascicle model was utilized in the development of a recruitment model tendon. This work suggested that subfascicle organization within a tendon specimen also plays a role in the development of the relaxation response. These studies highlight the importance of the collagen microstructure in the development of the time varying responses of tendon.

To my husband Pat whose insight, advice, and loving support has comforted and inspired me during the course of this research and to my parents who encouraged me to persevere.

### **ACKNOWLEDGMENTS**

I would like acknowledge Dr. Roger Haut for his guidance and support throughout the course of this project. Dr. Haut inspired me to face the challenges my research presented and made it possible for me to present and publish my research. I would also like to acknowledge Dr. Nicholas Altiero for his contributions to my research and for his assistance in preparing my work for publication. I also express my gratitude to Dr. Arnoczky and Dr. Beck for their participation on my committee and for making themselves available to me for consultation throughout my years of graduate education. I thank my co-authors, without whom I would not have been able to complete my studies: Pat Atkinson, Benjamin Ewers, and Vince Mendenhall. Finally I also wish to thank all those in the lab who have worked with me on a daily basis and who have made my graduate experience so memorable: Bill Newberry, Rich Banglmaier, Dana Dvorchek-Driksna, Cliff Beckett, and Jane Walsh.

### TABLE OF CONTENTS

LIST OF TABLES	v
LIST OF FIGURES	vi
INTRODUCTION	1
CHAPTER 1	
Patellar Tendon And Infrapatellar Fat Pad Healing	
After Harvest Of An ACL Graft	10
(to be published July 1998 in Journal of Surgical Research)	
Abstract	11
Introduction	12
Materials and Methods	13
Results	17
Discussion	
CHAPTER 2	
A Poroelastic Model That Predicts Some Phenomenological Responses	
of Ligaments and Tendons	30
(published in November 1997 in Journal of Biomechanical Engineering)	
Abstract	31
Introduction	
Methods	
Results	
Discussion	
CHAPTER 3	
A Microstructural Poroelastic Model For Patellar Tendon	63
(published in June 1997 ASME Summer Bioengineering Conference Proceedings)	
Äbstract	
Introduction	
Methods	
Results	
Discussion	
CHAPTER 4	
The Tensile and Stress Relaxation Responses of Human Patellar Tendon	
Varies with Specimen Cross Sectional Area	71
(submitted for consideration in Journal of Biomechanics)	/ 1
Abstract.	72
4 NLATE MALE	/ 4

Introduction	73
Methods	75
Results	<b>7</b> 9
Discussion	80
CHAPTER 5	
Extension of a Microstructural Model for a Subfascicle Toward a Description	
of Whole Tendon	97
(intended for submission to Journal of Biomechanics)	
Abstract	98
Introduction	99
Methods	102
Results	
Discussion	
CHAPTER 6	
A Subfascicle Recruitment Model for Tendon	131
Abstract	
Introduction	
Methods	
Results	
Discussion	
CHAPTER 7	
Conclusions and Recommendations for Future Work	156
Appendix A	
Porous Elastic Material Model	165
Appendix B	
Subfascicle model Abaqus code	169
Appendix C	
Fascicle model Abagus code	177

### LIST OF TABLES

CHAPTER 1		
Table 1: Biomechanical and biochemical data for goat patellar tendons		
and infrapatellar fat pads following harvest of a patellar tendon graft		
to reconstruct the ACL (mean ± one standard deviation)	25	
CHAPTER 2		
Table 1: Material Coefficients	51	
CHAPTER 4		
Table 1: Description of Specimens	88	
CHAPTER 5		
Table 1: Material Coefficients for Subfascicle FEM	119	
Table 2: Fascicle FEM Model Relaxation Response to 2% Strain	119	
CHAPTER 7		
Table 1: Comparison of Relaxation and Creep	163	

### LIST OF FIGURES

CHAPTER 1	
Figure 1	27
Figure 2	28
Figure 3	29
CHAPTER 2	
Figure 1	54
Figure 2a	55
Figure 2b	56
Figure 2c	57
Figure 3	58
Figure 4a	59
Figure 4b	60
Figure 5a	61
Figure 5c	62
CHAPTER 3	
Figure 1	69
Figure 2	
Figure 3	
Figure 4	
CHAPTER 4	
Figure 1	
Figure 2	
Figure 3	
Figure 4	
Figure 5	
Figure 6	
Figure 7	
Figure 8	96
CHAPTER 5	
Figure 1	122
Figure 2	123
Figure 3	
Figure 4	
Figure 5	
Figure 6	

Figure 7a	
Figure 7b	
Figure 8	
CHAPTER 6	
Figure 1	
Figure 2	
Figure 3	
Figure 4	
Figure 5	
Figure 6	
Figure 7	
Figure 8	
Figure 9	
Figure 10	
Figure 11	
Figure 12	
Figure 13	
Figure 14	
Figure 15	
CHAPTER 7	
Figure 1	164
Figure 2	164

#### INTRODUCTION

Most currently available tendon and ligament models consider the tissue to be entirely composed of collagen (Belkoff and Haut, 1992, Hurschler *et al.*, 1997, Kwan and Woo, 1989, Stouffer *et al.*, 1985,) and utilize a distribution function to describe the recruitment of collagen and capture the influence of the collagen structure on the tensile response (Belkoff and Haut, 1992, Hurschler *et al.*, 1997, Kwan and Woo, 1989). However, the collagen in tendon has been described as being arranged in subfascicles and fascicles (collections of subfascicles) which are enclosed by connective tissue sheaths (Yahia and Drouin, 1988). Danylchuk (1978) describes the collagen fasciculi as the portion of tendon responsible for its tensile strength. Kastelic (1980) modeled the collagen fascicle and suggested that the nonlinear tensile response of tendon might arise from collagen recruitment within the fascicle.

More recently, experimental studies have suggested that other tissue components, such as water (which comprises 60-70% of the weight of tendons and ligaments), might play a significant role in the tensile behavior of ligaments and tendons. For example, experiments suggest that human patellar tendons exhibit higher tensile modulus and ultimate strength when tested in a bath environment versus in air (Haut and Powlison, 1990). Similarly, the tendon is stiffer when tested in a hydrating solution versus a dehydrating solution (Haut, et. al 1995). Furthermore, both studies suggest that the time dependent responses of human tendon are influenced by water. For example, in relaxation

tests, specimens tested in a saline bath exhibit a larger and more rapid load relaxation versus those tested in air (Haut and Powlison, 1990). Similarly, specimens tested in a hydrating bath have greater load relaxation than those tested in a dehydrating bath (Haut et al., 1995).

In ligaments, increasing the water content causes the tissue to respond with greater cyclic load relaxation relative to ligaments with lower water content (Chimich et al., 1992). Data from cyclic tests also demonstrate monotonic decreases in rat tail tendon diameter from cycle to cycle (Lanir et al., 1988). Similar behavior has been documented in the rat medial collateral ligament (MCL) (Thielke et al., 1995). This deformation suggests densification of the collagenous structure and exudation of fluid, and is consistent with reports that glycosaminoglycans (GAGs) and water are exuded during tensile strain tests (Lanir et al., 1988; Hannifin and Arnoczky, 1994).

Effects associated with extracellular water have been observed experimentally, but few analytical models address the mechanism of its action. Chen et al. (1993) utilized a finite element analysis (FEA) to study permeability effects in tendon and ligament. The model includes a fluid phase moving around regular cylinders (meant to represent collagen fibers). Chen and Vanderby (1994) proposed a directionally sensitive permeability for tendons. The influence of water has also recently been incorporated in a model of the rabbit MCL (Wilson et al., 1994). Wilson's FEA model utilizes a continuum matrix of poroelastic material and spring elements attached at nodes to include the elastic stiffness of collagen. The model predicts that pressure within the MCL is negative during tensile deformation, implying that fluid flows into the structure. This result, however, is contrary

to current experimental data indicating positive internal pressures (Chen et al., 1995) in rabbit patellar tendon during tensile stretch and fluid exudation in the canine flexor tendon, rabbit MCL, and rat tail tendon under tensile strain (Hannifin and Arnoczky, 1994; Thielke et al., 1995; Lanir et al., 1988). Finally, most recently Chen et al. (1997) proposed a poroelastic cylinder model for tendon. In this model, however, it was necessary to assume an unreasonable Poisson's ratio of 0.65 in order to achieve the desired positive pressures upon extension.

These contrary results suggest that continuum characterizations of the tendon may not reflect mechanisms important to predicting the role of water in tensile load response. Lanir et al. (1988) describe the tendon on a microscopic scale as consisting of an arrangement of collagen fibrils embedded in a hydrophilic gel. While there is controversy in the literature concerning the hierarchical levels of collagen, it is generally accepted that fibrils are combined to form sub-fasciculi, fasciculi, and finally the whole structure (Danylchuk et. al, 1978; Viidik 1990; Yahia and Drouin 1988). It has been proposed that the morphology of collagen fibrils can be complex, ranging from being helically wound in the sub-fascicle (termed fascicle by Yahia and Drouin, 1988) in the patellar tendon to a both helical and planar waveforms in the anterior cruciate ligament (ACL). In the subfasciculi containing helically wound fibrils, the peripheral fibrils appear as undulated helices, while the central ones are normal helices (Yahia and Drouin, 1989). It has been previously suggested that the collagen in tendon and ligament interacts in such a way that it compresses the gelatinous matrix and creates a sensitivity to strain rate in the tissue (Lanir, 1978).

The purpose of this disseration was to build a microstructurally accurate model for a patellar tendon which could be used to study how the fluid present in tendon contributes to the tissue's mechanical responses.

The experimental study described in the first chapter of this dissertation was performed to gain insight into tendon healing following harvest of a patellar tendon graft. Changes in the tendon and the infrapatellar fat pad were examined in a goat model following reconstruction of the ACL, using an autogenic patellar tendon graft. This animal model approximates the clinical scenario for ACL reconstruction and the anthropometry of the human knee. Extensive proliferation was observed in the patellar tendon during the healing process. This proliferation appeared to have a negative effect on the fat pad which became fibrotic. A mechanical model for tendon formulated by Belkoff and Haut (1992), was fit to the tensile test data to quantify changes in the tensile response. This model suggested that the collagen structure in the tendon degraded during the healing process, becoming more disorganized. This work highlighted a need for models to help advance our understanding of the structure-function relationship in tendon such that a greater understanding of the healing process might be gained and healing might be improved.

In the second chapter a microstuctural finite element model for tendon was developed. In this development we hypothesized that longitudinal deformation of the more helically oriented fibrils in the subfascicles of patellar tendon might compress the matrix to generate hydraulic pressures and movement of unbound water during tensile stretch. By this mechanism the load might be shared between collagen and the surrounding matrix to influence the tensile response of the entire ligamentous or

tendonous structure. We assumed that the subfascicle may be considered a characteristic structure of ligament and tendon, which therefore should exhibit behaviors observed in the gross structure. The finite element model exhibited stress relaxation and strain rate sensitivity which were dependent on the level of hydration, and were qualitatively similar to those reported by other researchers. There were, however, several aspects of this model which were undesirable: a sealed boundary condition was applied to the model periphery, the "matrix" portion of the model alone reflected pressures in the subfascicle, and the tensile response of the model was linear. In order to address the limitations of this early model, a new, more microstructually accurate model was developed in Chapter 3. This model exhibited a continuous positive pressure profile under tensile load and a nonlinear tensile response.

In Chapter 4 a series of mechanical tests were performed in which quarters of human patellar tendons were sequentially sectioned. The tests were designed to describe both collagen recruitment, via a constant strain rate test, and the time dependent stress relaxation response of specimens harvested from a common location within the same donor. The objectives of these tests were to determine whether the responses of small portions of tendons, which were composed of several subfascicles, were qualitatively similar to those of whole tendon and to identify a relationship between mechanical behaviors of the small and large portions of tendon within the same subject. The experimental studies suggested that the constant deformation, stress relaxation response of human patellar tendon decreases as a function of the specimen cross sectional area. These experiments documented a 50% reduction in the rate and the amount of relaxation as the

specimen cross sectional area decreases from 20 to 1 mm<sup>2</sup>. The larger specimens which exhibited an increased relaxation response also contained a higher percentage of fluid than the smaller specimens. This additional fluid may have contributed to the increased relaxation in the larger specimens.

In Chapter 5 a quantitative subfascicle model was developed based on the experimental data collected in Chapter 4. Using this model potential explanations for the variation in the tissue's relaxation responses were investigated. The model's relaxation response was observed to increase when the water content of the model was increased, consistent with the experimental data. In addition the subfascicle model was extended to form a fascicle model consisting of two fascicles surrounded by an epitenon (a connective tissue membrane). The transversely oriented fibers within the epitenon caused the subfascicles to be pressed together under a tensile load, causing an increased relaxation response. This study suggests that both the tissue fluid content and the presense of oriented connective tissues surrounding the collagen fascicles induce the large relaxation response characteristic of whole human patellar tendon.

In the sixth chapter an analytic model was created to extend the response characteristics of the subfascicle into a model which was capable of describing tendon specimens of arbitrary cross section. The model was fit to experimental data described in Chapter 4 using the Marquardt's nonlinear least squares method. The fitted parameters suggest that the tissue hydration and subfascicle organization are separate influences on the mechanical response. The fitted models were also utilized to simulate the tissue's creep response. The creep and relaxation responses were nearly equivalent for the model

as posed. When a more aggressive relationship between strain and the rate of relaxation was assumed the model predicted more relaxation than creep, consistent with Thornton et al's (1997) experimental observations in the rabbit medial collateral ligament. Further study is required to develop an experimental basis for the strain/relaxation rate function.

In the final chapter concluding remarks are made relative to the benefits and drawbacks of the modeling approach applied in these studies. Potential extensions of the research are proposed.

Appendix A contains background information documenting the porous elastic material model. This material model was utilized to describe the matrix in the subfascicle model described in Chapter 2. This material was selected because it stiffens under compression and was therefore thought to be useful in producing the tensile stiffening response characteristic of tendon. As this model is not commonly used to describe biologic material, it was therefore eliminated in favor of a linear poroelastic material in subsequent chapters.

Appendix B contains the Abaqus code for the subfascicle model.

Appendix C contains the Abaqus code for the fascicle model.

#### REFERENCES

- Belkoff, S.M. and Haut, R.C. (1992) Microstructurally based model analysis of  $\gamma$  irradiated tendon allografts. J. Othop. Res. 10, 461-464.
- Chen, C., and Vanderby, R., 1997, A poroelastic model of streaming potential and interstitial fluid flow in ligament and tendon, In *Proceedings of the 1997 Bioengineering Conference*. Sun River, Oregon, pp. 185-186.
- Chen, C., McCabe, R., and Vanderby, R. Jr. (1995) Two electrokinetic phenomena in rabbit patellar tendon: pressure and voltage. In *Proceedings of the 1995 Bioengineering Conference*. Beaver Creek, Colorado.
- Chen, C. T. and Vanderby, R. (1994) 3-D finite element analysis to investigate anisotropic permeability for interstitial fluid flow in ligaments and tendons. In *Trans. of the* 40th Annual Meeting of Orthop. Res. Soc. New Orleans, LA.
- Chen, C. T., Vanderby, R., Graf, B. K., and Malkus, D. S. (1993) Interstitial fluid flow in ligaments and tendons: effects of fibril spacing and fluid properties. In *Proceedings of the 1993 Bioengineering Conference*, Breckenridge, Colorado.
- Chimich, D. D., Shrive, N. G., Frank, C. B., Marchuk, L., and Bray, R. C. (1992) Water content alters viscoelastic behaviour of the normal adolescent rabbit medial collateral ligament. *J. Biomech.* 25, 831-837.
- Danylchuk, K.D., Finlay, J.B. and Krcek, J.P. (1978) Microstructural organization of human and bovine cruciate ligaments. *Clinical Orthopaedics and Related Research*. **131**, 294-298.
- Hannafin, J.A. and Arnoczky, S.P. (1994) Effect of cyclic and static tensile loading on the water content and solute diffusion in canine flexor tendons: an in-vitro study. *J. Orthop. Res.* 12, 350-356.
- Haut, T.L., and Haut, R.C. (1997) The state of tissue hydration determines the strain-rate-sensitive stiffness of human patellar tendon. J. Biomech. 30, 79-82.
- Haut, R.C. and Powlison, A.C. (1990) The effects of test environment and cyclic stretching on the failure properties of human patella tendons. J. Orthop. Res. 8, 532-540.
- Hurschler, C., Loitz-Ramage, B., and Vanderby, R., (1997) A structurally based stress-stretch relationship for tendon and ligament. J. of Biomech. Eng. 119, 392-399.
- Kastelic, J., Palley, I., and Baer, E. (1980) A structural mechanical model for tendon crimping. J. Biomech. 13, 887-893.

- Kwan, M.K., and Woo, S. L-Y. (1989) A structural model to describe the nonlinear stress-strain behavior for parallel-fibered collagenous tissues. *J. Biomech. Eng.* 111, 361-363.
- Lanir, Y., 1978, "Structure--strength relations in mammalian tendon," *Biophysical J.*, Vol. 24, pp. 541-554.
- Lanir, Y., Saland, E. L., and Foux, A., 1988, "Physico-chemical and microstructural changes in collagen fiber bundles following stretch in-vitro," *Biorheology* J., Vol. 25(4), pp. 591-604.
- Stouffer, DC, Butler, DL, and Hosny, D. (1985) The relationship between crimp pattern and mechanical response of human patellar tendon-bone units. J. of Biomech. Eng. 107, 158-165.
- Thielke, R.J., Vanderby, R. Jr., and Grood, E.S. (1995) Volumetric changes in ligaments under tension. In *Proceedings of the 1995 Bioengineering Conference*. Breckenridge, Colorado.
- Thornton, G.A., Oliynyk, A., Frank, C.B., and Shrive, N.G., 1997, Ligament creep cannot be predicted from stress relaxation at low stress: A biomechanical study of the rabbit medial collateral ligament, *J. Orthop. Res.*, 15: 652-656.
- Viidik, A. 1990, "Structure and function of normal and healing tendons and ligaments" in **Biomechanics of Diarthrodial Joints Vol I**, (Edited by Mow, V.C., Ratcliffe, A., and Woo, S. L-Y.), p. 3-12, Springer-Verlag, N.Y.
- Wilson, A. N., Frank, C. B., Shrive, N. G. (1994) The behaviour of water in the rabbit medial collateral ligament. In *Second World Congress of Biomechanics*, (Edited by Blankevoort, L. and Kooloos, J. G. M.), pp. 226b. Amsterdam, The Netherlands.
- Yahia, L. H., and Drouin, G., 1989, "Microscopical investigation of canine anterior cruciate ligament and patellar tendon: collagen fascicle morphology and architecture," J. Orthop. Res., Vol. 7, pp. 243-251.
- Yahia, L. H., and Drouin, G., 1988, "Collagen structure in human anterior cruciate ligament and patellar tendon," J. Mat. Sci., Vol. 23, pp. 3750-3755.

### Chapter 1:

## Patellar Tendon And Infrapatellar Fat Pad Healing After Harvest Of An ACL Graft

Theresa S. Atkinson, Patrick J. Atkinson, Mendenhall, H. Vincent, and Roger C. Haut

### **ABSTRACT**

Clinical studies have documented proliferation of the host patellar tendon and fibrosis extending into adjacent tissues after reconstruction of the injured anterior cruciate ligament (ACL) using the central one third of the patellar tendon (PT) as the graft. Such generalized arthrofibrosis has been implicated in knee locking and as possible source of anterior knee pain. However, it is not clinically feasible to measure changes in tendon morphology and mechanical properties and degeneration of peripheral tissues over time following graft harvest. In a rabbit experimental model proliferative changes in the tendon and the infrapatellar fat pad have been documented following harvest of a central third tendon graft without ACL reconstruction. Studies in larger animals have shown significant reductions in the strength and stiffness of the healing patellar tendon, but without assessment of the peripheral tissue response. In the current study an ACL reconstruction was performed in a goat model using an autogenous patellar tendon graft. Extensive tendon and fat pad proliferation were observed along with significant reductions in the biomechanical properties of the host tendon. Significant fat pad fibrosis was documented using biochemical methods. The current data confirm that harvest of an autogenous PT graft for reconstruction of the ACL results in significant changes in the PT and adjacent tissues. These data may help explain some of the clinical complications documented in the reconstructed joint.

### INTRODUCTION

Reconstruction of the injured ACL using a full thickness central one third patellar tendon graft is currently standard practice (Aflietti et al., 1994), due to the graft's superior strength and the ability to anchor the graft via patellar and tibial bone blocks. However, significant reductions in the strength and stiffness of the healing patellar tendon have been observed in experimental studies (Burks et al., 1990, Linder et al., 1994, Kamps et al., 1994). In addition, clinical (Berg, 1992) and experimental (Atkinson et al., 1996) studies have documented a doubling of the cross sectional area and significant changes in the length of the healing tendon following harvest of the graft. Increased stress on the host tendon has been implicated in initiating this remodeling process. Other structures in the knee joint have also shown poor responses following patellar tendon graft harvest. Clinical studies have documented proliferation, or fibrosis, extending into tissues adjacent to the patellar tendon, such as the infrapatellar fat pad (Rosenburg et al., 1992, Olglivie-Harris and Giddens, 1994) and the joint capsule (Richmond and Assal, 1991, Cosgarea et al., 1994). Such proliferation may lead to loss of extension and contribute to post-surgical knee pain (Richmond and Assal, 1991). Advanced fat pad fibrosis (Hoffa's syndrome) is a clinically recognized source of anterior knee pain (Magi et al., 1991). Clinical studies have suggested that the removal of fibrotic fat pads can help alleviate pain (France et al., Kempf, 1980, Krebs and Parker, 1994). Our rabbit experimental model, in which a patellar tendon graft is harvested without ACL reconstruction, shows proliferation in the patellar tendon and fibrosis in the fat pad at six and twelve weeks following resection of the central third (Atkinson et al., 1996). At 52 weeks the patellar tendon shows

biomechanical and histological evidence of a return to normal tissue, and the fat pad shows decreased fibrosis. In our rabbit model, no bone blocks are excised during resection of the central third patellar tendon, and fat pad disruption is minimal. In the current study changes in the tendon and fat pad following reconstruction of the ACL, using an autogenic patellar tendon graft, were evaluated in a goat model. This model more closely approximates the clinical scenario for ACL reconstruction and the anthropometry of the human knee than the previous rabbit model. We hypothesized that this model would also exhibit proliferation in the patellar tendon, significant reduction in the biomechanical properties of the tendon, and fibrosis of the fat pad similar to our observations following resection of the central third of the patellar tendon in the rabbit model.

### MATERIALS AND METHODS

The right limbs of eighteen female goats (>40kg, >4yrs, mixed breed) were subjected to patellar tendon graft harvest and ACL reconstruction: six animals were sacrificed at each time point of time zero, 12 weeks and 52 weeks. The left limb served as an unoperated control for each animal. Time zero animals were sacrificed following surgery, while 12 and 52 week animals were allowed unrestricted mobilization on a farm. The procedures used in this study conformed to the Guide for the Care and Use of Laboratory Animals, National Research Council, Revised 1996.

### Operative Procedure

The patellar tendon (PT) was exposed via a lateral skin incision and clearing of the overlying subcutaneous tissue. A partial thickness PT graft, approximately 1 mm thick and 8 mm wide was harvested. Longitudinal incisions were made at the medial and lateral

margins of the tendon and a 1/3 thickness transverse incision was made in the tendon. Bone blocks, the width of the autograft, were then harvested at the patella and tibia. Two 1 mm diameter holes were drilled through these blocks, and non-absorbable #2 suture material was passed through the holes to aid in passage and fixation of the graft. The patella was then medially subluxed and the joint was held in full flexion. The fat pad and synovium surrounding the ACL were dissected longitudinally to provide visibility of the ACL insertions. The ACL was incised at the tibial and femoral insertions and removed. A tibial tunnel was constructed by drilling from the tibia, medial to the patellar tendon insertion, to a point slightly anterior and medial of the normal ACL insertion. posteriorly placed femoral tunnel was then drilled through the joint to the anterior origin of the lateral head of the gastrocnemius. A cancellous bone screw and spiked washer were placed in the femur. Isometry of the tunnel placement was checked at full extension and flexion using marked cotton tape. If necessary, the femoral tunnel was widened to insure isometric placement. The graft was then passed through the bone tunnels. The non-absorbable suture material was wrapped around the unthreaded end of the bone screw, and the screw was tightened. Small Kirschner wires were used to additionally fix the bone block. The graft was then placed under manual tension and the joint was cycled 20 times. The non-absorbable sutures on the tibial graft end were wrapped around a tibial bone screw and washer and a small force was applied to tension the graft. The tibial screw was tightened, and the tibial bone block additionally fixated with small Kirschner wires. The ACL graft was then observed through the entire range of motion.

impingement was noted, a femoral notchplasty was performed. The joint capsule, subcutaneous tissue, and skin were then closed using non-absorbable sutures.

### Biomechanical Analysis:

Following sacrifice, the fat pad was resected and immediately immersed in 10% buffered formalin. Patella-patellar tendon-tibia complexes were isolated from unoperated and operative sides at 12 and 52 weeks. The patellar tendon cross sectional area (CSA) was taken as the average of measurements taken at three longitudinal points using an area micrometer (Butler et al., 1983). At time zero the boundaries of the operated tendon were difficult to determine, thus these were harvested leaving some peripheral, non-load bearing tissues intact. The CSAs of these time zero tissues were determined following mechanical testing using photographs of intact tendon cross sections (NIH Image 1.6). Patellar tendon length was defined as the distance from the insertion at the distal patella to the insertion into the tibia and was measured by one individual with vernier calipers (Burks et al., 1990, Linder et al., 1994, Kamps et al., 1994). The patella and tibia were potted in a specially designed stainless steel box and tube, respectively. A stainless steel pin was carefully installed through a hole in the side of the tube to extend through both cortices of the midtibia to provide additional fixation. Mechanical experiments were conducted in a 0.15 M phosphate buffered saline (PBS) bath (pH 7.2) maintained at 37°C. The potted tibia was mounted on a vertical plate with an angle of 20 degrees between the long axis of the patella and the tibial shaft in the sagittal plane. To eliminate lateral loading, the vertical plate containing the tibia was secured to a X-Y table base and a universal joint connected the patella to the crosshead. The complex was preconditioned at 3% strain for 20 cycles at 1 Hz. It was immediately extended to failure in a materials testing machine (Instron model 1331) at a nominal strain rate of 100 %/s. An established analytic model (Belkoff and Haut, 1992) was used to obtain a numerical description of the load-displacement data. This model contains 2 parameters to describe the "toe" or initial nonlinear region of response ( $\mu$  and  $\sigma$ ) and a stiffness (k) to characterize the linear region. Based on the original development of the model (Belkoff and Haut, 1992), the parameter  $\mu$  describes the elongation required to straighten 50% of tendon fibers and  $\sigma$  is the standard deviation about that mean. The stiffness parameter (k) was determined from the load/displacement response and the  $\mu$  and  $\sigma$  values were obtained using an iterative curve fitting program. The ultimate (failure) load was determined from the load/displacement response. A tissue modulus was estimated by the product of stiffness and original tendon length divided by the CSA. These data provided an estimate of the substance tensile modulus and yield a measure of the quality of the tissue.

The fat pads of both limbs from two animals per time point were histologically processed, using standard methods, and stained with H & E. A portion of every test and unoperated fat pad was also assayed for its collagen content. Briefly, the wet fat pad tissue was minced and six 2.0-2.5 mg aliquots were weighed for each limb. The aliquots were freeze dried with liquid nitrogen, pulverized, then processed according to established methods to determine the content of hydroxyproline (Stegemann, 1958). The collagen content was then obtained from the hydroxyproline content (7.46 µg collagen/µg hydroxyproline).

A randomized ANOVA was used to compare the fat pad hydroxyproline, CSA, length, ultimate load, stiffness and model parameters ( $\mu$  and  $\sigma$ ) of the operated tendons at different time points (p $\leq$ 0.05, SigmaStat, Jandel Corp., San Rafael CA) and where significant differences were identified Student-Newman-Keuls (SNK) post-hoc testing was applied. Paired t-tests were used to compare the operative and contralateral unoperated data (p $\leq$ 0.05). Correlations (p $\leq$ 0.05) between fat pad hydroxyproline and patellar tendon cross sectional area, length, and stiffness were also obtained to investigate whether changes in tendon size or properties were related to changes in fat pad collagen content.

### RESULTS

One animal from the 12 week group and one from the 52 week group were not tested due to technical problems. The CSA of the operated tendon significantly increased from time zero to 12 and from 12 to 52 weeks (Table 1). The normalized (operated limb/contralateral limb) average CSA of the PT at time zero was 54%, while at 12 and 52 weeks the ratio was 237% and 184%, respectively. The tendon length decreased significantly from time zero to 12 weeks, and did not return to the unoperated length by 52 weeks. The ultimate load supported by the bone-tendon-bone complex increased significantly between time zero (22% of the unoperated limb load) and 12 weeks (54% of the unoperated limb load), and did not return to the unoperated level by 52 weeks. Four operated bone-tendon-bone preparations and 1 unoperated preparation failed due to avulsion at the distal pole of the patella and the remaining failed in the tendon midsubstance. The stiffness of the operated preparation increased significantly between time zero and 12 weeks (41% versus 69% of unoperated), and between 12 and 52 weeks

(69% versus 87%). The time zero tissue exhibited a "toe" response which was similar to that of the unoperated tissue, but with a lower stiffness (Figure 1). In contrast, at later times the operated tissue exhibited a more pronounced "toe region" region than the unoperated tissue (as evidenced by generally larger μ and σ values for the operated tendon). Histologic sections of the tendons indicated that the defect filled with collagen which appeared disorganized at 12 weeks and begans to show signs of order at 52 weeks (Figure 2). The estimated tensile modulus at time zero was 72% of the unoperated value. This parameter decreased significantly between time zero and 12 weeks (to 26% of unoperated). No significant change in the estimated modulus was detected between 12 and 52 weeks.

At time zero the tendon and fat pad morphology was not different from the unoperated tissues. Normal fat pads generally showed small amounts of collagen throughout the adipose tissue (Figure 3a). Extensive collagen infiltration was observed in fat pads at both 12 and 52 weeks (Figure 3b,c). Though not quantified in this study, neovascularization was also observed in fat pads from operated joints at these time points. The hydroxyproline content of the fat pad significantly increased between time zero and 12 weeks to 648% of the unoperated fat pad (Table 1). At 52 weeks the hydroxyproline content remained significantly higher than the unoperated level, however it dropped slightly from the 12 week level to 617% of the unoperated level. Increases in hydroxyproline content of the fat pad were correlated with increasing cross sectional area, and with decreasing length of the patellar tendon.

### **DISCUSSION**

This study was designed to investigate the effects of ACL reconstruction in a goat model using an autogenous PT graft on the mechanical and histological properties of the host patellar tendon. We hypothesized that extensive proliferation of the host tendon, significant reductions in the biomechanical properties of the tendon, and remodeling of the fat pad would follow surgery. Furthermore we suggested these changes would be similar to those observed in our rabbit model, where the ACL was not reconstructed.

Our results support these hypotheses, demonstrating significant changes to the tendon and fat pad in the goat model following ACL reconstruction using an autogenous, ipsilateral patellar tendon graft. The unoperated patellar tendon modulus was similar to that reported in Ng et al. (1995) (319 MPa vs. 302.5 MPa) but both of these were much higher than that reported by Jackson et al. (1993) (147.3 MPa). The ultimate load in the unoperated tendon was much higher than that documented in earlier studies (4334 N vs. 516.7 N (Ng et al., 1995) and 2714 N (Jackson et al., 1993), possibly due to the larger cross sectional area of the tendons (41.9 mm<sup>2</sup> vs. 13.7 mm<sup>2</sup> (Ng et al., 1995) and 28.3 mm<sup>2</sup> (Jackson et al., 1993)). This difference in size was most likely the result of different sized animals utilized in the studies (>40 kg in the current study vs. 33.2 kg average (Ng et al., 1995) and >25 kg (Jackson et al., 1993)). The operated tendon tissue was hypertrophic and the biomechanical properties were significantly reduced compared to unoperated limbs at all time points. The increase in the operated tendon cross section, decrease in tendon length, and improvement in tendon stiffness over time observed in the current study were also observed by Jackson et al. (1993) between 6 weeks and 6 months.

These changes were also similar to those observed in our rabbit model: at 12 weeks CSA 237% (goat) of unoperated as compared to 201% (rabbit), stiffness 69% compared to 75%,  $\sigma$  and  $\mu$  values higher than unoperated, and at 52 weeks some improvement toward unoperated levels. The ultimate load of the host tendon remained much below that found in the rabbit model (at 12 weeks 52% of unoperated, as compared to 80% in the rabbit model). This might be a result of the relatively large graft harvested in the current study (at time zero the CSA was 54% of the unoperated side, versus 67% in the rabbit model). Significant remodeling of the fat pad was evidenced by the replacement of adipose tissue by collagen, and development of new blood vessels. These changes were similar to those observed in our rabbit model (Atkinson et al., 1996). They were more significant than those noted in Muneta et al's (1993) rabbit model, where the ACL was reconstructed with an achilles tendon autograft and the animal was allowed limited motion. This difference may be due to increased compression applied to the fat pad in the current study resulting from the increased cross sectional area of the healing patellar tendon. This is supported by our finding that increased fat pad hydroxyproline content was correlated with tendon CSA. On the other hand, the genesis of fibrosis in the fat pad may be associated with biochemical changes not considered in the current study. The influx of enzymes associated with the healing patellar tendon, may encourage remodeling in the adjacent fat pad due to their shared vasculature (Linder et al., 1994, Paulos et al., 1983, Kohn et al., 1995).

A limitation of the current study was that the harvest procedure differed from that in the previous rabbit model: a partial thickness graft versus a central third in the earlier

studies. In both procedures, however, the character of the response appeared the same. This suggested that the tendon response may be initiated when stresses in the host are increased due to the removal of load bearing tissue. This etiology was previously suggested by observations in our rabbit model (Atkinson et al., 1996). Another limitation was that a visual technique was utilized to measure the time zero tendon cross sections. This likely caused the tendon area to be overestimated in the test case, where the cut surface likely allowed excessive fluid to be imbibed and expand the tendon, thereby reducing the time zero modulus. A further limitation of the study was that, while we associated anterior knee pain with fibrosis of the fat pad, we did not actually assess pain. In future studies it may be possible to assess pain by observation of the animal's stance forces (Bray et al., 1992) or gait. Finally, both the patellar tendon and fat pad were incised, thus making it difficult to determine whether the changes in the fat pad were related to the healing of the patellar tendon or to incision of the fat pad itself. The previous rabbit model, however, had minimal disruption of the fat pad and significant fat pad fibrosis was still observed. Taken together these data seem to suggest that the healing tendon may have a large influence on fat pad healing. Further studies are required to examine fat pad healing independent of tendon healing.

In conclusion, the current study suggests that significant remodeling of both tendon and fat pad take place following harvest of autogenous patellar tendon grafts. These changes were similar to those noted in our previous rabbit model. Increased stress on the patellar tendon due to harvest of load bearing tissue for ACL reconstruction may trigger the tendon proliferation and result in fibrosis of the fat pad. These changes may

help explain, in part, post-surgical complications such as infrapatellar contracture syndrome and anterior knee pain.

### **ACKNOWLEDGMENT:**

This investigation was supported, in part, by DePuy Incorporated, Warsaw, Indiana. The authors wish to gratefully acknowledge Mrs. Jane Walsh for her preparation of the histology slides, William Newberry and Benjamin Ewers for their assistance in the mechanical testing, and Mrs. Dana Dvorchek-Driksna for performing the biochemical assays on fat pads.

### **REFERENCES:**

- Aglietti, P., Buzzi, R., Zaccherotti, G., and DeBiase, P. Patellar Tendon Versus Doubled Semitendinosus and Gracilis Tendons for Anterior Cruciate Ligament Reconstruction. *The American Journal of Sports Medicine* 22(2):211, 1994.
- Atkinson, P., DeCamp, C., Kamps, B., Hespenheide, B., Zukosky, D., and Haut, R. Healing response of the patellar tendon after removal of its central third and implantation of an augmentation device. *Trans Orthop Res Soc* 43:751, 1996.
- Belkoff, S. M. and Haut, R. C. Microstructurally based model analysis of gamma-irradiated tendon allografts. *Journal of Orthopaedic Research* 10:461, 1992.
- Berg, E. Intrinsic Healing of a patellar tendon Donor Site Defect after Anterior Cruciate Ligament reconstruction. Clinical Orthopaedics 278:160, 1992.
- Bray, R., Shrive, N., Frank, C., and Chimich, D. The early effects of joint immobilization on medial collateral ligament healing in an acl-deficient knee: a gross anatomic and biomechanical investigation in the adult rabbit model. *Journal of Orthopaedic Research* 10:157, 1992.
- Burks, R., Haut, R., and Lancaster, R. Biomechanical and Histological Observations of the Dog Patellar Tendon After Removal of its Central One-third. *The American Journal of Sports Medicine* 18:146, 1990.
- Butler, D., Hulse, D., Kay, M., Grood, E., Shires, P., D'ambrosia, R., and Shoji, H. Biomechanics of Cranial Cruciate Ligament Reconstruction in dog. *Veterinary Surgery* 12(3):113, 1983.
- Cosgarea, A., DeHaven, K., and Lovelock, J. The surgical treatment of arthrofibrosis of the knee. *Amer J Sports Med* 22(2):184, 1994.
- France, E., Paulos, L., Abbott, P., and Roberts, P. Failure Characteristics of the medial Collateral Ligament of the Knee: Effects of high strain rate. Aviation Space and Environmental Medicine 58:488, 1987.
- Jackson, D. W., Grood, E. S., Goldstein, J. D., Rosen, M. A., Kurzweil, P. R., Cummings, J. F., Simon, T. M. A comparison of patellar tendon autograft and allograft used for anterior cruciate ligament reonstruction in the goat model. *Amer J Sports Med* 21(2):176, 1993.
- Kamps, B. S., Linder, L. H., DeCamp, C. E., and Haut, R. C. The influence of immobilization versus exercise on scar formation in the rabbit patellar tendon after excision of the central third. *American Journal of Sports Medicine* 22:803, 1994.

- Kempf, F. Treatment of mensicus defects with reference to our operative method: subtotal menisectomy, resection of hoffa's corpus adiposum, inner drainage. *Arch Orthop Traumat Surg* **96**:95, 1980.
- Krebs, V. and Parker, R. Arthroscopic resection of an extraossifying chondroma of the infrapatellar fat pad: end stage hoffa's disease? *Arthrosc: J Arthrosc Rel Surg* 10(3):301, 1994.
- Kohn, D., Deiler, S., and Rudert, M. Arterial blood supply of the infrapatellar fat pad: anatomy and clinical consequences. Arch Orthop Trauma Surg 114:72, 1995.
- Linder, L., Sukin, D., Burks, R., and Haut, R. Biomechanical and histologic properties of the canine patellar tendon after removal of the medial third. *The American Journal of Sports Medicine* 22(1):136, 1994.
- Muneta, T., Yamamoto, H., Takakuda, K., Sakai, H., and Furuya, K. Effects of Postopertative Immobilization on the Reconstructed Anteior Cruciate Ligament: An Experimental Study in Rabbits. *Amer J Sports Med* 21(2):305, 1993.
- Ng, G., Oakes, B. W., Deacon, O. W., McLean, I. D., and Lampard, D. Biomechanics of Patellar Tendon Autograft for Reconstruction of the Anterior Cruciate Ligament in the Goat: Three Year Study. *The Journal of Bone and Joint Surgery* 13:602, 1995.
- Magi, M., Branca, A., Bucca, C., and Langerame, V. Hoffa disease. *Ital J Orthop Traumatol* 17(2):211, 1991.
- Paulos, L., Butler, D., Noyes, F., and Grood, E. Intra-articular Cruciate Reconstruction. Clinical Orthopaedics and Related Research 172:78, 1983.
- Oglivie-Harris, D. and Giddens, J. Hoffa's disease: Arthroscopic resection of the infrapatellar fat pad. Arthrosc: J Arthrosc Rel Surg 10(2):184, 1994.
- Richmond, J. and Assal, M. Arthroscopic management of arthrofibrosis of the knee, including infrapatellar contracture syndrome. *Arthrosc: J Arthrosc Rel Surg* 7(2):144, 1991.
- Rosenburg, T. D., Franklin, J. L., Baldwin, G. N., and Nelson, K. A. Extensor Mechanism Function After Patellar Tendon Graft Harvest for Anterior Cruciate Ligament Reconstruction. *The American Journal of Sports Medicine* **20(5)**:519, 1992.
- Stegemann, H. Mikro vestimmurg von hydroxyproline mit chloramin-tund p-dimethylamino benzaldehyd. Hoppe-Seylers Z. *Physiol Chem* 41, 1958.

## **TABLES**

Table 1: Biomechanical and biochemical data for goat patellar tendons and infrapatellar fat pads following harvest of a patellar tendon graft to reconstruct the ACL (mean  $\pm$  one standard deviation).

Measured Parameter	Unoperated (n=16)	0 weeks (n=6)	12 weeks (n=5)	52 weeks (n=5)
Tendon Cross	41.9±3.9 <sup>d</sup>	22.8±5.3 <sup>a,b,c</sup>	99.3±12.1 <sup>a,c,d</sup>	77.0±14.8 <sup>a,d</sup>
Sectional Area (mm²)				
Tendon Length (mm)	40.8±2.4	41.5±2.4 <sup>b,c</sup>	36.4±3.3 <sup>c,d</sup>	30.6±4.0 <sup>a,b,d</sup>
Ultimate Load (N)	4334±831 <sup>d</sup>	946±244 <sup>a,b,c</sup>	2354±675 <sup>a,d</sup>	2454±462 <sup>a,d</sup>
Tensile Stiffness (N/mm)	319±45 <sup>d</sup>	130±25 <sup>a,b,c</sup>	221±26 <sup>a,c,d</sup>	276±29 <sup>a,b,d</sup>
model parameter μ (mm)	0.683±.480	0.292±0.142	1.730±0.929 <sup>d</sup>	1.193±0.435 <sup>d</sup>
model parameter σ (mm)	0.502±0.337	0.194±0.124	1.090±0.598 <sup>d</sup>	0.906±0.455 <sup>d</sup>
Tensile Modulus (MPa)	313±32	255±96 <sup>b,c</sup>	80±12 <sup>a,d</sup>	115±34 a,b,d
Fat Pad Collagen (μg/mg wet tissue)	22.3±25.6	23.1±21.7 <sup>b,c</sup>	144.6±80.6 <sup>a,d</sup>	137.6±69.2 <sup>a,d</sup>

a - significantly different than unoperated, paired t-test (p<0.05).

b - significantly different from 12 weeks, ANOVA (p<0.05).

c - significantly different from 52 weeks, ANOVA (p<0.05).

d - significantly different from time 0, ANOVA (p<0.05).

## **FIGURE LEGENDS**

Figure 1: Composite load-elongation curves for the unoperated and three operated groups constructed using the average values of the parameters  $\mu$  (elongation required to straighten 50% of tendon fibers),  $\sigma$  (the standard deviation about that mean) and the linear stiffness (K) as determined by the non-linear curve fitting program

Figure 2: Tendon coronal sections (H&E, 100X) A) Typical unoperated tendon, B) 12 and C) 52 week operated patellar tendons. Note a minimal distribution of mature fibroblasts in the unoperated tissue versus the marked hypercellularity and cell immaturity in the operated tissues at 12 and 52 weeks. Also note poor collagen alignment at 12 weeks but improved collagen alignment and crimping at 52 weeks.

Figure3: Fat pad cross sections (H&E, 40X). A) Time zero operated and unoperated fat pads, B) 12 week operated fat pads showing extensive fibrosis and neovascularization (arrow) and

C) 52 weeks showing reduced fibrosis.

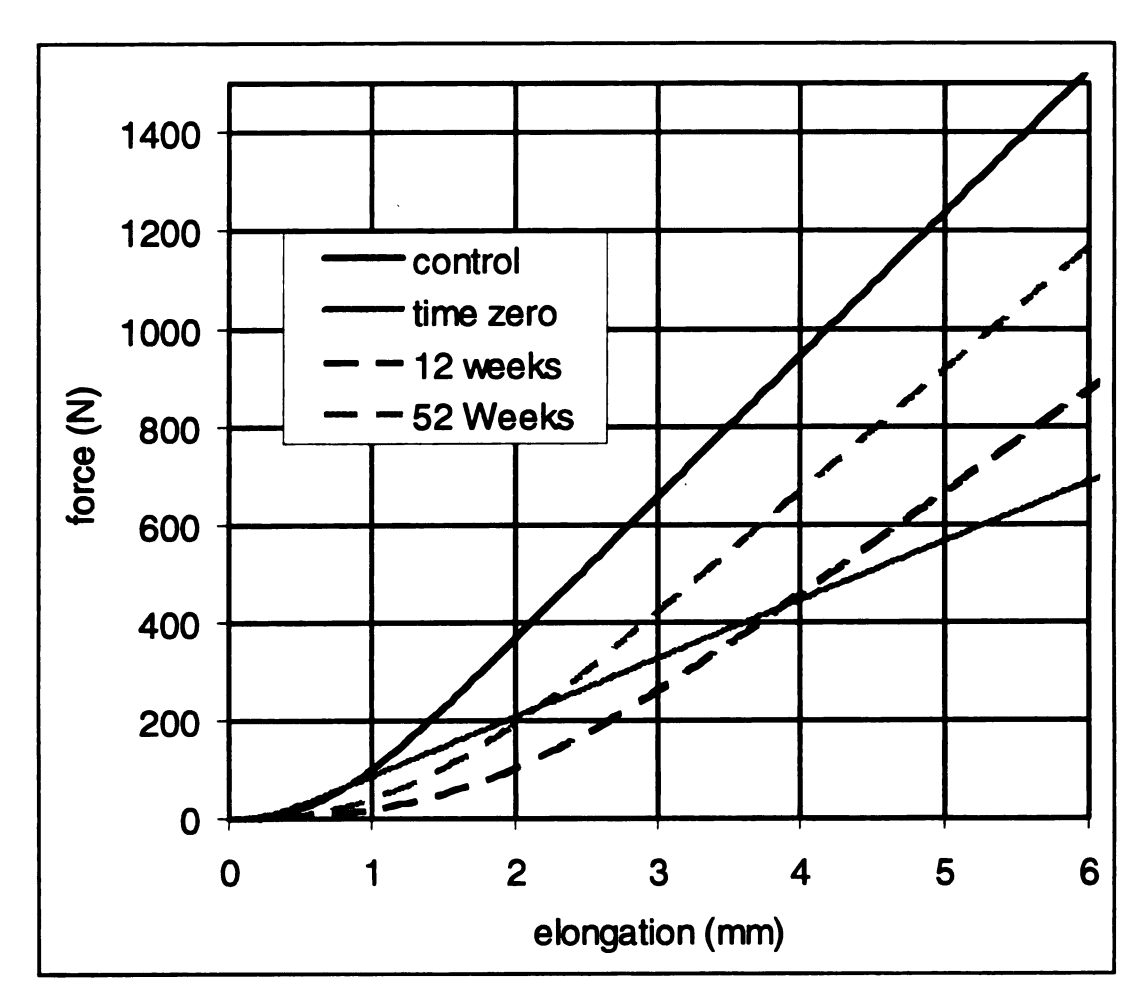


Figure 1

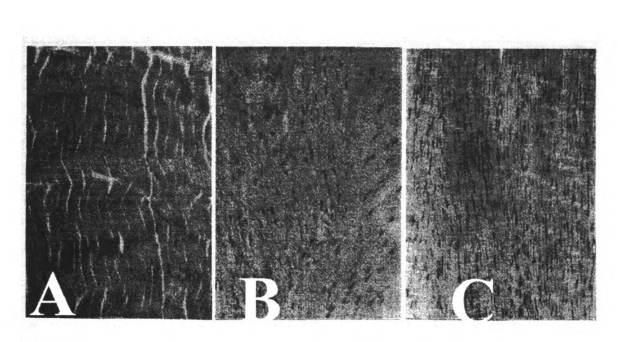


Figure 2

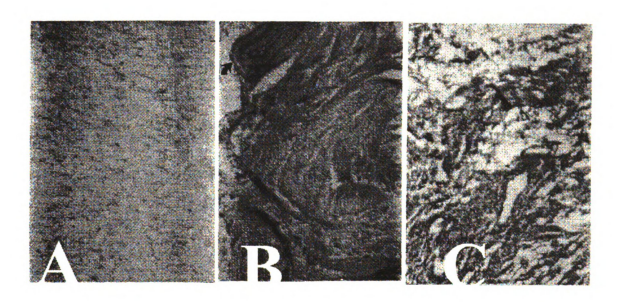


Figure 3

Footnotes:

Sponsored in part by DePuy, Incorporated of Warsaw Indiana.

# Chapter 2:

# A Poroelastic Model That Predicts Some Phenomenological Responses of Ligaments and Tendons

Theresa S. Atkinson, Roger C. Haut, and Nicholas J. Altiero

#### ABSTRACT:

Experimental evidence suggests that the tensile behavior of tendons and ligaments is in part a function of tissue hydration. The models currently available do not offer a means by which the hydration effects might be explicitly explored. To study these effects a finite element model of a collagen sub-fascicle, a substructure of tendon and ligament, was formulated. The model was microstructurally-based and simulated oriented collagen fibrils with elastic-orthotropic continuum elements. Poroelastic elements were used to model the interfibrillar matrix. The collagen fiber morphology reflected in the model interacted with the interfibrillar matrix to produce behaviors similar to those seen in tendon and ligament during tensile, cyclic, and relaxation experiments conducted by others. Various states of hydration and permeability were parametrically investigated, demonstrating their influence on the tensile response of the model.

### INTRODUCTION:

Tendons and ligaments provide stability and control for the motion of joints. Thus, their function plays an important role in musculoskeletal biomechanics. Assessment of the mechanical properties of these tissues is important in development of various surgical techniques for joint reconstruction. In these assessments, the role of collagen fibers in the tissue has been highlighted and correlated to various disease states. Models which refer to various collagen morphologies have been used to characterize the results of these studies (Belkoff and Haut, 1991; Lanir, 1978; Kwan and Woo, 1989).

More recently, experimental studies have suggested that other tissue components, such as water (which comprises 60-70% of the weight of tendons and ligaments), might

play a significant role in the tensile behavior of ligaments and tendons. For example, experiments suggest that human patellar tendons exhibit higher tensile modulus and ultimate strength when tested in a bath environment versus in air (Haut and Powlison, 1990). Similarly, the tendon is stiffer when tested in a hydrating solution versus a dehydrating solution (Haut, et. al 1995). Furthermore, both studies suggest that the viscoelastic properties of human tendon are influenced by water. For example, in relaxation tests, specimens tested in a saline bath exhibit a larger and more rapid load relaxation versus those tested in air (Haut and Powlison, 1990). Similarly, specimens tested in a hydrating bath have greater load relaxation than those tested in a dehydrating bath (Haut et al., 1995).

In ligaments, increasing the water content causes the tissue to respond with greater cyclic load relaxation relative to ligaments with lower water content (Chimich et al., 1992). Data from cyclic tests also demonstrate monotonic decreases in rat tail tendon diameter from cycle to cycle (Lanir et al., 1988). Similar behavior has been documented in the rat medial collateral ligament (MCL) (Thielke et al., 1995). This deformation suggests densification of the collagenous structure and exudation of fluid, and is consistent with reports that glycosaminoglycans (GAGs) and water are exuded during tensile strain tests (Lanir et al., 1988; Hannifin and Arnoczky, 1994).

Effects associated with extracellular water have been observed experimentally, but few analytical models address the mechanism of its action. Chen et al. (1993) utilized a finite element analysis (FEA) to study permeability effects in tendon and ligament. The model includes a fluid phase moving around regular cylinders (meant to represent collagen

fibers). Chen and Vanderby (1994) proposed a directionally sensitive permeability for tendons. The influence of water has also recently been incorporated in a model of the rabbit MCL (Wilson et al., 1994). Wilson's FEA model utilizes a continuum matrix of poroelastic material and spring elements attached at nodes to include the elastic stiffness of collagen. The model predicts that pressure within the MCL is negative during tensile deformation, implying that fluid flows into the structure. This result, however, is contrary to current experimental data indicating positive internal pressures (Chen et al., 1995) in rabbit patellar tendon during tensile stretch and fluid exudation in the canine flexor tendon, rabbit MCL, and rat tail tendon under tensile strain (Hannifin and Arnoczky, 1994; Thielke et al., 1995; Lanir et al., 1988).

These contrary results suggest that continuum characterizations alone of the tendon may not reflect mechanisms important to predicting the role of water in tensile load response. Lanir et al. (1988) describe the tendon on a microscopic scale as consisting of an arrangement of collagen fibrils embedded in a hydrophilic gel. While there is controversy in the literature concerning the hierarchical levels of collagen, it is generally accepted that fibrils are combined to form sub-fasciculi, fasciculi, and finally the whole structure (Danylchuk et. al, 1978; Viidik 1990; Yahia and Drouin 1988). It has been proposed that the morphology of collagen fibrils can be complex, ranging from being helically wound about a sub-fascicle (termed fascicle by Yahia and Drouin, 1988) axis in the patellar tendon to a both helical and planar waveforms in the anterior cruciate ligament (ACL). In the sub-fasciculi containing helically wound fibrils, the peripheral fibrils appear as undulated helices, while the central ones are normal helices (Yahia and Drouin, 1989).

It has been previously suggested that the collagen in tendon and ligament interacts in such a way that it compresses the gelatinous matrix and creates a sensitivity to strain rate in the tissue (Lanir, 1978). We hypothesize that longitudinal deformation of the more helically oriented fibrils in the sub-fascicular structure of patellar tendons and ACLs might compress the matrix to generate hydraulic pressures and movement of unbound water during tensile stretch. By this mechanism the load might be shared between collagen and the surrounding matrix to influence the tensile response of the entire ligamentous or tendonous structure. Danylchuk (1978) states that the connective tissue sheaths between fascicles and sub-fascicles, contain collagen which is oriented perpendicular to the long axis of the structure and thus provides a binding function rather than significant tensile strength. We therefore assumed that the sub-fascicle may be considered a characteristic structure of ligament and tendon which therefore should exhibit behaviors observed in the gross structure

#### **METHODS:**

The fibril structure and matrix interaction were idealized for the purpose of building a simple model. This simple model consists of an outer ring composed entirely of helically oriented fibrils, and an internal region comprised of a water-based matrix (Fig. 1). These regions interact to support tensile loads. Further simplifications of this conceptual model were made in order to provide the basis for a finite element model. The sub-fascicle's cross section was assumed to be circular and of constant diameter throughout its length. Thus, it was only necessary to model a representative section from the center of a centrally located sub-fascicle.

A finite element model, consisting of 84, 20 noded 3-dimensional continuum elements, was developed using a commercial code (ABAQUS, Hibbitt, Karlsson, and Sorensen, Inc. Pawtucket R.I.). The cubic elements consisted of nodes at the midpoint of each edge possessing three degrees of freedom for displacement, and nodes at the corners possessing an additional degree of freedom for pressure. The model's radius, 37.5 µm, was an average of those scaled from micrographs of the human patellar tendon (Yahia and Drouin 1988). The length of the model was chosen to be 10.0µm to maintain an approximately 1 to 1 relationship between the lengths of the element sides in a majority of the elements and to help avoid numerical ill-conditioning. The fibrous outer ring was modeled as an orthotropic poroelastic material, where the selection of orthotropic material properties was intended to produce deformations consistent with helically oriented collagen fibrils. The fibril alignment, measured as a 62° inclination from vertical on one SEM of a tendon (Yahia and Drouin, 1988, Figure 8), was attained by setting the 2 direction of the orthotropic outer ring at this inclination. For simplicity, the fibril morphology was assumed to be purely helical, at a constant angle of orientation through the sub-fascicle's thickness.

Little information is available documenting material properties of collagen sub-fascicles. One study suggests that rabbit patellar tendon fascicles have a modulus of approximately 225MPa (Yamamoto et al., 1995). Rat tail tendon (RTT) has been described as being composed of 1-3 collagen fascicles (Kastelic et. al, 1978) with a tensile modulus of approximately 600MPa (Haut, 1983). In this study the tensile modulus in the fibril direction was assumed to be 600MPa (Table 1). Unfortunately, there is no

information on the transverse or shear moduli of collagen sub-fascicles or fascicles. We assumed that the fibrous portion of the model was weak transverse to the fibril direction.

Thus, the transverse moduli were assumed to be one order of magnitude less than the fibril direction modulus, and the shear moduli less than the transverse. Poisson's ratios consistent with an orthotropic material were then selected.

The central core was modeled as nonlinear poroelastic. The poroelastic material model, originally developed to describe soil behavior, is similar in formulation to the biphasic model currently applied to cartilage (Suh and Spilker, 1994; Mow et al., 1984). The poroelastic matrix of tendon and ligaments may be similar to cartilage in that it is a fiber embedded permeable structure which contains water, proteoglycans and other constituents (Mow and Hayes, 1991; Thielke et al., 1995).

The nonlinear poroelastic material stiffens upon compression. This is accomplished through moderation of the shear modulus in the following way:

$$G = \left[ \frac{3(1-2\nu)(1+e_o)}{2(1+\nu)\kappa} \right] \left( P + P_t \right) \exp\left(\epsilon_{vol}^{el}\right)$$

where  $e_0$  is the initial voids ratio (volume fraction of fluid/volume fraction of solid), P is the internal pressure,  $P_t$  is the elastic ultimate strength,  $\epsilon^{el}_{vol} = \ln J^{el}$  is the elastic portion of volume change, v is Poisson's ratio, and  $\kappa$  is the log bulk modulus (relating the logarithm of pressure to the dilatation) (Abaqus Theory Manual, Zienkiewicz and Naylor, 1972). Thus, G increases with compaction and pressure. Assuming that the volume fraction of water in tendon is similar to the weight fraction (70% of the wet weight is water), an initial voids ratio of 2.33 (=.7/.3) was used for the nonlinear poroelastic portion of the

model (Haut, 1993; Mow and Hayes 1991), however, e<sub>0</sub>=1.0 (50%) was also investigated. Based on the assumption that fluid in tendon is similar to that in other tissues, the log bulk modulus of the nonlinear poroelastic core was obtained from data for fluid in the human annulus fibrosis (Best et al., 1984). Poisson's ratio was assumed to be 0.49. The tensile modulus of the material was then derived such that the initial shear modulus of the inner core approximately matched the shear moduli of the outer poroelastic ring.

Fluid flow was assumed to obey Darcy's law, i.e.:

$$v = -k dp/dr$$

where v is the fluid velocity, k is the permeability, and p is the pressure. This law is applicable to low flow rate problems and is used in biphasic models of cartilage (Mow and Hayes, 1991). The influence of permeability on flow rate can be complex and is known to be a nonlinear function of deformation in cartilage (Mow et al. 1984). Since k is unknown for tendon, it was assumed constant. In the past, similar assumptions have been utilized in cartilage models (Suh and Spilker, 1994). The permeability of cartilage has been reported from 1.45x10<sup>-15</sup> (bovine) to 2.17x10<sup>-15</sup>m<sup>4</sup>/Ns (human patellar groove) (Mow and Hayes, 1991). Permeabilities in the range 1.0x10<sup>-12</sup> to 1.45x10<sup>-27</sup>m<sup>4</sup>/Ns were investigated in the current study.

The orthotropic poroelastic material of the outer ring was assumed to be capable of holding water with permeabilities similar to those of the core portion of the model.

Initial voids ratios of 1.0 and 2.33, similar to those used in the core were assigned to this portion, but values as low as 0.01 were also examined. All the materials in the model

were assumed to be fully saturated and the outer ring was assumed to be perfectly attached to the inner core.

## **Boundary Conditions:**

All loading was prescribed through displacement control. The bottom of the model was constrained to planar motion with 4 nodes separated by  $90^{\circ}$  constrained to radial motion. The top of the model was also constrained to planar motion (r and  $\theta$  free). A uniform displacement was applied across the top of the model. The top and bottom were assumed to be sealed in order to represent conditions in a long thin fascicle at the center of a tendon. The outer boundary of the model was also sealed. This sealed boundary condition was dictated by the use of continuum elements in the ring portion of the model (rather than modeling discrete collagen fibers), which would experience a positive dilatation under tensile loading and thus tend to draw in water if a perfectly draining boundary condition were applied. This drawing in of water would compete with the movement of water from the core part of the model and thus obscuring effects the model was designed to study. The sealed boundary condition forced fluid to flow according to gradients developed as result of the applied stress and not as a function of a drainage pressure applied as a boundary condition.

Relaxation experiments, similar to those performed by Haut et al. (1995), were simulated with the model with an initial, suddenly applied, 3% strain followed by a 180s period of constant deformation. Constant strain-rate tensile tests, also similar to those in Haut et al. (1995), were simulated using constant strain rates of 0.5%/s and 50%/s. Cyclic extension tests, similar to those performed by Chen (1995), Chimich et al. (1992),

and Hannifin and Arnoczky (1994), were simulated using a 0.5 cycle per second 4% strain triangular ramp.

Parametric studies were also performed during the simulated relaxation and constant strain rate tests in which moduli, permeability, and voids ratio were varied in both the ring and core portions of the model.

Newton's method with backward time integration was utilized to solve the coupled flow and deformation equations simultaneously. Since pilot studies indicated that shear deformations exceeded 10%, nonlinear deformation terms were included in the analysis.

Due to the unsymmetric nature of the coupled flow equations, the unsymmetric matrix solver was used in all solutions.

#### **RESULTS**

## **Constant Deformation Relaxation:**

In the simulated relaxation experiments the model indicated an initially high reaction force which slowly relaxed to a lower, steady state level (Fig. 2 (a)). The relaxation response was highly sensitive to permeability and water content. Increasing permeability caused the sub-fascicle to relax to the steady state response faster. If k was less than  $1 \times 10^{-19} \text{m}^4/\text{Ns}$ , the relaxation phenomenon was lost in the time frame of the current study (0-180s). If it was greater than  $1 \times 10^{-16}$ , the initial peak in the force was lost. Increased initial water content, reflected by an increase in e<sub>0</sub>, tended to increase the peak force, steady state force and the amount of relaxation. Higher percentages of relaxation resulted when the water content and voids ratio were the same throughout the sub-fascicle, rather than varied between the fibrous ring and the poroelastic core.

The internal pressures predicted during the constant deformation experiments also exhibited a dependence on water content and permeability. During this test the internal pressure within the sub-fascicle was initially high, but decreased to a lower steady state value (Fig. 2 (b)). Pressures central to the sub-fascicle were high, and decreased radially (Fig. 2 (c)). The core portion of the model always experienced a negative dilatation. At steady state the pressures in the model were either positive, slightly negative or close to zero depending on the material properties selected. Combinations of properties which produced large negative pressures in the fibrous ring portion of the model resulted in negative steady state pressures. Increasing e<sub>o</sub> increased the initial internal pressure.

Increasing k increased the rate of pressure decay. Increased ultimate tensile strength of the poroelastic core, P<sub>t</sub>, tended to decrease the peak pressure in the middle of the fascicle. The pressure at each location was constant through the model's length, and the initial pressure resulting in the fibrous ring was always negative.

The deformation of the ring elements was such that the fiber axis became more aligned with increasing axial load causing the element to twist helically (Fig. 3). In addition, the radial deformation during these relaxation tests indicated that the subfascicle's radius decreased slightly as a function of time.

## Cyclic Loading:

During cyclic loading the sub-fascicle's internal pressures followed the applied loading (Fig. 4 (a)). The peak internal pressures were positive, and the pressures when the displacement returned to zero were slightly negative. The peak pressures and axial force varied as a function of the extension, decreasing with increasing numbers of cycles. During

the extension, the pressures at the center of the model were higher than those at the edge (Fig. 4 (b)).

### Tensile Deformation at Varied Rates:

During simulated constant strain rate experiments the sub-fascicle stiffness was dependent on initial water content, as defined by  $e_o$ . As the initial water content was increased, the model's stiffness increased (Fig. 5 (a)). The sub-fascicle's stiffness was also dependent on the values chosen for k. Increasing k caused the stiffness to decrease for  $1 \times 10^{-12} < k < 1 \times 10^{-15} m^4/Ns$ . At low permeability, there was no difference in stiffness due to changes in  $e_o$ . Increasing the various elastic moduli caused the model's stiffness to increase accordingly.

The model's stiffness was dependent on strain rate if  $k>1\times10^{-14} m^4/Ns$  (Fig. 5 (b)). Faster rates of extension produced a stiffer response. Increasing  $P_t$ , or the transverse elastic moduli in the fibrous ring portion, or decreasing the permeability in any part of the model, decreased the sensitivity of stiffness to strain rate.

The force/deformation response of the model was linear for small strains.

#### **DISCUSSION:**

Many of the model's predicted relaxation behaviors were consistent with experimentally-observed tendon and ligament data. The peak force, rate of relaxation and relaxed force exhibited by the model depended on e<sub>o</sub>, the initial ratio of water to substrate. When the amount of water in the sub-fascicle decreased, the initial force, steady state force, and the rate of relaxation decreased. This caused the reduced relaxation modulus (slope of the normalized force, logarithm time curve) to decrease. This behavior is

consistent with Haut et al.'s (1995) observations and exhibits the same time varying character as that noted in Lanir et al. (1988) and Chimich et al.'s (1992) work. The peak force and rate of relaxation shown in the model also depended on k. Parametric studies demonstrated that the ability of the elastic part of the model to take on water was primarily governed by the permeability parameter. In the current model the core portion exhibited dilatation and water flow behaviors hypothesized to exist in the matrix of a subfascicle. The ring portion loaded the matrix in a twisting manner, which we hypothesize is similar to the effect produced by collagen fibrils within the sub-fascicle. In this model the ring also acted as a sink for water. Water moved out of the nonlinear poroelastic core material into the ring portion of the model similar to how we hypothesize it would move out of the real sub-fascicle, and ultimately out of the entire structure. Water motion out of tissues has been observed experimentally (Chimich et al., 1992; Lanir et al., 1988; Hannifin and Arnoczky, 1994). The water motion phenomena in the model was readily seen in the simulated relaxation, where water initially trapped in the compressed poroelastic core of the model, diffused out into the fibrous ring portion thus softening the poroelastic portion and decreasing the overall tensile stress.

The model's pressure profile was also similar to that in a recently reported experiment which indicated that the internal pressure developed in a rabbit patellar tendon during cyclic loading is positive and follows the loading profile (Chen et al., 1995). The model also predicted a concurrent decrease in the diameter of the sub-fascicle during the test. This phenomenon was consistent with experimental observations in rat tail tendon (Lanir et al., 1988) and in rat MCL (Thielke et al. 1995). It has been suggested that this

decreasing cross sectional area indicates compaction and water motion out of the interfibrillar matrix (Hannifin and Arnoczky, 1994; Lanir et al., 1988; Thielke et al., 1995). These phenomena are consistent with observations made in the current parametric studies using the poroelastic model.

During cyclic extension, the model's internal pressures were positive on extension, negative on the return to zero displacement, and the peak pressures and forces decreased with increasing number of cycles. This behavior was similar to Chen et al.'s (1995) experimental pressure measurements in the rabbit patellar tendon. This pressure pattern was also consistent with water motion radially out of the poroelastic portion (into the elastic portion) during extension and back in when the displacement returned to zero. These predictions suggest that fluids tend to leave the sub-fascicle during cyclic loading, consistent with recent experimental findings (Hannifin and Arnoczky, 1994; Lanir et al., 1988). The predicted relaxation during cyclic loading was similar to that observed in ligaments (Chimich et al., 1992).

In Chen et al.'s (1995) experiment, the magnitude of the measured pressure was significantly less than the tensile stress, suggesting a lack of load sharing between the fibers and matrix. In the current study, cyclic loading tests showed the peak predicted pressures in the matrix portion of the sub-fascicle were similar to the average stress (average force/area). Thus, the current model suggested there was load sharing. It is possible that Chen's pressure probe provided a leakage path for water. On the other hand, the model describes a very small unit of the tendon and predicted pressures might not reflect gross pressures measured in the tendon. This difference might also be attributed to

possible differences in the water content of rabbit patellar tendon and human tendon. As the pressures predicted in the model also depend on the voids ratio and permeability, additional parameter studies performed under cyclic loading may provide more insight into these experimentally observed behaviors.

In simulated constant rate of deformation tensile tests (10%/s) the sub-fascicle's stiffness increased when the voids ratio (water fraction) increased. Similar behavior has been noted in tendons when the test environment was used to alter the water content (Haut and Powlison, 1990, Haut et al., 1995). This behavior resulted in the model when the voids ratio was increased in either both the elastic and poroelastic parts or just in the poroelastic part. Variation of the initial amount of water in the elastic part does not in itself change the stiffness of the elastic portion. However, anything that alters the ability of the elastic portion to accept water from the poroelastic portion effected the stiffness of the poroelastic portion and thus the stiffness of the total model. The sub-fascicle stiffness also exhibited a dependence on permeability. Increasing the permeability tended to make the model more compliant. Although no direct evidence exists documenting the permeability of tendons, previously Haut and Powlison attributed the increased compliance of  $\gamma$ -irradiated tendons to increased permeability. At lower permeability, changes in the voids ratio did not effect the sub-fascicle stiffness. This suggests that the water acts as a stiffening agent only when the permeability of the tendon is sufficiently high. The force-deformation curve provided by the model was linear, unlike the forcedeformation curves for a gross tendon or groups of fascicles (Butler, et. al 1986). This discrepancy is attributed to the simplified fibril morphology incorporated in the model.

Factors such as variation of fibril orientation through the sub-fascicle thickness, the undulation of fibrils, sub-fascicle recruitment and sub-fascicle interactions were not examined in the current study, but should be addressed in future models.

When the rate of deformation was changed from 10%s to other rates of extension the model exhibited rate sensitivity. During fast extension (50%/s) the model predicted a stiffer response than that during slow extension (.5%/s), similar to Haut et al. (1995). This behavior was highly dependent on the tissue permeability, with no rate dependence exhibited at  $k<1\times10^{-14}$ m<sup>4</sup>/Ns. This suggests that the water motion in the tissue might cause rate sensitivity when the permeability of the tendon is sufficiently high.

Deformation in the model's outer ring was consistent with collagen fibrils reorienting into a tighter, more axially aligned helix. This deformation produced a wringing
effect in the sub-fascicle, compressing the hydrophilic gel portion to generate positive
pressure. This particular deformation may then be very important in producing many of
the observed mechanical behaviors particular to tendons and ligaments.

Although the model exhibits behaviors consistent with many experimentally observed behaviors, several problems remain which must be addressed in its further development. The distribution and morphology of collagen fibrils in the sub-fascicle have been simulated by the use of a fibrous ring attached to the outside of the core, matrix material. As the ring material is somewhat compressible, it experienced a positive dilatation under tensile load leading to negative negative pressures in the ring. Yet, on the other hand, the model exhibited a wringing out of the core and thus water motion out of the sub-fascicle. We hypothesize that water flow effects exhibited by the core of our

model will occur throughout a real sub-fascicle as real fibrils experience rigid body motion motion as they align along the loading axis. Improvements such as distributing elements throughout the matrix to represent fibrils, might be a more realistic microstructural model of the sub-fascicle. Another limitation of the current model is that the thin connective tissue sheaths which separate sub-fascicles have not been included in the model. However, we hypothesize that these thin sheaths do not play an active role in the tensile response of tendon and ligament, rather they act to bind sub-fascicles and fascicles into the gross structure. The model's tensile response was compared qualitatively to that of whole tendon or ligament, however interactions between subfascicles and extra-fascicular materials must be evaluated experimentally before a whole tendon model can be developed. Strategies to utilize the model to quantitatively describe whole tendon and ligament behavior remain to be explored. Appropriate material properties must also be obtained. The bulk modulus (K) of the interstitial fluid, the fascicle's elastic modulus, the angle of fibril orientation and other geometric properties need to be measured. Other material properties, such as the transverse elastic moduli and the shear moduli might be assumed, or could be derived based on SEM studies of fibril reorientation during tensile loading with the use of this analytical model. The model also suggests that parameters such as the tissue permeability (k), and voids ratio (e<sub>o</sub>) are extremely important. These parameters might be measured using standard permeability tests and measurements of water content.

The model demonstrates that when structural aspects, i.e. collagen morphology and orientation, and aspects of how collagen interacts with the hydrophilic base matrix

material are taken into account, a reasonable mechanical response results. The sub-fascicle modeled here is similar in form to those found in both the patellar tendon and ACL. Other fascicle morphologies also exist in the ACL and require further study, but the approach taken in modeling this structure may serve as a basis for such a model. We suggest that future improvements in the understanding of ligament and tendon mechanics will necessarily involve the study of microstructure and the measurement of parameters not previously considered. Thus, we propose that analytical models which incorporate tissue water content and microstructural information will be important tools in future research.

#### REFERENCES

- **Abaqus Theory Manual**, Version, 5.4, Hibbitt, Karlsson and Sorenson, Inc. 1994, pp. 4.4.1.
- Belkoff, S. M. and Haut, R.C., 1992, "Microstructurally based model analysis of  $\gamma$  irradiated tendon allografts", J. Othop. Res., Vol. 10, pp. 461-464.
- Best, B. A., Setton, L. A., Guilak, A., Ratcliffe, A., Weidenbaum, M. and Mow, V. C., 1989, "Permeability and compressive stiffness of annulus fibrosus: variation with site and composition," *Trans. Orthop. Res. Soc.*, Vol. 14, p. 354.
- Butler, D.L., Matthew, D.K, and Donald, C.S., 1986, "Comparison of material properties in fascicle-bone units from human patellar tendon and knee ligaments", *J. Biomech.*, Vol. 19, No. 6, pp. 425-432.
- Chen, C., McCabe, R., and Vanderby, R. Jr., 1995, "Two electrokinetic phenomena in rabbit patellar tendon: pressure and voltage," *Bioengineering Conference*. *ASME*, Beaver Creek, Colorado, pp. 31-32.
- Chen, C. T., Vanderby, R., Graf, B. K., and Malkus, D. S., 1993, "Interstitial fluid flow in ligaments and tendons: effects of fibril spacing and fluid properties," *Bioengineering Conference. ASME*, Breckenridge, Colorado, pp. 399-402.
- Chen, C. T. and Vanderby, R., 1994, "3-D finite element analysis to investigate anisotropic permeability for interstitial fluid flow in ligaments and tendons," *Trans. Orthop. Res. Soc.*, p. 643.
- Chimich, D. D., Shrive, N. G., Frank, C. B., Marchuk, L., and Bray, R. C., 1992, "Water content alters viscoelastic behaviour of the normal adolescent rabbit medial collateral ligament," *J. Biomech.*, Vol. 25(8), pp. 831-837.
- Danylchuk, K.D., Finlay, J.B. and Krcek, J.P., 1978, "Microstructural organization of human and bovine cruciate ligaments", Clinical Orthopaedics and Related Research, No. 131, pp. 294-298.
- Hannafin, J. A. and Arnoczky, S. P., 1994, "Effect of cyclic and static tensile loading on the water content and solute diffusion in canine flexor tendons: an in-vitro study," *J. Orthop. Res.*, Vol. 12, pp. 350-356.
- Haut, R.C., 1983, "Correlation between strain-rate-sensitivity in rat tail tendon and tissue glycosaminoglycans," ASME Biomechanics Symposium, pp. 221-224.

- Haut, R. C., 1993, "The mechanical and viscoelastic properties of the anterior cruciate ligament and of ACL fascicles," *The Anterior Cruciate Ligament: Current and Future Concepts*, (Edited by Jackson, D. W., et al.), Raven Press, Ltd., New York.
- Haut, R. C. and Powlison, A. C., 1990, "The effects of test environment and cyclic stretching on the failure properties of human patella tendons," *J. Orthop. Res.*, Vol. 8, pp. 532-540.
- Haut, T. L., Jayaraman, R.C., and Haut, R.C., 1995,"Water content determines the strain rate sensitive stiffness of human patellar tendon", Advances in Bioengineering, BED-Vol 31, pp. 61-62.
- Kastelic, J., Galeski, A. and Baer, E., 1978, "The multicomposite structure of tendon", *Connective Tissue Res.*, Vol 6, pp.11-23.
- Kwan, M.K., and Woo, S. L-Y., 1989, "A structural model to describe the nonlinear stress-strain behavior for parallel-fibered collagenous tissues", *J. Biomech. Eng.*, Vol. 111, pp.361-363.
- Laible, J. P., Pflaster, D., Simon, B. R., Krag, M. H., Pope, M., Haugh, L. D., 1994, "A dynamic material parameter estimation procedure for soft tissue using a poroelastic finite element model," *J. Biomech. Eng.*, Vol. 116(1), pp. 19-29.
- Lanir, Y., 1978, "Structure--strength relations in mammalian tendon," *Biophysical J.*, Vol. 24, pp. 541-554.
- Lanir, Y., Saland, E. L., and Foux, A., 1988, "Physico-chemical and microstructural changes in collagen fiber bundles following stretch in-vitro," *Biorheology J.*, Vol. 25(4), pp. 591-604.
- Mow, V. C., Holmes, M. H., and Lai, W. M., 1984, "Fluid transport and mechanical properties of articular cartilage: a review," *J. Biomech.*, Vol. 17(5), pp. 377-394.
- Mow, V. C., and Hayes, W. C., 1991, *Basic Orthopaedic Biomechanics*, Raven Press, Ltd., New York, New York, pp. 143-243.
- Simbeya, K. W., Shrive, N. G., Frank, C. B., and Matyas, J. R., 1993, "A micro-mechanical finite element model of the rabbit medial collateral ligament," *Recent Advances in Computer Methods in Biomechanics and Biomedical Engineering*, (Edited by Middleton, J., Pande, G., and Williams, K.), pp. 240-249, Books and Journals Ltd, Swansea.

- Suh, J., and Spilker, R. L., 1991, "Indentation analysis of biphasic articular cartilage: nonlinear phenomena under finite deformation," *J. Biomech. Eng.*, Vol. 116, pp. 1-9.
- Thielke, R.J., Vanderby, R. Jr., and Grood, E. S., 1995, "Volumetric changes in ligaments under tension," *Bioengineering Conference*. *ASME*, Breckenridge, Colorado. pp.197-198.
- Viidik, A. 1990, "Structure and function of normal and healing tendons and ligaments" in **Biomechanics of Diarthrodial Joints Vol I**, (Edited by Mow, V.C., Ratcliffe, A., and Woo, S. L-Y.), p. 3-12, Springer-Verlag, N.Y.
- Wilson, A. N., Frank, C. B., Shrive, N. G., 1994, "The behaviour of water in the rabbit medial collateral ligament," *Second World Congress of Biomechanics*, (Edited by Blankevoort, L., and Kooloos, J. G. M.), p. 226b, Amsterdam, The Netherlands.
- Yahia, L. H., and Drouin, G., 1989, "Microscopical investigation of canine anterior cruciate ligament and patellar tendon: collagen fascicle morphology and architecture," *J. Orthop. Res.*, Vol. 7, pp. 243-251.
- Yahia, L. H., and Drouin, G., 1988, "Collagen structure in human anterior cruciate ligament and patellar tendon," J. Mat. Sci., Vol. 23, pp. 3750-3755.
- Yamamoto, E., Kozaburo, H., and Yamamoto, N., 1995, "Mechanical properties of collagen fascicles of stress-shielded patellar tendons in the rabbit," *Bioengineering Conference*, pp. 199-200, Beaver Creek, Colorado.
- Zienkiewicz, O.C. and Naylor, D.J., 1972, "The adaptation of critical state solid mechanics theory for use in finite elements", **Stress-Strain Behavior of Soils**, Parry, R.H.G. ed., Foulis and Co, , pp. 537-543.

**Table 1 Material Coefficients** 

Elastic Moduli	Value	Poisson's Ratio	Value	Shear Moduli	Value
E1	30MPa	v12	.01	G1	.5 MPa
E2	600MPa	v23	.25	G2	.5 MPa
E3	30MPa	v13	.25	G3	.5 MPa

Figure legends:

Fig. 1 Conceptualization of the geometry of a fascicle used as the basis of the finite element model.

Fig. 2 (a) The effects of voids ratio and permeability on stress relaxation in a constant deformation (3% strain) test. The forces were normalized by the peak force in the  $e_o$ =2.33, k=1.45x10<sup>-19</sup>m<sup>4</sup>/Ns load case. For each load case, k and  $e_o$  were constant throughout the model. The initial normalized force in the load cases  $e_o$ =1, k=1.45x10<sup>-19</sup> m<sup>4</sup>/Ns and 5.45x10<sup>-18</sup> m<sup>4</sup>/Ns was 0.95. The material constants for the outer ring are given in Table 1. The material constants in the poroelastic matrix were v=0.45,  $\kappa$ =0.047, and  $P_t$ =3.4x10<sup>5</sup> Pa.

Fig. 2 (b) The effects of voids ratio and permeability on fascicle internal pressure during stress relaxation a constant deformation (3% strain) test. The pressures were normalized by the peak for in the  $e_0=2.33$ ,  $k=1.45\times10^{-19}$  m<sup>4</sup>/Ns load case.

Fig. 2 (c) The variation of pressure in the radial direction during the  $e_o=1.0$  and  $k=1.45\times10^{-19}$  m<sup>4</sup>/Ns load case.

Fig. 3 Deformation of the model at 3% strain (magnified x 10) during a constant deformation test. The elements shear to the left, bringing the fiber axis (initially oriented at 62° to the right) more directly in line with the tensile load.

Fig. 4 (a) Fascicle internal pressures during cyclic deformation. Pressures were normalized by the peak positive pressure. Orthotropic material properties are given in Table 1,  $e_o=0.01$  and  $k=1.45\times10^{-19} \text{m}^4/\text{Ns}$ . Poroelastic properties were  $e_o=1.0$ ,  $k=1.45\times10^{-14} \text{m}^4/\text{Ns}$ , v=0.49,  $P_t=3.4\times10^4$  Pa, and  $\kappa=0.047$ .

Fig. 4 (b) Fascicle pressures as a function of radial distance at the peak of the 1st cycle.

Fig. 5 (a) The effect of voids ratio and permeability during constant strain rate tensile deformation (10%/s). Forces were normalized by the force at 4.8% strain in the  $e_o$ =2.33, k=1.45x10<sup>-19</sup>m<sup>4</sup>/Ns load case. The lines for the load cases  $e_o$ =1, k=1.45x10<sup>-19</sup> m<sup>4</sup>/Ns and  $e_o$ =2.33, k=1.45x10<sup>-19</sup> m<sup>4</sup>/Ns are on top of one another. The material constants in the ring portion of the model are given in Table 1. The material constants in the poroelastic matrix were v=0.45,  $\kappa$ =0.047, and  $P_t$ =3.4x10<sup>4</sup> Pa.

Fig. 5 (b) The effect of strain rate on the tensile response of the fascicle. For both tests  $e_o=2.33$  and  $k=1.45\times10^{-17} \text{m}^4/\text{Ns}$ . The material constants in the ring portion of the model are given in Table 1. The material constants in the poroelastic matrix were v=0.45,  $\kappa=0.047$ , and  $P_i=3.4\times10^4$  Pa.

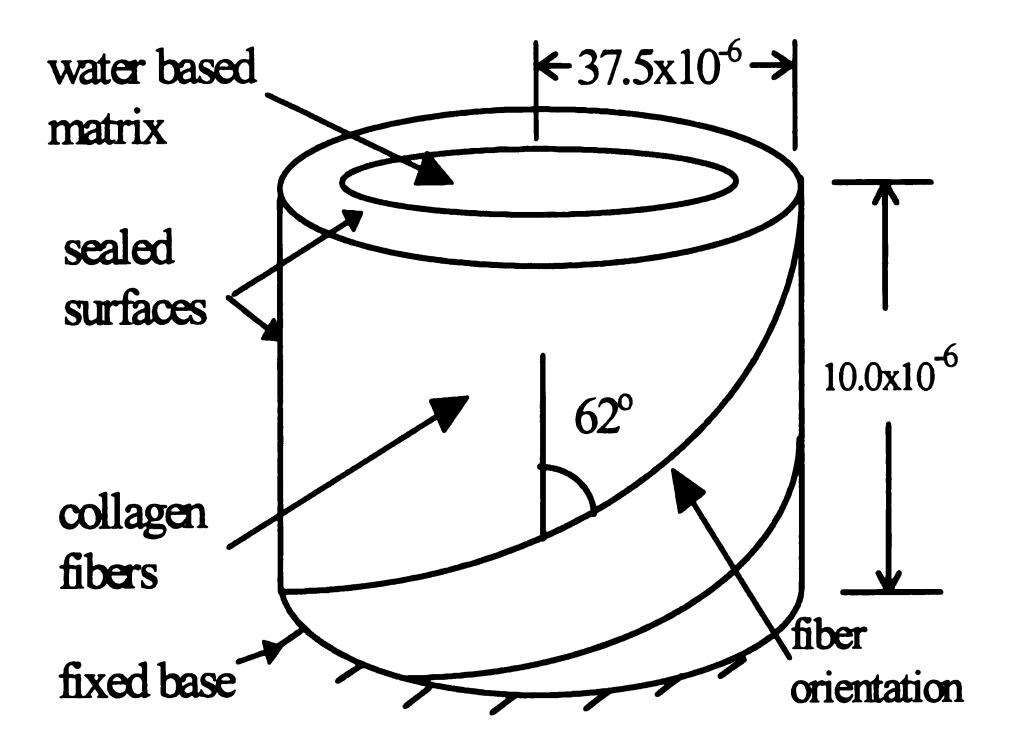
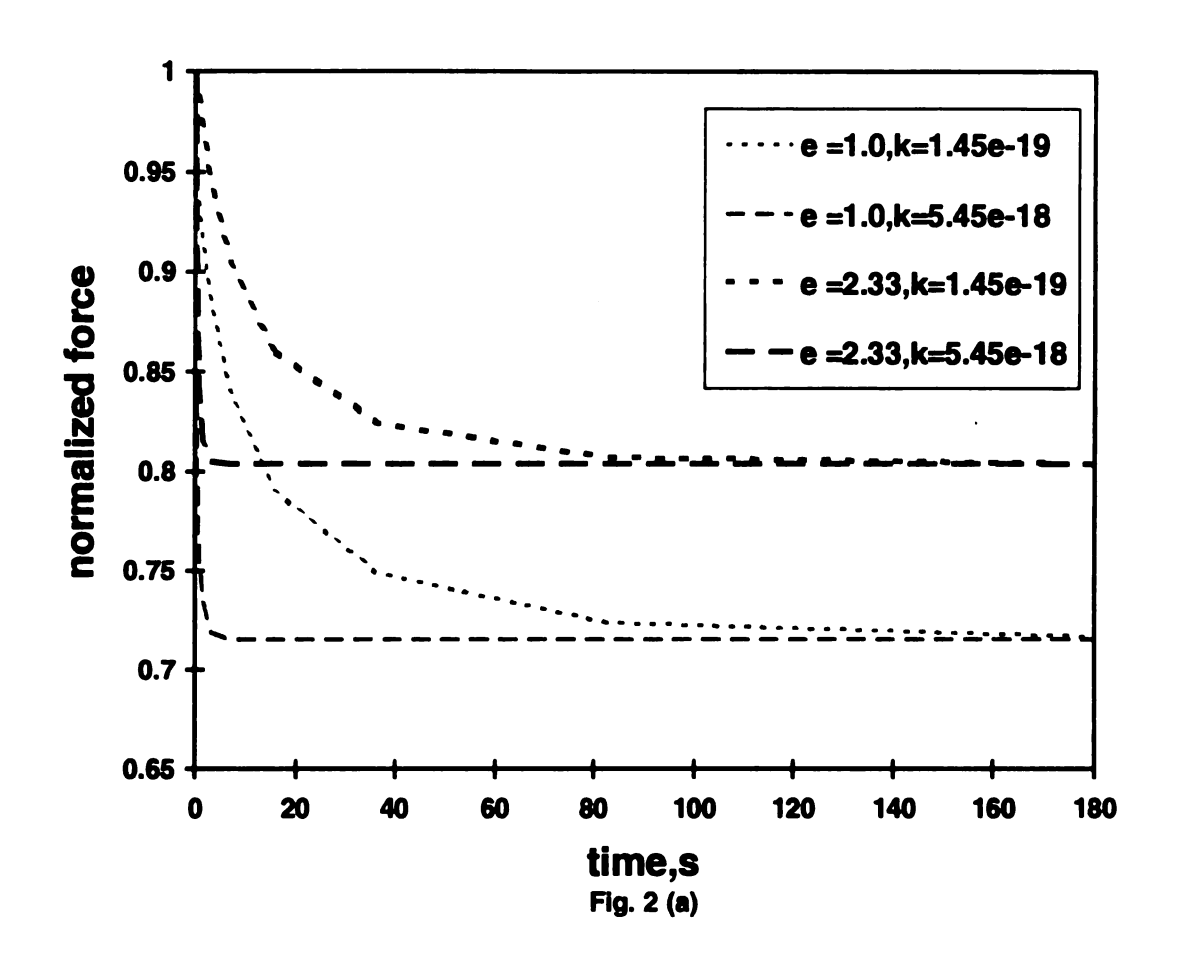
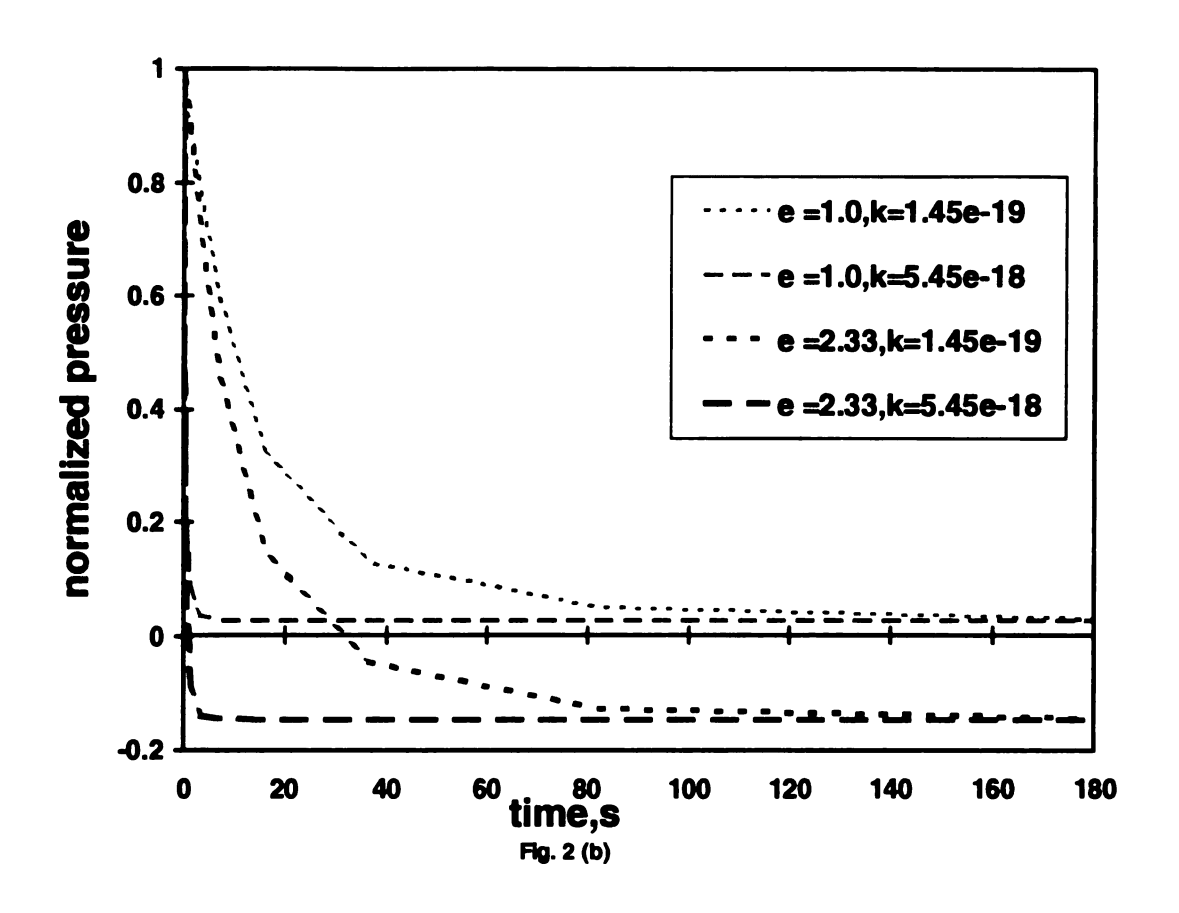
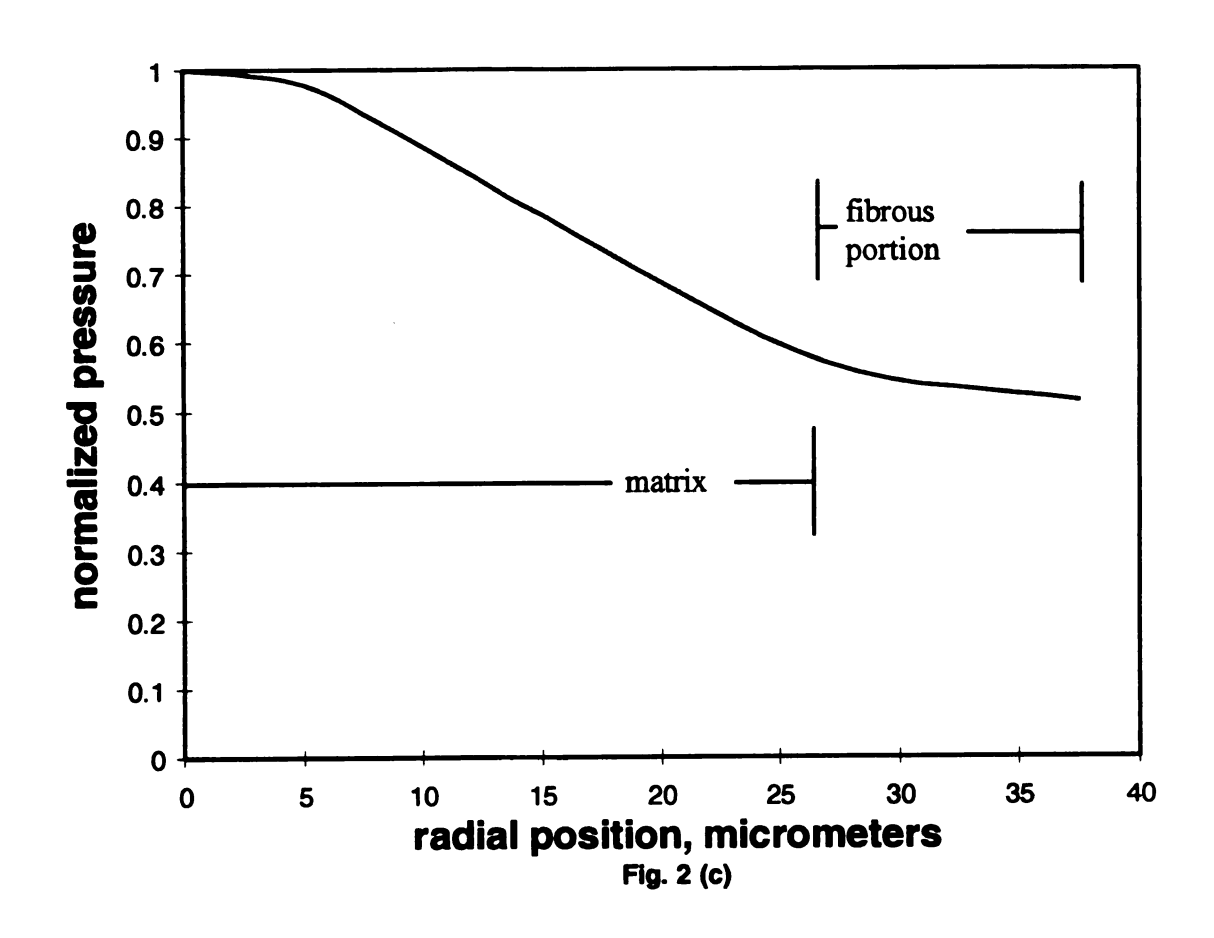
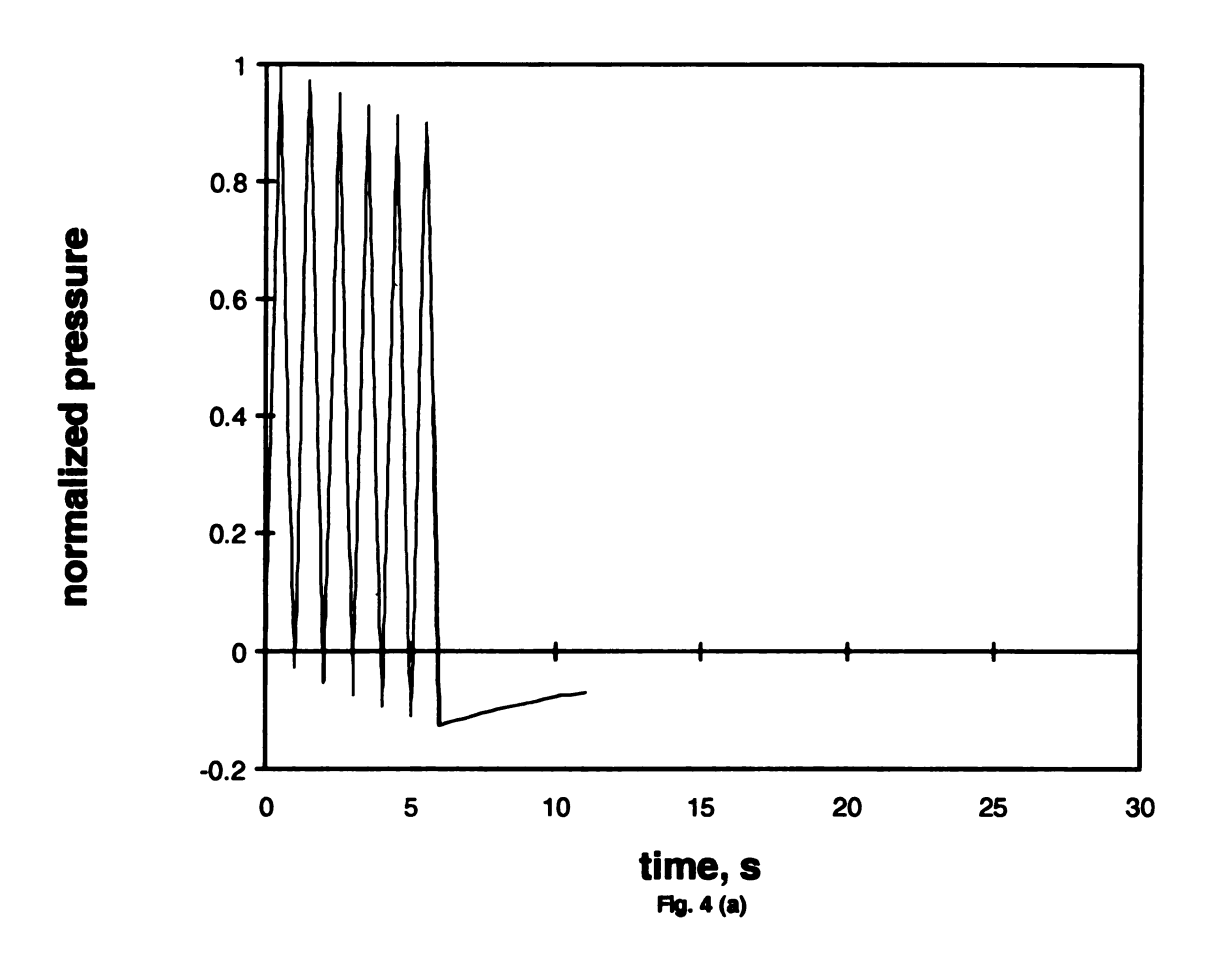


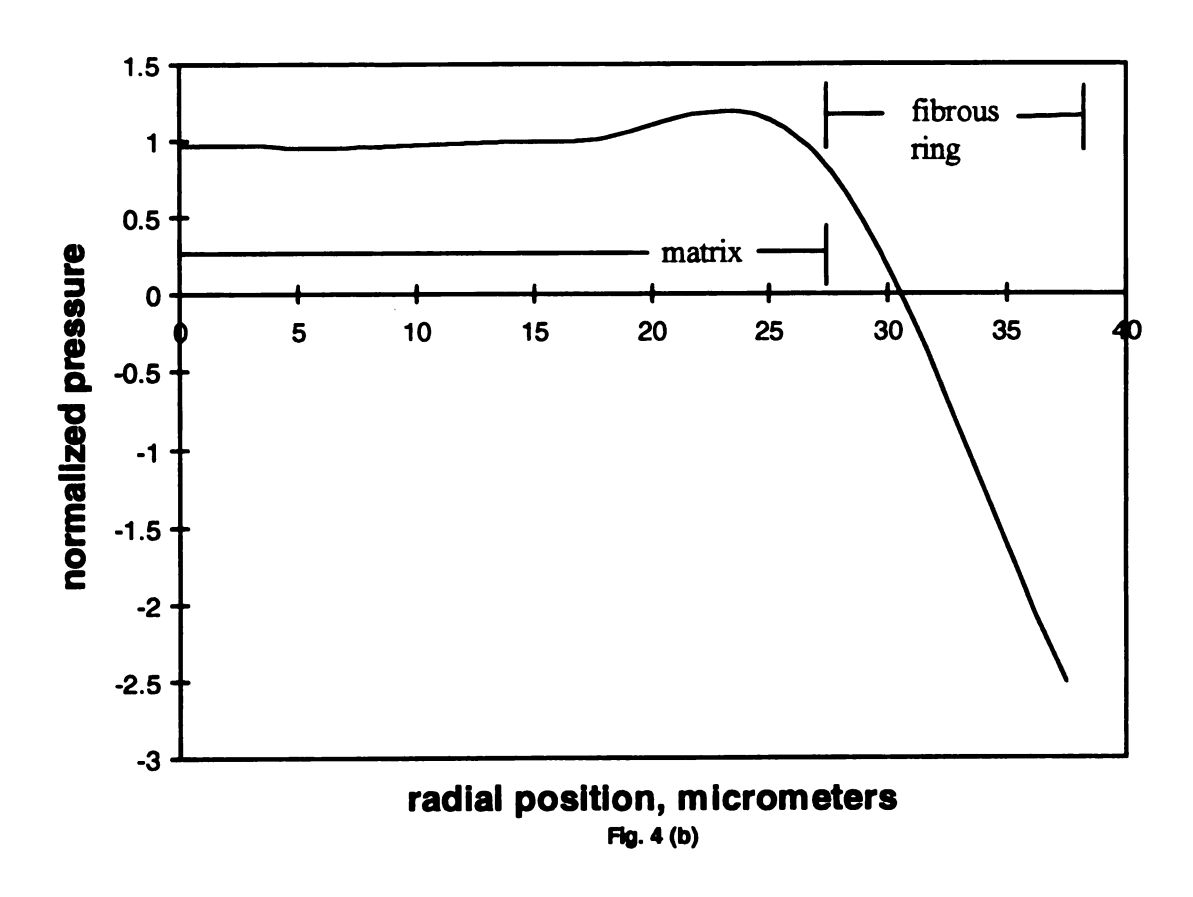
Figure 1

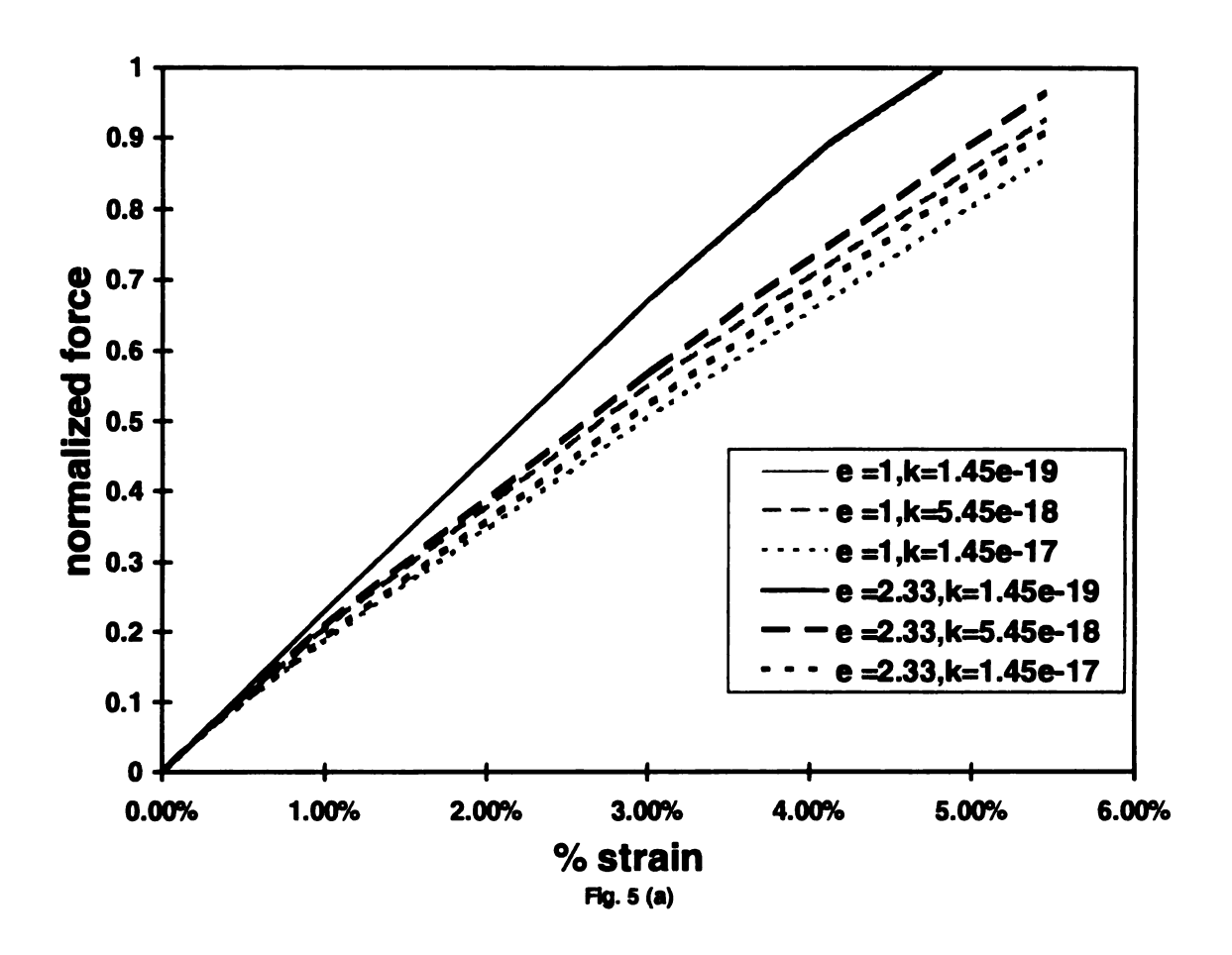


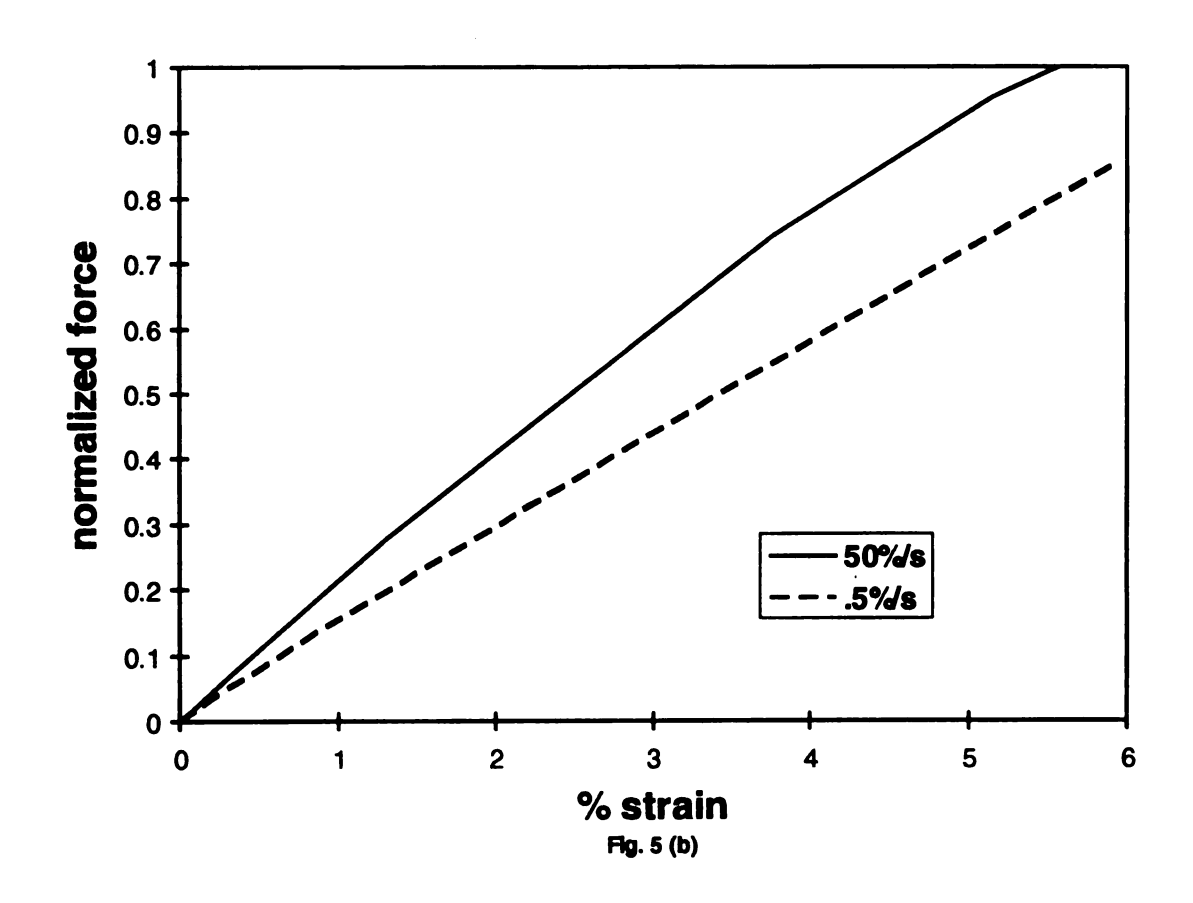












# Chapter 3:

## A Microstructural Poroelastic Model For Patellar Tendon

Theresa Atkinson, Roger Haut, and Nicholas Altiero

#### **ABSTRACT:**

In order to study potential influences of water content on tendon tensile response a finite element model of a subfascicle (a microstructural element of tendon) was constructed. Although this model exhibited mechanical responses which were similar to those observed in whole tendon and ligament, it was preliminary in nature and as such contained some undesirable compromises. These compromises related to boundary conditions imposed as a result of the simplification of the subfascicular geometry. In the current study a more detailed description of the subfascicular microstructure was encorporated in a model. This model was shown to exhibit reasonable relaxation and tensile responses as well as a realistic pressure profile throughout the subfasicle.

### **INTRODUCTION:**

Predicting and measuring the mechanical response of tendon is important in the development and assessment of various orthopaedic reconstruction techniques (which frequently utilize these tissues as graft materials). Recent experimental studies (Haut et al., 1995, Haut and Powlison, 1990) indicate that water, which comprises approximately 60-70% of the total weight of the tendon, might play a significant role in dictating the tensile response of ligaments and tendon. Several studies performed by other researchers (Hannifin and Arnoczky, 1994, Lanir et al, 1995, Thielke et al, 1995) suggest that fluids are exuded from these tissues and internal pressures are positive under tensile loads. Predicting how variations in water content might influence tendon mechanical response is desirable given the variation in hydrating methods and solutions utilized by investigators in the evaluation of tendon and ligament response. The effect of hydration on tensile

behavior of tendon was recently investigated with a finite element model of a patellar tendon subfascicle (Atkinson et al., 1997). The model exhibited stress relaxation and strain rate sensitivity which were dependent on the level of hydration, and were qualitatively similar to those reported by other researchers. There were, however, several aspects of this model which were undesirable: a sealed boundary condition was applied to the model periphery, the "matrix" portion of the model alone reflected pressures in the subfascicle, and the tensile response of the model was linear. In order to address the limitations of this early model, a new, more microstructually accurate model has been developed.

## **METHODS:**

The original model was based on Yahia and Drouin's (1988) description of the microstucture of tendon and ligament wherein he identifies a helical arrangement of collagen in the sub-fascicular structures present in PT and the ACL. Jozsa et al (1991) also describes a fibre (subfascicle) composed of helically oriented collagen fibres as the basic unit of tendon found in various human tendons, i.e.: Achilles, quadriceps, and extensor pollicis longus. We idealized the helically oriented collagen fibers as rings of fibers separated by matrix (Figure 1).

In the original model the collagen fiber effects were contained in a single ring of fibers located on the periphery of the model. In the current model the fiber effect was modeled with a distribution of concentric rings throughout the model.

In order to incorporate both solid and fluid effects into the mechanical response of the model, poroelastic material was utilized, which has the same form as the linear biphasic model when linear elastic behavior is assumed for the solid portion. An orthotropic

poroelastic material was utilized to simulate oriented fibers within 8 fibrous rings, where the  $E_2$  direction represented the fiber modulus. Material properties were selected to achieve a material which was strongest in the fiber direction, weaker in the orthogonal directions and weakest in shear ( $E_1$ = $E_3$ = 300MPa,  $E_2$ = 600MPa,  $G_{1,2,3}$ =3MPa) in order to achieve a twisting effect consistent with tightening of helically wound fibers. Poisson's ratios for the orthotropic materials were selected to be consistent with the elastic moduli. The fiber orientation angle within each ring varied from 5° from vertical at the innermost ring to 25° at the outermost. The matrix material was assumed to be isotropic poroelastic (E=2MPa, v=0.1).

As the fascicle is a reasonably long continuous structure, a 3 dimensional slice from the middle was modeled. The top and bottom surfaces of the model were sealed to represent conditions in a long fiber. The outer boundary of the model was assumed to be perfectly draining. The bottom plane of the model was constrained to in plane motions with 4, nodes 90° apart, additionally constrained to radial motion. The top plane was assumed to deform uniformly in the z direction with r and  $\theta$  free.

The model was utilized to simulate a relaxation experiment with 3% strain induced in 1ms and tensile tests at strain rates of .1%/s and 10%/s.

## **RESULTS:**

Positive pressures throughout the model indicated a negative dilatation during tensile stretch (Fig. 2). The model's relaxation resulted from water exudation (Fig. 3). Water moved radially from the center to the periphery. The nonlinear tensile response resulted from reorientation of the simulated fibers with the load (Fig. 4).

## **DISCUSSION:**

Incorporation of the microstructural aspects of tendon structure, such as fiber organization, in poroelastic structures can lead to models which exhibit realistic tensile behaviors. These new mathematical models for parallel fibered connective tissues may prove especially useful in understanding the roles of fiber organization and tissue hydration during various states of healing. The new models will, however, require further validation studies.

## **REFERENCES:**

- Atkinson, T.S., Haut, R.C. and Altiero, N.J. (1997) A poroelastic model that predicts some phenomenological responses of ligaments and tendons. *J. Biomech. Eng.* 119, 400-405.
- Hannafin, J. A. and Arnoczky, S. P., 1994, "Effect of cyclic and static tensile loading on the water content and solute diffusion in canine flexor tendons: an in-vitro study," *J. Orthop. Res.*, Vol. 12, pp. 350-356.
- Haut, T.L., and Haut, R.C. (1997) The state of tissue hydration determines the strain-rate-sensitive stiffness of human patellar tendon. J. Biomech. 30, 79-82.
- Haut, R. C. and Powlison, A. C., 1990, "The effects of test environment and cyclic stretching on the failure properties of human patella tendons," *J. Orthop. Res.*, Vol. 8, pp. 532-540.
- Jozsa, L., Kannus, P., Balin, J.B., Reffy, A., 1991, Three-Dimensional Ultrastructure of Human Tendons, *Acta Anat*, Vol. 142, pp. 306-312, 1991.
- Lanir, Y., 1978, "Structure--strength relations in mammalian tendon," *Biophysical J.*, Vol. 24, pp. 541-554.
- Lanir, Y., Saland, E. L., and Foux, A., 1988, "Physico-chemical and microstructural changes in collagen fiber bundles following stretch in-vitro," *Biorheology J.*, Vol. 25(4), pp. 591-604.
- Thielke, R.J., Vanderby, R. Jr., and Grood, E.S. (1995) Volumetric changes in ligaments under tension. In *Proceedings of the 1995 Bioengineering Conference*. Breckenridge, Colorado.
- Yahia, L. H., and Drouin, G. (1988) Collagen structure in human anterior cruciate ligament and patellar tendon. J. Mat. Sci. 23, 3750-3755.

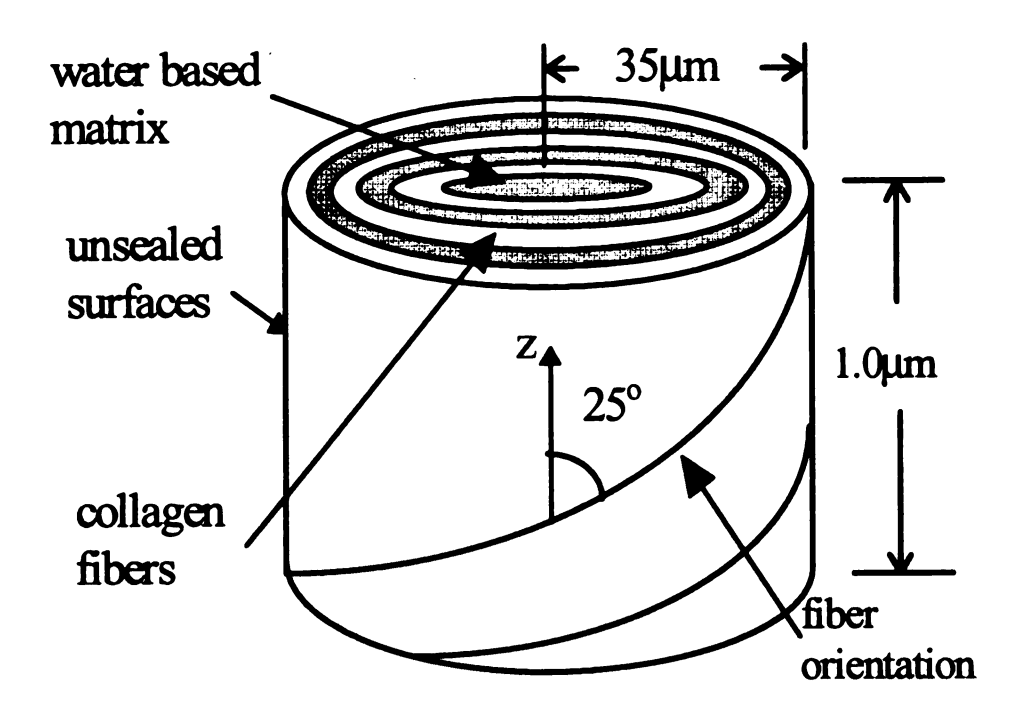


Figure 1

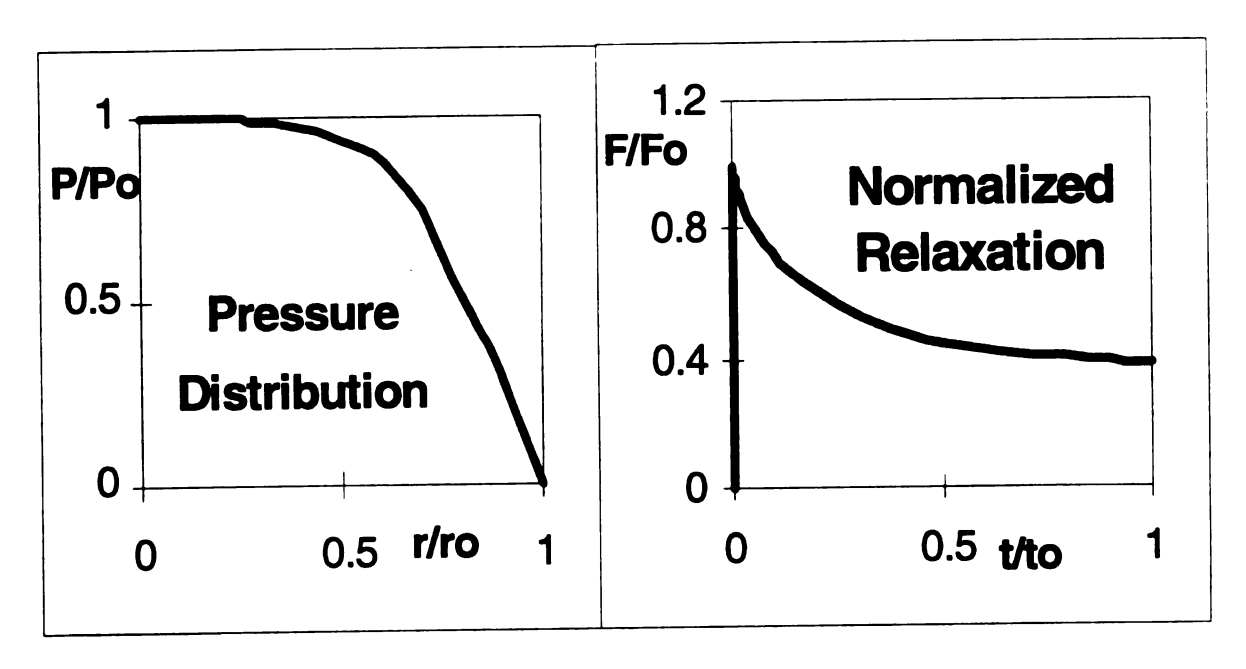


Figure 2 Figure 3

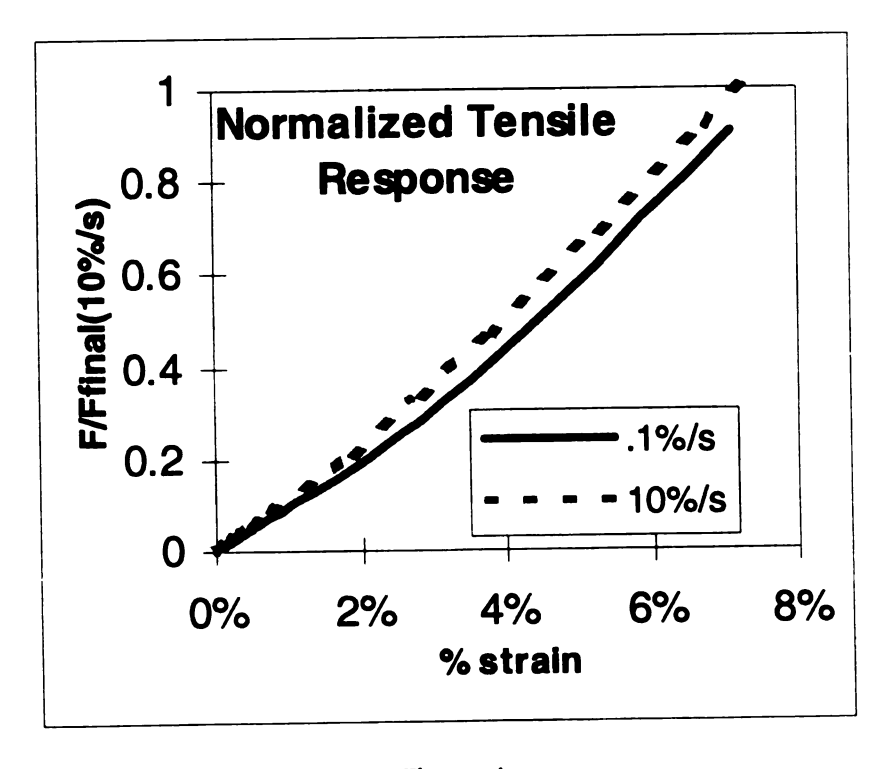


Figure 4

## Chapter 4:

The Tensile and Stress Relaxation Responses of Human Patellar Tendon Varies with Specimen Cross Sectional Area

Theresa S. Atkinson, Benjamin Ewers and Roger C. Haut

## ABSTRACT:

In order to provide insight into the mechanical response of the collagen fascicle structures in tendon, a series of constant strain rate and constant deformation, stress relaxation mechanical tests were performed on human patellar tendon specimens of various sizes. These data described the stress relaxation and constant strain rate tensile responses as a function of cross sectional area and water content. The experimental data suggested that small portions of tendon exhibit a higher tensile modulus, a slower rate of relaxation and a lower amount of relaxation in comparison to larger specimens from the same location in the same tendon. The variation of the mechanical response with respect to specimen cross sectional area was nonlinear. These data suggest that the structural level present in a specimen has a strong influence on its tensile and stress relaxation responses.

## INTRODUCTION:

Most currently available tendon and ligament models consider the tissue to be entirely composed of collagen (Belkoff and Haut, 1992, Hurschler *et al.*, 1997, Kwan and Woo, 1989, Stouffer *et al.*, 1985,) and utilize a distribution function to describe the recruitment of collagen and capture the influence of the collagen structure on the tensile response (Belkoff and Haut, 1992, Hurschler *et al.*, 1997, Kwan and Woo, 1989). However, the collagen in tendon has been described as being arranged in subfascicles and fascicles (collections of subfascicles) which are enclosed by a connective tissue sheaths (Yahia and Drouin, 1988). Danylchuk (1978) describes the collagen fasciculi as that portion of tendon responsible for its tensile strength. Kastelic (1980) modeled the collagen fascicle and suggested that the nonlinear tensile response of tendon might arise from collagen recruitment within the fascicle.

More recently, the fluid present in these tissues has been shown to contribute to their mechanical responses (Chen et al., 1995, Chen et al., 1994, Chen et al., 1993, Chimich et al, 1992, Haut and Haut, 1997, Haut and Powlison, 1990, Thielke et al, 1995). Recent efforts have been made to improve the characterization of these tissues to take the influence of fluid into account (Atkinson et al., 1997, Chen and Vanderby, 1997, Wilson et al., 1994). Atkinson et al. (1997) modeled the collagen subfascicle. This model achieved stress relaxation and strain rate sensitivity via interaction between the subfascicle's collagen fiber structure and an internal hydrated matrix. The model response was qualitatively similar to that reported for whole tendon and ligament.

Previous experimental studies have suggested that the tensile load/deformation response of small portions of tendon is qualitatively similar to that of whole tendon (Butler et al., 1986, Stouffer et al., 1985). These experiments, however, do not describe how the properties of small portions of tendon relate to those of larger segments in the same subject, nor do they document time dependent phenomena such as stress relaxation behavior. Currently, the mechanical behavior of the microstructural elements of tendon, i.e. fascicles and subfascicles, is not well defined and it is unclear how the mechanical response of whole tendon might be attributed to the collective responses of these structures.

In the current study a series of mechanical tests were performed in which quarters of human patellar tendons were sequentially sectioned. The tests were designed to describe both collagen recruitment, via a constant strain rate test, and the time dependent stress relaxation response of specimens harvested from a common location within the same donor. The objectives of these tests were to determine whether the responses of small portions of tendons, which were composed of several subfascicles, were qualitatively similar to those of whole tendon and to identify a relationship between mechanical behaviors of the small and large portions of tendon within the same subject. We hypothesized that the small portions of tendon would behave qualitatively like whole tendon, exhibiting a nonlinear stress strain response and stress relaxation. We also hypothesized that the whole tendon response might be described by linear superposition of the responses of the smallest pieces of tendon.

### **METHODS:**

All testing was performed using four pairs of human cadaver knees obtained from the Michigan Tissue Bank (Table 1). Specimens were maintained at -20° C until the day prior to testing, when they were thawed in room temperature 0.1 M phosphate buffered saline (PBS), pH 7.2, in preparation for dissection. All soft tissue structures, excluding the patellar tendon, were removed from the patellar and tibial bone blocks. The paratenon and fat pad were removed from the tendon surface. The patellar tendons were separated into quarters with bone blocks maintained at each end (Figure 1). Six specimens were selected from the quarters: one from each cadaver and an additional specimen from cadavers 2 and 3 (Table 1). The remaining tissue was returned to -20°C storage. The specimens were inspected under a dissecting microscope and damaged portions were removed. At all times the specimens were kept moist with a spray of 0.1M PBS. Specimens were potted in grips using room temperature curing epoxy. The cross sectional area of each specimen was measured at 3 locations using a constant pressure area micrometer (Butler et al., 1983). The length of each piece was measured from bone to bone at 3 locations. The specimens were then stored overnight at -4 C. The following day the specimens were equilibrated at least 60 minutes at room temperature in distilled water. This bath was selected to increase the tendon's hydration and thereby enhance the tissue's hydration dependent response (Haut and Haut, 1997). The tissues were mounted for tests in a servohydraulic test machine (Instron model 1331) in a vertical orientation with the patellar bone block attached to a 100 lb load cell. The specimen was positioned such that it was axially

aligned between the patellar and tibial bone blocks. The specimen was immersed in a 37° C distilled water bath and allowed to equilibrate, while slack, for 5 minutes. A small preload was applied (2N) and the specimen alignment was visually verified. A constant strain (2%) relaxation experiment was then conducted. The peak strain was achieved at a cross head displacement rate of 123 mm/s (the maximum displacement rate of the equipment) and was held constant for 180s while force data was gathered at 15 Hz. Immediately following relaxation, the specimen was returned to slack for 2s, then subjected to a subfailure tensile test (peak strain of 5%) at a grip-to-grip strain rate of 1%/s (sample rate 100 Hz).

Following the tensile test the specimen was returned to slack, the bath was drained and a portion of the specimen was carefully resected (approximately 1/4 of the cross section). This resected portion was gently patted with gauze to remove excess fluid, then weighed on a digital scale (Sartorius, model R160D) to determine its wet weight. The cross sectional area of this portion was determined using the constant pressure area micrometer. The remaining, intact piece of tendon was removed from the test fixture and allowed to re-equilibrate in a distilled water bath for at least 30 minutes. After re-equilibration the specimen was again mounted in the test fixture and retested following the protocol described above. This process was repeated (except that for very small specimens the preload was 0.2N) until it was not physically possible to harvest a smaller portion of the tendon.

Following the mechanical testing each piece of each specimen was dried in an oven and the dry weight determined. The total wet weight of the specimen at each level of

dissection was then determined by adding the wet weights of the pieces that made up the specimen. The total dry weight was similarly obtained using the dry weights. The percent of water at each level of dissection was assumed to be 1- total dry/wet weight.

As it is possible that the serial sectioning protocol used in the first series of tests may have induced some artifact due to repeated testing, a second series of experiments was performed to verify the trends observed in the first series. The specimens in the second series were those which had been previously set aside and returned to the freezer during preparation for the first series of tests (Table 1). One quarter sized specimen was selected from each cadaver to serve as the "large" sized specimen. Two small specimens were harvested to help insure that at least one of the specimens would be able to complete the test protocol. As it has been previously reported that the mechanical response of human patellar tendon varies spatially across the structure (Chun et al., 1989), the "small" specimens were harvested from locations consistent with those of the contralateral "large" specimen (Figure 1). The specimens' cross sectional areas and lengths were determined as described in the first series of experiments. The specimens were potted and mounted as described earlier. In these tests the experimental protocol developed in the first series of tests was repeated, however, at the conclusion of the tensile test the whole specimen was transected. The specimen's wet weight and cross sectional area were determined. Each specimen was then dried in an oven and reweighed to determine the dry weight. The percentage of fluid in the tissue at the time of test was assumed to be equal to 1- dry/wet weight.

The data from the first series of tests were analyzed to determine the stiffness in the linear range (N/mm cross head displacement) during the constant strain rate tests. The end of the toe region of the tensile response (the start of the linear region) was identified as the point where the difference between the line describing the linear range and the experimental curve exceeded 5%. A paired t-test was used to compare the length of the "toe" region in the large and smallest specimens. A tensile modulus was calculated by multiplying the stiffness by the specimen length and dividing by the cross sectional area. The rate of relaxation (N/lns) and amount of relaxation ((1-Force\_r/Force<sub>initial</sub>) were obtained from the normalized relaxation response. The tensile modulus, rate of relaxation, and amount of relaxation were plotted versus cross sectional area for each specimen, and appropriate trend lines were fit to the data. An F-test was used to determine whether there were significant differences between the slopes of the fitted lines. Where there were no significant differences, the data were combined and a general trend identified. Paired ttests where also used to identify significant differences between the responses of the small and large specimens in the second series of tests (one of the two small specimens was selected at random and paired with it's contralateral large specimen) to confirm that the differences observed in the first series of tests were present when a specimen was tested only once. The correlation of tensile modulus, rate of relaxation and amount of relaxation with water content and the correlation of water content with cross sectional area was obtained within each specimen. Statistical significance in all tests was set at p<0.05.

### **RESULTS:**

In the first series the initial specimen cross sectional areas ranged from 3.2 to 16.2 mm<sup>2</sup>, and the final, dissected specimens ranged in size from  $4 \times 10^{-2}$  to  $0.2 \text{ mm}^2$ . In the second series of tests the cross sectional areas of the larger portions of tendon ranged from 14.5 to 21.7 mm<sup>2</sup>, while those of the small portions ranged from 0.1 to 2.6 mm<sup>2</sup>. The tensile response of a small portion of tendon (cross sectional area < 1 mm<sup>2</sup>) was nonlinear with a toe region persisting to between 0.3 to 1.4% strain (Figure 2), while that of larger specimens exhibited a significantly longer to eregion to approximately 1.4 - 2.8 % strain. The tensile modulus was found to increase nonlinearly with decreasing cross sectional area in each series of experiments. A natural logarithm, linear relation fit these data well (Figure 3). There was no significant difference between the slopes of the fitted curves for specimens from cadavers 1,2,4 and 3 (Il location), therefore these data were combined and a general trend line was plotted. The medial-central (lc) specimen from cadaver 3 exhibited a modulus-area trend with a significantly steeper slope (Figure 4). The general effect of specimen cross sectional area on modulus was consistent between all specimens. The small specimens from the second series of tests also exhibited tensile moduli which were significantly larger than the moduli of the matched contralateral larger specimens. These data followed the general trend demonstrated in the first series of experiments (data points on Figure 4).

The rate of relaxation increased nonlinearly with increasing cross sectional area, and the rate-area relationship was also described well by a natural logarithm, linear function (Figure 3). There was no significant difference between the slopes of the rate-area

functions for all specimens, therefore a general trend line was computed using all specimens (Figure 5). The small specimens in the second series of tests relaxed at a rate which was significantly slower than that of the larger specimens. The trend was comparable to that observed in the first series of tests (points on Figure 5).

The amount of relaxation nonlinearly increased with increasing cross sectional area, and a natural logarithm, linear function fit the data (Figure 3). There was a significant difference in the slope of the relaxation/area function for specimens 2 (lc) and 3 (ll), as compared to the other specimens. Two trend lines describing the amount of relaxation/area relationship were therefore generated to describe these groups, but the cross sectional area effect was consistent between specimens (Figure 6). The large specimens from the second series of tests also relaxed significantly more than the smaller specimens (data points on Figure 6).

A strong overall linear relationship was identified between the rate of relaxation and the amount of relaxation for all specimens (Figure 7). There was also a significant positive correlation between the percentage of water present and the rate and amount of relaxation a specimen exhibited for specimens 1,2(lc),3(lc), and 4 (Figure 8). The percentage of water in the larger pieces was generally larger than that of the smaller, however there was only a significant correlation in specimen 3(ml).

### **DISCUSSION:**

Previously, the mechanical strength of tendon (Danylchuk et al., 1978) and the "toe" region of the tensile response (Atkinson et al., 1997, Kastelic et. al., 1980) have been attributed to the collagen fasciculi within the tissue. There have been, however, few

mechanical studies that attempt to isolate these structures to evaluate the tensile response of human tendon fasciculi and no documentation of their time varying response. The intent of the current study was to document the mechanical response of tendon as the specimen was sequentially sectioned into a specimen which might be described as a small group of collagen subfascicles. The experiments demonstrated that small specimens exhibited a slightly nonlinear tensile response, unlike that of larger specimens where the "toe" region persisted to greater strains. The tensile modulus of the specimens increased nonlinearly as the specimen cross section decreased. In constant strain, stress relaxation tests the smaller specimens relaxed at a slower rate than the larger specimens, and they did not relax as much as the larger specimens. These findings suggest that there may be structural influences in both the tensile and relaxation, or time dependent, responses of tendon beyond those found in a small group of subfascicles. There was also significant overall correlation between water content and the rate and amount of relaxation, with the specimens with higher water content relaxing faster and relaxing more. These data suggested that tissue hydration also played a role in the production of the time dependent response of the tissue.

The tensile modulus obtained for large specimens in the current study compared favorably to those previously reported in Haut and Haut (1997). In that study halves of human patellar tendon exhibited an average tensile modulus of 203 MPa (average cross sectional area of 52 mm²) compared to an average of 200 MPa for similarly sized specimens in the current study (as obtained using the trend function fit to the data). The modulus of small specimens exceeded that of large specimens in the current study.

Previous studies have also suggested that the tensile modulus of a small piece of tendon is greater than that of whole tendon (Butler et al., 1987, Stoeffer et al., 1985). Butler et al. (1986) suggests that the modulus of a small specimen of tendon may be more descriptive of the collagen in tendon as the "fascicle initial length and cross section can be more accurately determined" and "fiber bundles...tend to be more parallel than in whole tissues". The increased modulus could also have been due to a decrease in the amount of areolar connective tissue in smaller samples of the tendon (Danylchuk et al, 1978, Yahia and Drouin, 1988). Danylchuk et al. (1978) previously suggested that "a precise definition of the tensile strength of ligament ought to take into account the relative contributions of collagen fasciculi and connective sheaths...". In the current study the toe region of the tensile response of the small specimens was minimal. This finding suggested that some mechanism other than collagen recruitment within the fascicle or subfascicle, potentially whole subfascicle or fascicle recruitment, contributed to the creation of the "toe" region in a large specimen.

The rate of relaxation for the large specimens in the current study approached that observed in Haut and Haut (1997) (0.143 N/ln(s) for an area of 52 mm<sup>2</sup>). Also in the Haut and Haut (1997) study, tissues tested in a dehydrating solution (sucrose) exhibited a slower rate of relaxation than those tested in distilled water. A similar trend was observed in the current study where the rate of relaxation decreased with decreasing fluid content. Previously Stouffer *et al.* (1985) reported that no relaxation was observed in tendon specimens ranging in size from 0.33-0.72 mm<sup>2</sup> during tensile testing, where the specimens were "slowly elongated" then held at a fixed position for several minutes to facilitate

82

strain measurement in a 0.9 M, 37°C saline bath. In that study it was the authors intent to describe the specimens steady state tensile response and the slow rate of extension may have allowed fluids inside of the specimens to escape during deformation thus losing the relaxation response. On the other hand, the distilled water bath selected in the current study likely magnified the relaxation response, as intended.

In the current experiments the large specimens, which relaxed faster and more than smaller specimens, also tended to contain more fluid. This fluid might have caused the tissue to swell and therefore exhibit a higher permeability and more relaxation. The influence of free fluid might also explain the strong linear relationship identified between the rate of relaxation and the amount of relaxation. On the other hand, the faster rate of relaxation in the large pieces might also be attributed to structural influences, as the larger pieces which exhibited faster relaxations also exhibited longer toe regions in their tensile response. This longer toe suggests that there might have been more "squeezing" effect in these tissues as the collagen structures reorient to align with the load. As the specimen cross sectional area and the water content of the tissue were not significantly correlated in most cases, it may be that both structure and fluid content contribute to the creation of the relaxation response.

The current study was limited in that it was not possible to document the microstructure present in the tested specimens, as the specimens were dehydrated for determination of water content. The dehydrated portions, however, were examined under a light microscope and axially aligned structures were identified. The study was also limited in that it was not possible to measure the amount of fluid in the specimens prior to

each test. As fluids are known to move out of these tissues when stretched (Hannafin and Arnoczky, 1994, Lanir *et al.*, 1988), the "pre-test" fluid content was likely higher than that measured in the current study. The study was also limited in that distilled water was used instead of a physiologic saline solution. In the future these response data need to be studied in physiological baths. In addition to these limitations, the study was limited in that the number of cadaver tendons included in the study, 4, was small in number. However, the trends in mechanical responses observed in the current study were consistent between cadavers and in specimens drawn from various sites within the tendons, suggesting that the observed variation of mechanical response was general.

In conclusion, the experiments suggested that while small portions of tendon behave qualitatively similar to large portions, there were significant quantitative effects of specimen size on the stress relaxation and constant strain rate, tensile responses of the tendon. These experimental data indicated that the whole tendon response could not be predicted by linear superposition of the responses of small portions of the tendon, thus disproving our initial hypothesis. These data also suggest that tissue fluid and structural organization of collagenous structures larger than the subfascicle likely play major roles in the response of a whole tendon.

## **REFERENCES:**

- Atkinson, T.S., Haut, R.C. and Altiero, N.J. (1997) A poroelastic model that predicts some phenomenological responses of ligaments and tendons. *J. Biomech. Eng.* 119, 400-405.
- Atkinson, T.S., Haut, R.C. and Altiero, N.J. (1996) A microstructural poroelastic model for patellar tendon. In *Proceedings of the 1997 Bioengineering Conference*, Sunriver, Oregon.
- Belkoff, S.M. and Haut, R.C. (1992) Microstructurally based model analysis of  $\gamma$ -irradiated tendon allografts. J. Othop. Res. 10, 461-464.
- Butler, D.L., Noyes, F.R., Walz, K.A., and Gibbons, M.J. (1987) Biomechanics of human knee ligament allograft treatment. In *Trans. of the 33rd Annual Meeting of the Orthop. Res. Soc.* San Francisco, CA.
- Butler, D.L., Kay, M.D., and Stouffer, D.C. (1986) Comparison of material properties in fascicle-bone units from human patellar tendon and knee ligaments. *J. Biomech.* 19, 425-432.
- Butler, D., Hulse, D., Kay, M., Grood, E., Shires, P., D'ambrosia, R., and Shoji, H. (1983) Biomechanics of Cranial Cruciate Ligament Reconstruction in dog. *Veterinary Surgery.* 12, 113.
- Chen, C.T., and Vanderby, R. (1997) A poroelastic model of streaming potential and interstitial fluid flow in ligament and tendon. *Advances in Bioengineering*, **36**, 185-186.
- Chen, C., McCabe, R., and Vanderby, R. Jr. (1995) Two electrokinetic phenomena in rabbit patellar tendon: pressure and voltage. In *Proceedings of the 1995 Bioengineering Conference*. Beaver Creek, Colorado.
- Chen, C. T. and Vanderby, R. (1994) 3-D finite element analysis to investigate anisotropic permeability for interstitial fluid flow in ligaments and tendons. In *Trans. of the 40th Annual Meeting of Orthop. Res. Soc.* New Orleans, LA.
- Chen, C. T., Vanderby, R., Graf, B. K., and Malkus, D. S. (1993) Interstitial fluid flow in ligaments and tendons: effects of fibril spacing and fluid properties. In *Proceedings of the 1993 Bioengineering Conference*, Breckenridge, Colorado.
- Chimich, D. D., Shrive, N. G., Frank, C. B., Marchuk, L., and Bray, R. C. (1992) Water content alters viscoelastic behaviour of the normal adolescent rabbit medial collateral ligament. *J. Biomech.* **25**, 831-837.

- Chun, K.J., Butler, D.L, Bukovec, D.B., Gibbons, M.J., and Stouffer, D.C. (1989) Spacial variation in material properties of fascicle-bone units from human patellar tendon. In *Trans. of the 35th Annual Meeting of the Orthop. Res. Soc.* Las Vegas, Nevada.
- Danylchuk, K.D., Finlay, J.B. and Krcek, J.P. (1978) Microstructural organization of human and bovine cruciate ligaments. *Clinical Orthopaedics and Related Research*. **131**, 294-298.
- Hannafin, J.A. and Arnoczky, S.P. (1994) Effect of cyclic and static tensile loading on the water content and solute diffusion in canine flexor tendons: an in-vitro study. *J. Orthop. Res.* 12, 350-356.
- Haut, T.L., and Haut, R.C. (1997) The state of tissue hydration determines the strain-rate-sensitive stiffness of human patellar tendon. J. Biomech. 30, 79-82.
- Haut, R.C. and Powlison, A.C. (1990) The effects of test environment and cyclic stretching on the failure properties of human patella tendons. J. Orthop. Res. 8, 532-540.
- Hurschler, C., Loitz-Ramage, B., and Vanderby, R., (1997) A structurally based stress-stretch relationship for tendon and ligament. J. of Biomech. Eng. 119, 392-399.
- Kastelic, J., Palley, I., and Baer, E. (1980) A structural mechanical model for tendon crimping. J. Biomech. 13, 887-893.
- Kwan, M.K., and Woo, S. L-Y. (1989) A structural model to describe the nonlinear stress-strain behavior for parallel-fibered collagenous tissues. *J. Biomech. Eng.* 111, 361-363.
- Lanir, Y., Saland, E. L., and Foux, A. (1988) Physico-chemical and microstructural changes in collagen fiber bundles following stretch in-vitro. *Biorheology J.* **25**, 591-604.
- Stouffer, DC, Butler, DL, and Hosny, D. (1985) The relationship between crimp pattern and mechanical response of human patellar tendon-bone units. *J. of Biomech. Eng.* **107**, 158-165.
- Thielke, R.J., Vanderby, R. Jr., and Grood, E.S. (1995) Volumetric changes in ligaments under tension. In *Proceedings of the 1995 Bioengineering Conference*. Breckenridge, Colorado.
- Wilson, A. N., Frank, C. B., Shrive, N. G. (1994) The behaviour of water in the rabbit medial collateral ligament. In *Second World Congress of Biomechanics*, (Edited by Blankevoort, L. and Kooloos, J. G. M.), pp. 226b. Amsterdam, The Netherlands.

Yahia, L. H., and Drouin, G. (1988) Collagen structure in human anterior cruciate ligament and patellar tendon. J. Mat. Sci. 23, 3750-3755.

**TABLE 1: Description of Specimens** 

cadaver number	age	sex	cause of death	series 1 harvest location, left/right knee, initial cross sectional area (mm²)	series 2 harvest location, left/right knee, cross sectional area (mm <sup>2</sup> )
1	52	М	M.C. Infarction	lc, right, 3.2	mc, right, 8.7 mc, right, 2.3 mc, right, 1.3
2	17	M	motor vehicle accident	ll, right, 15.4 lc,right, 9.8	lc, left, 2.7 lc, right, 0.8 lc, right, 1.2
3	52	F	ventricular fibrillation	lc, right, 6.1 mc, right, 16.2	ll, left, 18.1 ll, right, 0.6 ll, right, 1.2
4	19	F	motor vehicle accident	ll, left, 5.4	mm, right, 17.7 mm, left, 0.2 mm, left, 0.1

## Figure Legends:

Figure 1: The specimens were harvested to provide approximately quarter sized pieces of tendon for the first series of experiments (which were subsequently sectioned during the testing) and one quarter sized piece and two smaller pieces for the second series of tests. The small pieces in the second series of tests were harvested from a location consistent with that of the contralateral quarter sized piece, to help minimize the influence of spatial variation across the tendon. The harvest locations were denoted as: ll=most lateral, lc=lateral-central, mc=medial-central, and mm=most medial.

Figure 2: The constant strain rate, tensile responses of smaller specimens exhibited a shorter toe region than that of larger specimens (specimen 3, lateral-central).

Figure 3: The data obtained by sequentially sectioning each specimen was plotted versus the specimen cross sectional area and a natural-logarithm, linear relation fit the data well.

Figure 4: A natural logarithm, linear relationship existed between specimen cross sectional area and tensile modulus for specimens in series 1. The data from series 2, denoted by the points (•), follow the trends observed in series 1.

Figure 5: The natural logarithm, linear relationship describing the variation in the rate of relaxation (as obtained from the normalized relaxation response) with specimen cross sectional area from experimental series 1 and data points from specimen tested in series 2.

Figure 6: The natural logarithm, linear relationship describing the variation in the amount of relaxation with specimen cross sectional area from experimental series 1 and data points from specimen tested in series 2.

Figure 7: The relationship between the amount of relaxation and the rate of relaxation exhibited by a specimen was linear.

Figure 8: There was a significant correlation between the percentage of fluid present in the specimen and the rate and amount of relaxation in 4 of the 6 specimen tested. The plot describes a typical relationship between the percentage of fluid and the rate and amount of relaxation exhibited (specimen 2, lateral-central).

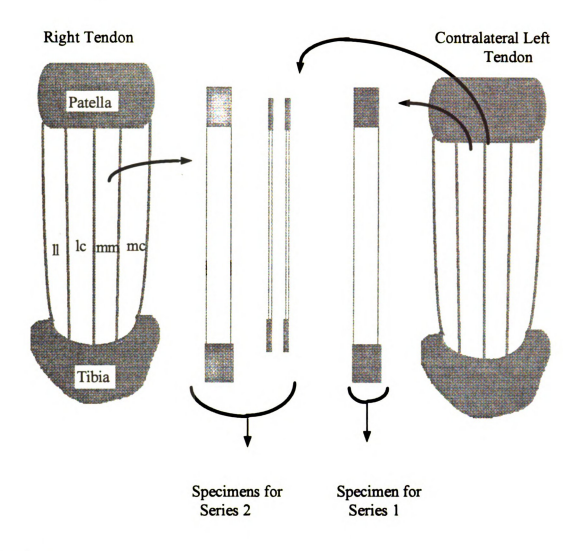
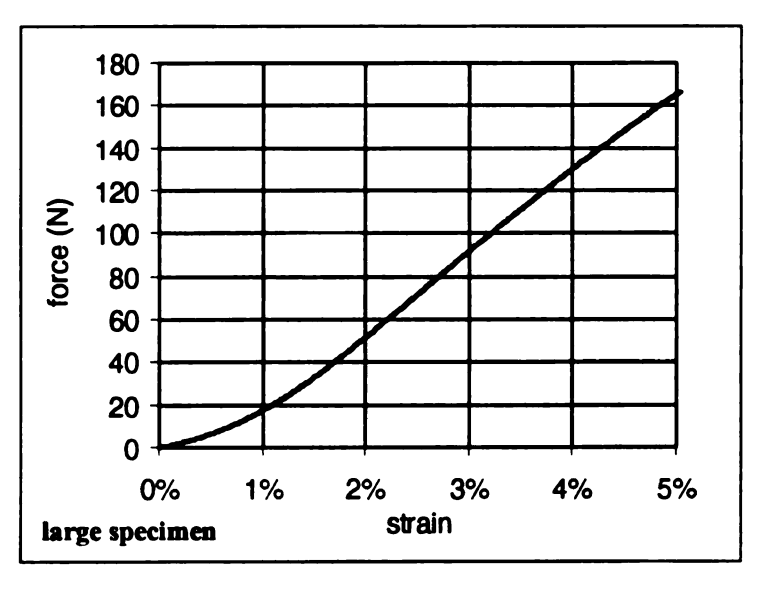


Figure 1



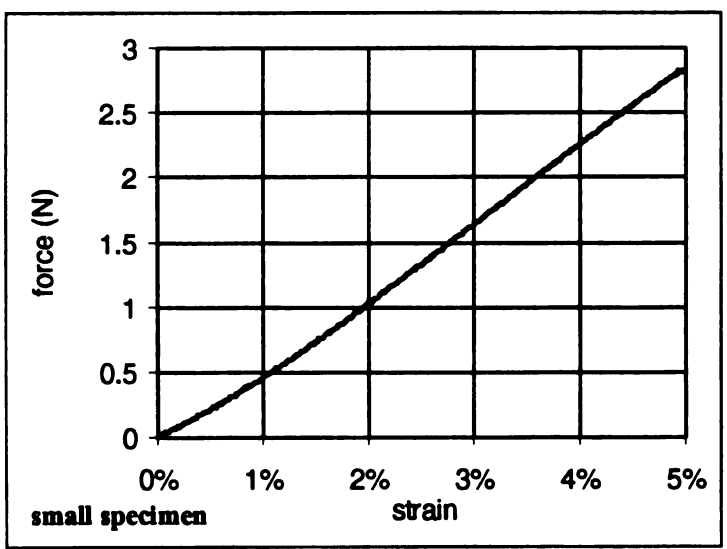


Figure 2

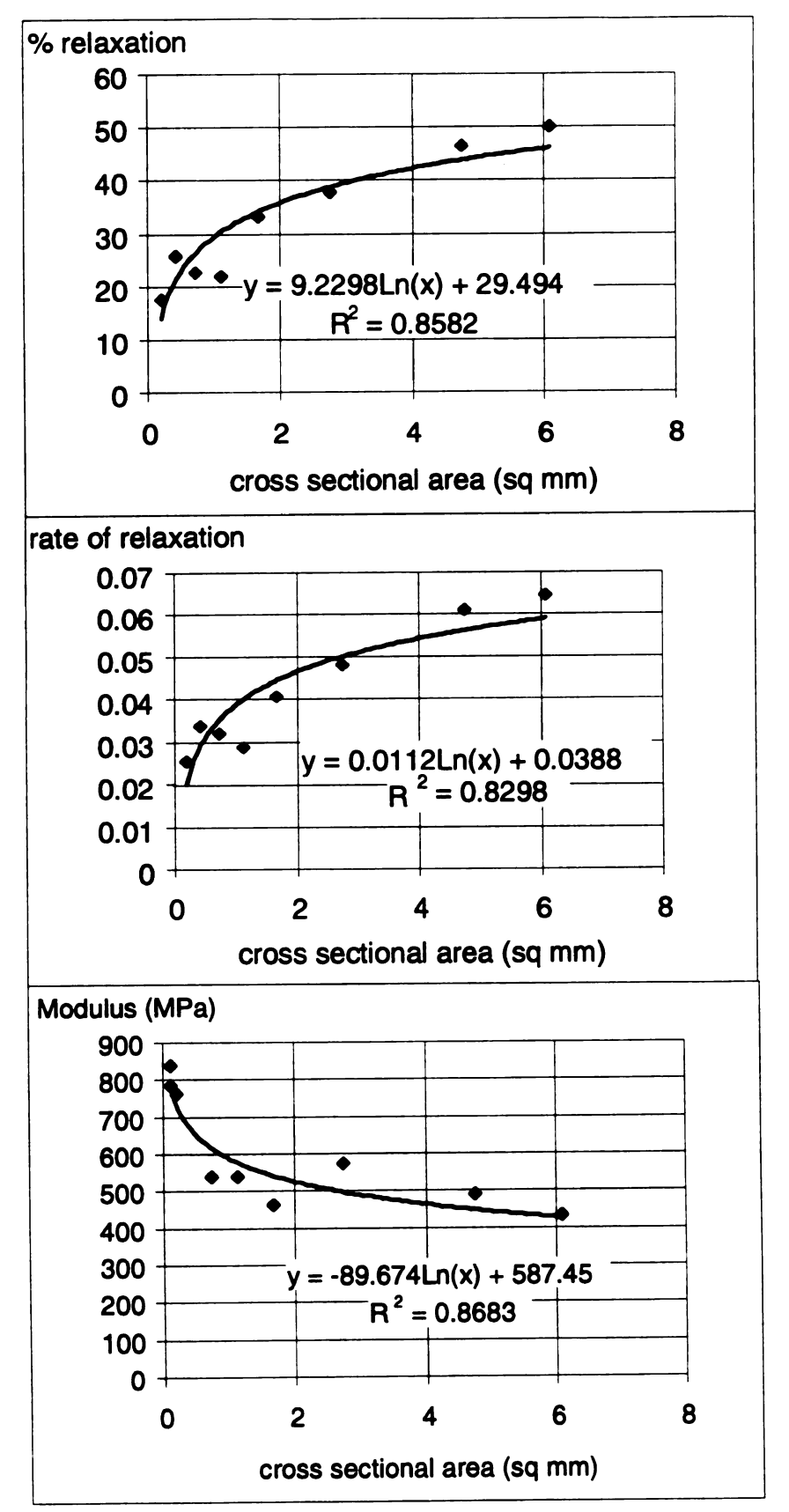


Figure 3

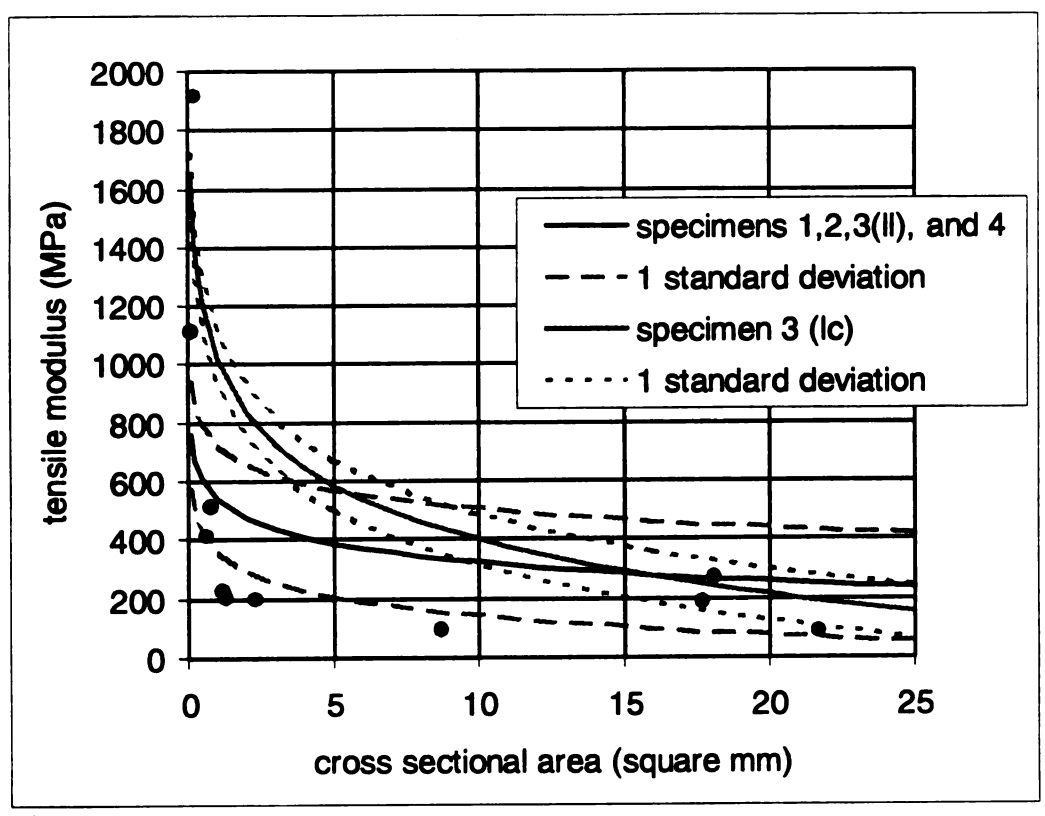


Figure 4

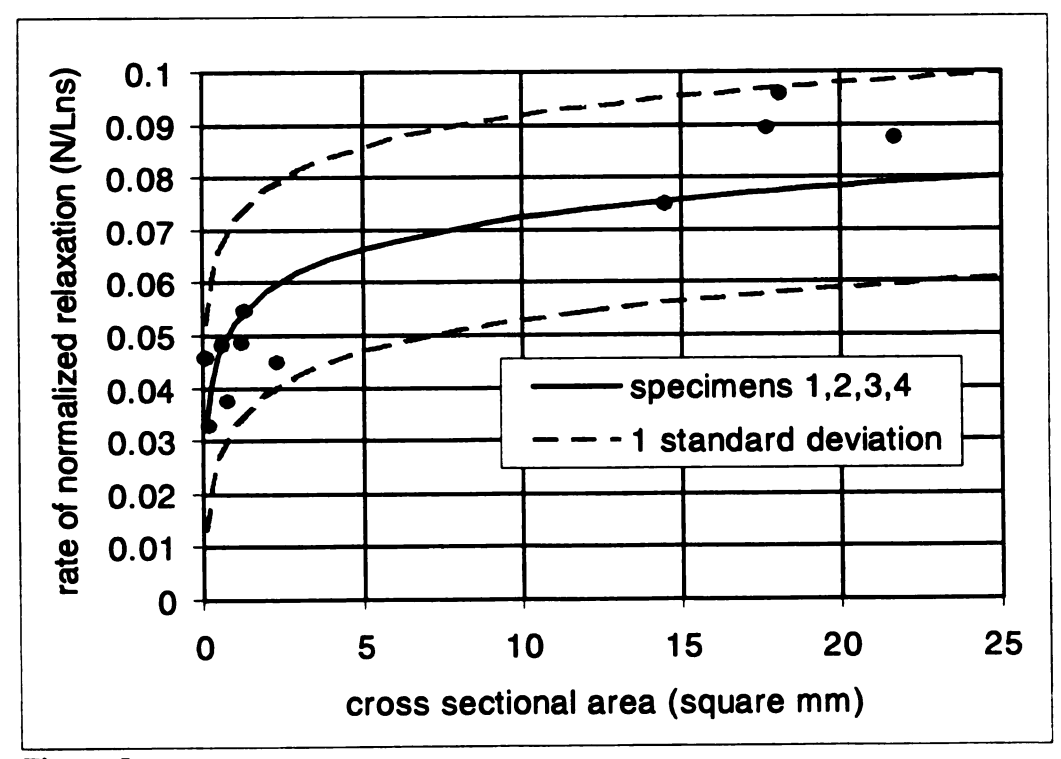


Figure 5

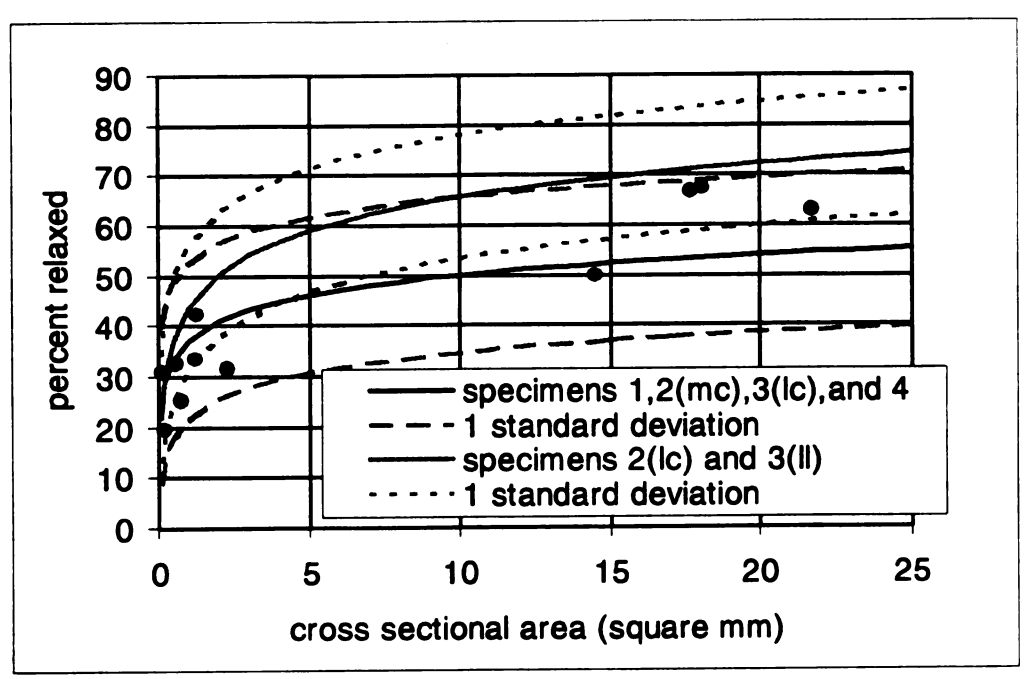


Figure 6

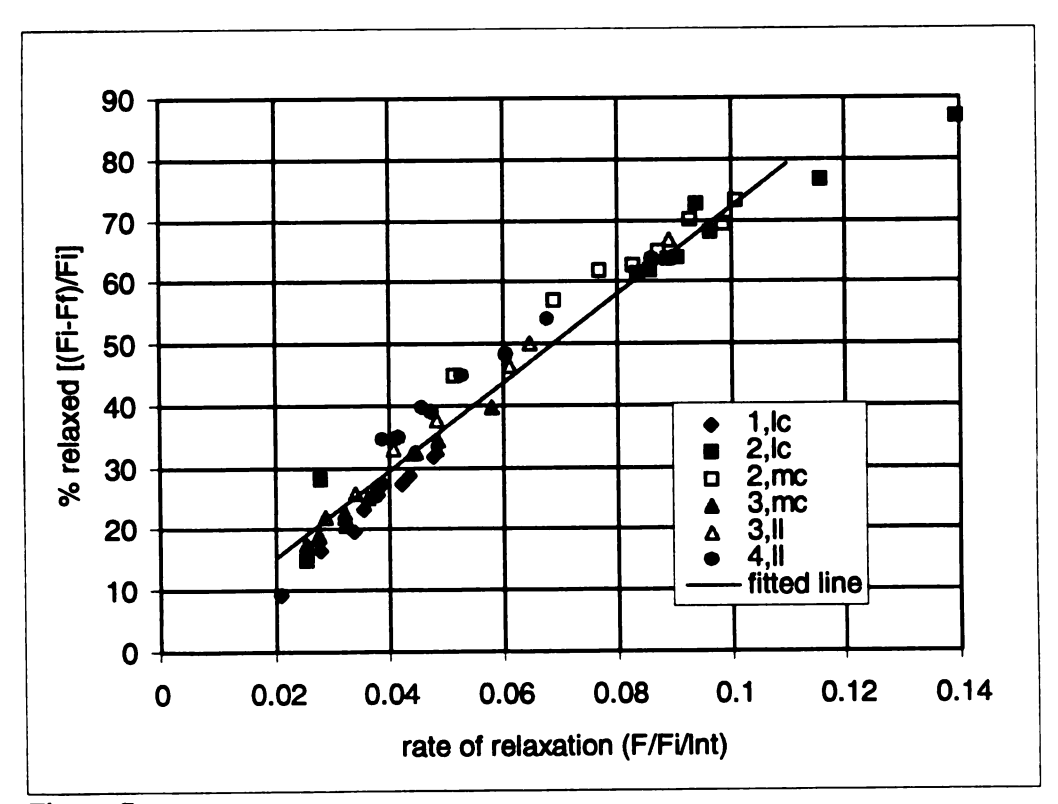


Figure 7

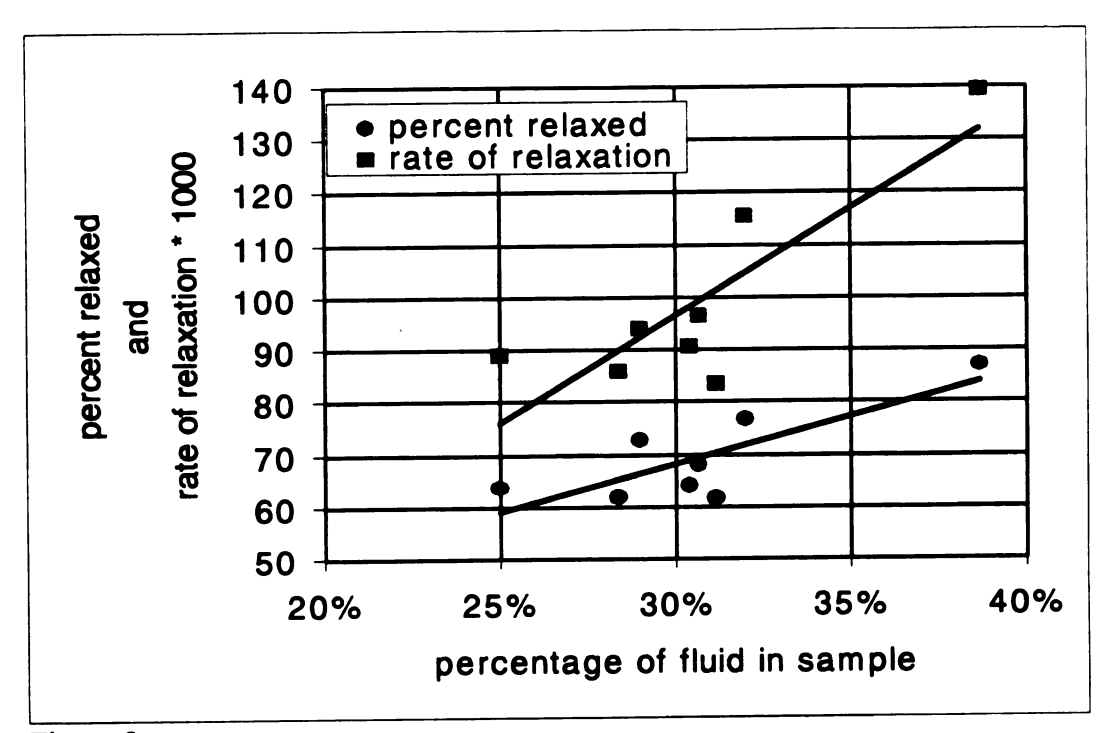


Figure 8

# Chapter 5:

Extension of a Microstructural Model for a Subfascicle Toward a Description of Whole Tendon

Theresa S. Atkinson, Roger C. Haut and Nicholas J. Altiero

### ABSTRACT:

A finite element model of a collagen subfascicle (a microstructural element of tendon) was previously constructed to describe the role of solid structure and fluid motion in the mechanical response of tendon. In the current study, this model was able to quantitatively match subfascicle relaxation and constant strain rate tensile responses as described in a previous experimental study. The subfasicle model was extended to form a simple fascicle model consisting of two subfascicles surrounded by epitenon. In previous experiments, a difference in the rate and amount of relaxation was observed between tendon specimens with small cross sectional areas (<1 mm<sup>2</sup>) and large specimens (20 mm<sup>2</sup>), with large specimens relaxing faster and more than small. The fascicle and subfascicle models were utilized to explore whether increased subfascicle hydration and/or the presence of an epitenon layer surrounding fascicles in the large specimen could help explain this variation. The subfascicle model suggested that increased fluid in the subfascicle might explain a portion of the increased relaxation response exhibited by larger specimens. The fascicle model suggested that transversely oriented fibers in the connective tissues surrounding the fascicles can produce subfascicle interaction, which will increase the rate and amount of relaxation. The analysis suggested that the presence of connective tissue in tendon may play an important role in defining the relaxation response of a whole tendon.

# **INTRODUCTION:**

Predicting and measuring the mechanical response of tendon is important in the development and assessment of various orthopaedic reconstruction techniques which frequently utilize these tissues as graft materials. Lanir (1979) hypothesized that the collagen structure has an important effect on the tissue's function. Many models assume that a tendon or ligament's mechanical response can be predicted if the geometric organization and mechanical properties of the collagen are known (Belkoff and Haut, 1992, Hurschler et al., 1997, Kastelic et al, 1980, Kwan and Woo, 1989, Stouffer et al., 1985). Tissue hydration has also been shown to contribute to the mechanical response of the tissue (Chen et al., 1995, Chen et al., 1994, Chen et al., 1993, Chimich et al, 1992, Haut and Haut, 1997, Haut and Powlison, 1990, Thielke et al, 1995). However, at this time, relatively little is known about how the collagen microstructure and fluid motion in tendon contribute to the observed relaxation and tensile responses.

The microstructure of tendon has been described as being composed of collagen fascicles which in turn are composed of subfascicles (Danylchuk et al, 1978, Yahia and Drouin, 1988). The subfascicles are the smallest repeating structural element of the tissue and their structure in the patellar tendon has been documented by Yahia and Drouin (1989). Atkinson et al. (1997a) suggested that the collagen subfascicle might be the fundamental structural unit within the tendon. They devised a finite element method (FEM) model of the structure, based on descriptions by Yahia and Drouin (1988), where a band of collagen was helically oriented about a central core of matrix. This model suggested that the helical orientation causes the collagen to compress the interfibrillar

matrix causing fluid motion and relaxation. The model's mechanical response, however, was compared qualitatively to that of whole tendon or ligament since the response of a subfascicle is largely unknown.

More recently, an experimental study suggests that very small pieces (crosssectional areas) of tendon, which may be composed of less than 10 subfascicles, exhibit relaxation and tensile responses which are qualitatively similar to that of whole tendon (Atkinson et al., 1998). This study, however, demonstrated significant quantitative differences in the rate and amount of relaxation between tendon specimens with small and large cross sectional areas (Figure 1). The experiments documented a 50% reduction in the rate and the amount of relaxation when the specimen cross sectional area decreased from 20 to 1 mm<sup>2</sup>. In the study the larger specimens, which exhibited the increased relaxation response, also contained a higher percentage of fluid than the smaller specimens. The experimental data for the small specimens suggested that the subfascicle model produced an appropriate mechanical response. However, the variation of the relaxation response with specimen size suggested that a linear superposition of independent subfascicles could not be used to predict the whole tendon response. Linear superposition would result in a rate and amount of relaxation in whole tendon equivalent to those of the subfascicle.

Two potential explanations for the observed increase in relaxation with increasing specimen cross section readily present themselves. It is possible that the additional fluid present in the large specimens may signify more fluid within the specimen's constituent subfascicles. This increased fluid may have contributed to the observed increased

relaxation response. It is also possible that connective tissue structures present between subfascicles and fascicles, likely present in greater proportion in the large specimens, may play a role in increasing the rate and amount of relaxation. In ligament, fascicles are covered by a connective tissue sheath termed epitenon (Danylchuk et al, 1978, Clark and Sidles, 1990, Jozsa et al 1991). Thin projections from the epitenon, termed endotenon, subdivide the fascicles into subfascicles (Danylchuk et al., 1978). The endotenon and epitenon are described as areolar connective tissues carrying small blood vessels, lymphatics and nerves (Elliott, 1965). These areolar tissues bind the fasciculi into functionally independent units (Danylchuk et al., 1978, Chowdhury et al, 1991), allowing them to move with respect to each other (Yahia et al, 1994, Clark and Sidles, 1990). Danylchuk et al. (1978) describes the collagen fibers within the epitenon as having the same diameter as those in the fasciculi. They are, however, "randomly situated in a coiled manner along the long axis of the fasciculi" (Danylchuk et al., 1978). In an extensive study of human tendon microstructure Jozsa et al (1991) describes the collagen fibrils in the epitenon as "crossed over each other and the longitudinal axis of the tendon at various angles forming an irregular network." Some of the fibers of the epitenon are fused with those of the fascicle (Jozsa et al. 1991, Yahia and Drouin, 1988). The epitenon may provide a binding function and thereby play a role in the relaxation response in tendon.

The current study was performed to explore whether increased fluid in the subfascicle or the presence of connective tissue structures might have produced the increasing rate and amount of relaxation observed in the large specimens in the previous experimental study. In order to explore these possibilities, a quantitative subfascicle

model was developed using previously obtained experimental data (Atkinson et al., 1998). The fluid content in this model was then increased to determine whether this might increase the rate and amount of relaxation. The model was also utilized in the construction of a fascicle model, consisting of two subfascicles surrounded by epitenon. Fiber orientations within the epitenon were visualized with scanning electron microscopy (SEM). These orientations were simulated to explore whether the presence of an epitenon layer might enhance the relaxation response.

#### **METHODS:**

The subfascicle finite element model utilized in the current study was a modification of the previously described subfascicle model (Atkinson et al, 1997a,b). Briefly, the model represents Yahia and Drouin's (1989) description of a subfascicle in patellar tendon (wherein collagen fibers are wrapped in a helix about the subfascicle's axis) using a representative 3-D section of a cylindrical subfascicle with a 50  $\mu$ m radius (Figure 2). The helically oriented collagen fibers were wrapped around the periphery of the model, and the matrix within the subfascicle was collected in the center. The top and bottom surfaces of the model were sealed (as the subfascicle is a long and thin structure) and the outer boundaries were assumed to be perfectly draining. The bottom plane of the model was constrained to in plane motions with 4 nodes, 90° apart, additionally constrained to radial motion. The top plane was assumed to deform uniformly in the z direction with r and  $\theta$  free. The matrix portion, in the center of the model, was assumed to be a linear isotropic poroelastic material. An orthotropic poroelastic material simulated the helically oriented fibers within the fibrous rings, where the E<sub>2</sub> direction represented the

fiber modulus. The properties of the orthotropic material were selected to achieve a nearly incompressible material, which was weak in shear. These properties allowed the fiber portion to helically twist in a nearly rigid body fashion. The fiber direction of the orthotropic outer ring was a 20° declination from vertical, the approximate fiber orientation scaled from SEM images presented by Yahia and Drouin (1988) and the crimp angle exhibited in young rat tail tendon (Kastelic et al, 1978). Fluid flow was assumed to obey Darcy's law and the permeability was assumed to be constant.

This modified subfacicle model was fit to relaxation data for a small specimen taken from the previous experimental study (cadaver 2, lateral-central harvest location, Atkinson et al, 1998). This specimen exhibited a stiffness and rate of relaxation which were near the average for similarly sized specimens. It was assumed that this experimental data contained the response of 7 subfascicles (the number of subfasicles, each with a radius of 50 um, that fit into the specimen cross sectional area). As the fasciculi provide the majority of the tensile strength in tendon (Danylchuk et al., 1978, Yahia and Drouin, 1988), the contribution of other connective tissue structure to the strength or stiffness of the specimen was neglected. Each subfascicle was assumed to carry 1/7 th of the load. As the endotenon is a relatively thin projection of the epitenon, its influence was neglected and each of the seven subfascicles were assumed to exhibit equal, normalized, relaxation responses. The potential influence of any epitenon present in the specimen was also neglected at this point, as the influence of this structure was to be evaluated later in the study. The relaxation test was simulated by axially deforming the subfascicle model to 2% strain in 1 ms, while leaving the top of the model free to undergo radial and angular

deformations, then holding this strain for 180 s. Fluids were allowed to drain freely from the lateral boundaries of the model at all times. Constant strain rate tensile tests were modeled at a deformation rate of 1 %/s, while the boundary of the model was assumed to drain freely.

An iterative fitting process was employed to obtain a quantitative match between the experimental relaxation response and the response of the subfascicle FEM model. This process involved maintaining a constant relationship between the tensile moduli in the "fiber" part of the model  $(E_2/E_1=E_2/E_3=2)$ , so that the transverse moduli were less than the fiber modulus, E<sub>2</sub>). The Poisson's ratios were held constant, and the shear moduli were assumed to be equal and much smaller than the tensile moduli. The elastic modulus of the matrix was assumed to be equal to the shear moduli of the "fibers," as the matrix was assumed to be much softer than the collagen fiber portion of the model. This also decreased the number of independent parameters included in the model. The Poisson's ratio of the matrix was assumed to be 0.2, as experimental studies of ligament suggest that these tissues might be highly compressible (Thielke, et al., 1995). The iterative fitting process utilized a linear interpolation scheme, where the fiber and matrix moduli were sequentially varied to match the initial and final forces in the relaxation experiment. The model permeability was then varied to fit the time varying character of the response. The tensile response of the model was compared to the experimental response to verify the model's fit.

Once a fitted model was obtained, it was used to examine whether increased subfascicle hydration might explain the increased relaxation observed in the large

specimens of the previous experimental study (Atkinson et al., 1998). As there does not appear to be an accepted practice for simulating increased water content in tendon, the increased fluid was simulated using three independent methods. In the first approach the permeability (k) of the subfascicles in the large, more hydrated specimen was determined using the relationship suggested by Argoubi and Shirazi-Adl (1996):

$$k = k_o \left[ \frac{e(1+e_o)}{e_o(1+e)} \right]^2 \exp \left[ M \left( \frac{1+e}{1+e_o} - 1 \right) \right]$$
 equation 1

where e<sub>o</sub> was the voids ratio (V<sub>fluid</sub>/V<sub>solid</sub>) and k<sub>o</sub> was the permeability from the "fitted" subfascicle model, and e was the voids ratio of a subfascicle from a large specimen. M is a constant used to fit experimental data. In the current study, M was assumed to be 1 as larger values yield unrealistic increases in the permeability. The voids ratio in the "fitted" subfascicle model was 1.857, based on the amount of fluid (65% fluid) in the small specimen (Atkinson et al 1998). The subfascicles in large specimens from the previous study contained approximately 75% fluid, which translated into a voids ratio of 3. Using these values in equation 1 suggested that the subfascicles in large specimens would have a permeability twice that of the small specimens. In the second and third approaches, changes in water content were simulated by varying the steady-state material properties of the matrix portion of the model. In an isotropic poroelastic or biphasic material the Poisson's ratio is a measure of the fluid efflux through the tissue, with small ratios associated with greater efflux (Mow et al. 1991), and thus more movable fluid present in the tissue. Therefore in the second approach Poisson's ratio of the matrix was set to 0.0 in the model to simulate increased movable fluid in the large specimens. It has also been

suggested that the aggregate modulus of a biphasic material might be a function of the fluid content of the tissue. McFarland et al. (1986) observed a decreased tensile modulus concurrent with an increase in the fluid content in patellar tendon sections used as grafts. Thus, the steady state modulus of the tendon may decrease when the water content increases. In the third approach an increase of fluid within the subfascicle was simulated by decreasing the modulus of the matrix in the subfascicle model by 10%.

Although increased fluid in the subfascicle may increase the relaxation response, it is also possible that structural elements outside of the subfascicle, such as the epitenon, may play a role. In order to examine whether an epitenon layer surrounding fascicles enhances the relaxation response, a simple fascicle model was constructed from two "fitted" subfascicle models surrounded by an thin epitenon layer (Figure 3). The epitenon was assumed to be perfectly attached to the subfascicles, based on Jozsa et al (1991) and Yahia and Drouin's (1988) observations of binding fibers between the structures. The thickness of the epitenon layer (1/12 of the fascicle major axis) was taken from average thicknesses measured in coronal transmission electron micrographs of human anterior cruciate ligament (Hart et al, 1990). The fiber orientations in the epitenon were visualized for two human patellar tendons, where the tissues were prepared using Danylchuk et al's (1978) methods. Briefly, the tissues were fixed for 9 days (Histochoice) then transversely sectioned with a razor. The sections were digested in hyaluronidase (15000 units/150ml sodium acetate buffer, pH 5.4, 0.1 M, 37 °C) for 12 h, dehydrated in increasing concentrations of ethanol, then critical point dried, mounted on aluminum stubs, sputter coated and examined with a Jeol JSM 6400V scanning electron microscope.

Danylchuk et al. (1978) suggested that only the orientation of the collagen fibers in the epitenon distinguished it from the fasciculi. The epitenon was therefore simulated using the collagen fiber material model. The orientation of the fibers was varied based on our micrographs. The relaxation response of the fascicle was compared to that of two non-connected subfascicles.

#### **RESULTS:**

In simulated relaxation the subfascicle FEM model exhibited a peak force, rate of relaxation and relaxed force which were qualitatively similar to that defined by 1/7th of the response of a small specimen from the previous experimental study (Figure 4). The material properties required to obtain agreement between the subfascicle model and this experimental relaxation response (Table 1) resulted in a subfascicle with a total effective modulus of 0.85 GPa. The pressure in the model was positive at all times with a peak internal pressure in the center of the model of 6.5 MPa or 0.8% of the effective modulus. Although the model coefficients were obtained by fitting the model to a small specimen's relaxation response, the model's tensile response was similar to the specimen's tensile response, except the model's response was linear while that from the experiments was slightly nonlinear (Figure 5).

In relaxation simulations, when the subfascicle's water content was assumed to increase from 65% to 75%, the permeability, by equation 1, increased to 10.2e-19 m<sup>4</sup>/Ns or two times the "fitted model" permeability. This produced a rapid rate of relaxation, such that steady-state was achieved approximately 10s faster than with the original permeability (Figure 6, arrows). The peak and steady state forces in the model were

equivalent to those in the 65% water content case. When an increase in fluid content was simulated by decreasing the Poisson's ratio of the matrix from 0.2 to 0.0, the model exhibited negligible change in the rate and amount of relaxation. However, when the modulus was decreased 10%, the rate and amount of relaxation increased approximately 12%.

The SEM visualization of the patellar tendon revealed epitenon surrounding the fascicles in the patellar tendon (Figure 7a). The SEM micrographs suggested a disorganized, but relatively transverse, fiber direction in the epitenon (Figure 7b). As the fiber direction in the epitenon appeared to vary somewhat from location to location in the micrographs, fiber orientations from 0° (horizontal, transverse to the length of the tendon) to -60° from horizontal were investigated in the fascicle model. In simulated relaxation tests with the fascicle model the pressure in each subfascicle was positive and continuous for all epitenon fiber directions (Figure 8). The fascicle model indicated that the rate and amount of relaxation increased as the direction of the collagen in the epitenon became more transversely oriented (Table 2). With more transverse orientations of the collagen the epitenon tended to push the subfascicles together under a tensile load, increasing the amount of twisting in each subfascicle, resulting in higher internal pressures in the model. At the -5° fiber orientation the amount of relaxation and the rate of relaxation of the structure increased by 39% and 18%, respectively, over that of two independent fascicles. In cases where the rate and amount of relaxation were increased, the pressure in the center of the subfascicles was also increased. For the -5° case the pressure increased 13% over that without an epitenon. In comparison, with an isotropic epitenon layer the internal

pressure and the amount of relaxation were 39% and 66% less than a model with no epitenon.

## **DISCUSSION:**

The subfascicle FEM model exhibited behaviors that were qualitatively similar to those of a representative small specimen from a previous experimental study. The collagen fiber modulus suggested by the model, 6.7 GPa, was somewhat higher than that previously reported for pure collagen, 0.6 - 2 GPa (Haut, 1983; Lanir, 1979). The effective modulus of the whole structure (0.85 GPa) was, however, within this range. In the subfascicle model the collagen fibers account for approximately one quarter of the subfascicle's cross section. This amount was based on the assumption that the interfibrillar matrix accounted for a substantial portion of the subfascicle's cross sectional area. This assumption was based on the relatively high volume of water in tendon and ligament as indicated by the ratio of wet to dry weight (Chimich, et al., 1992). The previously reported collagen moduli suggest that collagen may account for a somewhat greater portion of the subfascicle's cross section than was assumed in the model. The linearity of the subfascicle's tensile response was attributed to the relatively crude collagen fiber representation utilized in the current study. In a subfascicle the collagen fibers are distributed throughout the cross section and Yahia and Drouin (1989) suggests that the peripheral fibers are undulated and helically oriented, while those at the center form a simple helix. In a previous study, a more sophisticated subfascicle model was developed which incorporated distributed collagen fibers which were inclined at various helical angles (Atkinson et al, 1997b). This model exhibited a nonlinear tensile response. However, this

model was not utilized in the current study, as the radial distribution of collagen fiber orientations in the subfascicles is unknown, and the model was not well suited to the iterative fitting process used in the study due to the solution time required. In the future it may be possible to obtain a description of the orientation of collagen fibers within the subfascicle using SEM.

An important limitation of fitting the subfascicle model to the experimental data was that the experimental specimen likely contained some connective tissues as well as subfascicles. This endotenon may have contributed to the observed relaxation response which was attributed to the subfascicle. In the small specimens utilized in the previous experimental study (Atkinson et al, 1998), however, the epitenon was likely transected or removed. The relaxation response observed was therefore more likely closer to that of a single subfascicle than that observed in large specimens where more fascicles were likely surrounded with an intact epitenon.

In the current study it was suggested that the relaxation response was attributed to fluid motion out of the subfascicle, resulting in a local redistribution of fluid. This concept is consistent with Atkinson et al's (1998) experimental data which suggests that relaxation does not result from gross fluid motion out of the specimen as decreased rates of relaxation were observed in specimens with shorter flow paths (smaller cross sections), rather than faster rates. It is also consistent with Hannifin and Arnoczky's (1994) findings that large molecules are not taken up by tendon under cyclic load, suggesting that large scale fluid transfer between the tendon and its surrounding does not occur. The permeability of the subfascicle obtained in the current study,  $10^{-19}$  m<sup>4</sup>/Ns, was below the

10<sup>-15</sup> m<sup>4</sup>/Ns range obtained in confined compression testing of 3.175 mm diameter coupons from rabbit flexor tendon (Malaviya, et al. 1995). Confined compression yields a gross effective permeability in the direction of compression. However, as the patellar tendon is generally loaded in tension, this measure may not be reasonable. In the fascicle model it was suggested that the relaxation response of whole tendon may result from fluid motion out of subfascicles into adjoining connective tissues. In this case the subfascicle permeability, suggested here, would more accurately describe the state of fluid flow in the tissue. The current study also suggested that there might be local regions of high pressure within the subfascicles in the tendon. However the pressure between fascicles, in the connective tissues, might be lower. A low pressure between fascicles would be consistent with low pressures (.001 MPa) measured within rabbit patellar tendon under cyclic load (Chen et al, 1995).

In the previous experimental study (Atkinson et al, 1998), large specimens contained a greater percentage of fluid and exhibit faster rates of relaxation and a larger amount of relaxation than smaller specimens. This trend was also observed in Haut and Haut's (1997) study where specimens tested in a distilled water relaxed faster than those tested in a dehydrating sucrose solution. There does not appear to be consensus in the literature on how to accommodate variation in water content into a biphasic analysis. In the current study three methods were utilized to reproduce the influence of variation in tissue hydration. Variations in permeability and Poisson's ratio could not reproduce the variation in response observed in large specimens. Decreasing the elastic modulus of the matrix caused a moderate increase in the relaxation response of the subfascicle FEM.

suggesting that a portion of the difference between small and large tendon specimens might be due to variation in water content. However, the current study would suggest that variations in the water content of the subfascicles can only account for a portion of the observed variation of the relaxation response.

The fascicle model suggested that transversely oriented fibers in the epitenon increase the subfascicle deformations thereby increasing the pressurization of the matrix, resulting in an increase in the rate and amount of relaxation. This model described a single, simple subfascicle, but it suggests that a transversely oriented epitenon might cause the relaxation response to continue to increase as greater numbers of subfascicles and fascicles are grouped together to represent the larger specimens. The epitenon has been described as a continuous network of connective tissues throughout the tissue (Jozsa et al., 1991, Yahia and Drouin, 1989) composed of transversely oriented fibers (Danylchuk et al., 1978). The possible existence of a continuous transversely oriented network may be further supported by experimental studies documenting a 10 MPa transverse modulus for human medial collateral ligament (Quapp and Weiss, 1997). The potential influence of the epitenon in a large section of tendon therefore appeared to be more significant than the influence of increased fluid, and may help explain the marked increase in relaxation of larger specimens observed in the previous experiments.

There were several limitations in the current study. The collagen fiber angle in the model was assumed to be 20° declined from vertical. It was not possible to verify this assumption as the specimens tested in the experimental study were dehydrated for determination of water content. Previous SEM studies, however, suggest that this

orientation is reasonable (Yahia and Drouin, 1978, Kastelic et al, 1978). Another limitation was that a rather simplified model was fit to the experimental data, however this model provided a reasonable approximation to the subfascicle tensile response and vielded a positive pressure profile. It was also impossible to determine the morphology of the connective tissues as the specimens in the previous experimental study were destroyed during the determination of water content. SEM, however, evidence suggests that the fibers in these tissues are not longitudinally aligned in the tendon (Yahia and Drouin, 1988) Danylchuk et al, 1978, Jozsa et al, 1991). A further limitation was that the fascicles were assumed to be aligned longitudinally in the tendon. In the anterior cruciate ligament (ACL) the arrangement of the fascicles and subfascicles has been described as 3-dimensional where these units exhibit an undulating course and are arranged in various directions and are interwoven (Strocchi, et al 1992, Elliott, 1965). Danylchuk indicates that the ratio of the area occupied by the connective tissue sheaths to the area occupied by the collagen fasciculi varies along the longitudinal course of the ACL, further suggesting a structure in which the fasciculi are not perfectly parallel. If a similar structure exists in the patellar tendon, it might also play a role in the production of the relaxation response. In future studies it will be important to document the microstructure of tendon specimens so that models may be created which represent the specific microstructural elements present.

In conclusion, the current study suggested that connective tissues surrounding the collagen fasciculi might exhibit a binding function that theoretically could increase the pressurization of collagen subfascicles to generate more and faster relaxation in fascicles versus individual subfascicles. This effect is postulated to become even more pronounced

as many fascicles are grouped together to form a whole tendon. The study further suggested that increases in the degree of tissue hydration can lead to increased relaxation responses in ligaments and tendons.

#### **REFERENCES:**

- Atkinson, T.S., Ewers, B.J, and Haut, R.C., 1998, "The tensile and stress relaxation responses of human patellar tendon varies with specimen cross sectional area," submitted to *J. Biomech.*, 5/98.
- Atkinson, T.S., Haut, R.C. and Altiero, N.J.,1997a, "A poroelastic model that predicts some phenomenological responses of ligaments and tendons," *J. Biomech. Eng.*, Vol. 119, pp. 400-405.
- Atkinson, T.S., Haut, R.C. and Altiero, N.J., 1997b, "A microstructural poroelastic model for patellar tendon," In *Proceedings of the 1997 Bioengineering Conference*, Sunriver, Oregon, pp. 573-574.
- Argoubi, M. and Shirazi-Adl, A., 1996, "Poroelastic creep response analysis of a lumbar motion segment in compression," *J. Biomechanics*, Vol. 29(10), pp. 1331-1339.
- Belkoff, S. M. and Haut, R.C., 1992, "Microstructurally based model analysis of γ irradiated tendon allografts", J. Othop. Res., Vol. 10, pp. 461-464.
- Butler, D.L., Matthew, D.K, and Donald, C.S., 1986, "Comparison of material properties in fascicle-bone units from human patellar tendon and knee ligaments", *J. Biomech.*, Vol. 19, No. 6, pp. 425-432.
- Chen, C., McCabe, R., and Vanderby, R. Jr., 1995, "Two electrokinetic phenomena in rabbit patellar tendon: pressure and voltage," *Bioengineering Conference*. *ASME*, Beaver Creek, Colorado, pp. 31-32.
- Chen, C. T. and Vanderby, R., 1994, "3-D finite element analysis to investigate anisotropic permeability for interstitial fluid flow in ligaments and tendons," *Trans. Orthop. Res. Soc.*, p. 643.
- Chen, C. T., Vanderby, R., Graf, B. K., and Malkus, D. S., 1993, "Interstitial fluid flow in ligaments and tendons: effects of fibril spacing and fluid properties," *Bioengineering Conference ASME*, Breckenridge, Colorado, pp. 399-402.
- Chimich, D., Shrive, N., Frank, C., Marchuk, L., and Bray, R., 1992, "Water content alters viscoelastic behaviour of the normal adolescent rabbit medial collateral ligament," *J. Biomech.*, Vol. 25(8), pp. 831-837.
- Chowdhury, P., Matyas, J.R., and Frank, C.B., 1991, "The "epiligament" of the rabbit medial collateral ligament: a quantitative morphological study", *Conn. Tiss. Res.*, Vol 27, pp. 33-50
- Clark, J.M., and Sidles, J.A., 1990, "The interrelation of fiber bundles in anterior cruciate ligament," J. Orthop. Res., Vol. 8(2), 180-188.

- Danylchuk, K.D., Finlay, J.B. and Krcek, J.P., 1978, "Microstructural organization of human and bovine cruciate ligaments", Clinical Orthopaedics and Related Research, No. 131, pp. 294-298.
- Elliott, D.H., 1965, "Structure and function of mammalian tendons," *Biol. Rev.*, Vol. 40, pp. 394-421.
- Hannafin, J. A. and Arnoczky, S. P., 1994, "Effect of cyclic and static tensile loading on the water content and solute diffusion in canine flexor tendons: an in-vitro study," *J. Orthop. Res.*, Vol. 12, pp. 350-356.
- Hart, R.A., Woo, S. L-Y., Newton, P.O., 1990, "Ultrastructural Morphology of Anterior Cruciate and Medial Collateral Ligaments: An Experimental Study in Rabbits," *J. Orthop. Res.*, 10: 96-103.
- Haut, R.C., 1983, "Correlation between strain-rate-sensitivity in rat tail tendon and tissue glycosaminoglycans," ASME Boimechanics Symposium, pp. 221-224.
- Haut, R. C. and Powlison, A. C., 1990, "The effects of test environment and cyclic stretching on the failure properties of human patella tendons," *J. Orthop. Res.*, Vol. 8, pp. 532-540.
- Haut, T.L., and Haut, R.C., 1997, "The state of tissue hydration determines the strain-rate-sensitive stiffness of human patellar tendon," J. Biomech. Vol 30, pp. 79-82.
- Haut, R.C. and Powlison, A.C., 1990, "The effects of test environment and cyclic stretching on the failure properties of human patella tendons," *J. Orthop. Res.*, Vol 8, pp. 532-540.
- Hurschler, C., Loitz-Ramage, B., and Vanderby, R., 1997, "A structurally based stress-stretch relationship for tendon and ligament," *J. of Biomech. Eng.*, Vol. 119, pp. 392-399.
- Jozsa, L. Kannus, P., Balint, J.B., Reffy, A., 1991, "Three-dimensional ultrastructure of human tendons," *Acta. Anat.*, Vol. 142, pp. 306-312.
- Kastelic, J., Palley, I., and Baer, E., 1980, "A structural mechanical model for tendon crimping," J. Biomech., Vol. 13, pp. 887-893.
- Kastelic, J., Galeski, A. and Baer, E., 1978, "The multicomposite structure of tendon", Connective Tissue Res., Vol 6, pp.11-23.

- Kwan, M.K., and Woo, S. L-Y.,1989, "A structural model to describe the nonlinear stress-strain behavior for parallel-fibered collagenous tissues," *J. Biomech. Eng.*, Vol. 111, pp. 361-363.
- Lanir, Y., 1979, "A structural theory for the homogeneous biaxial stress-strain relationships in flat collagenous tissues," J. Biomechanics, Vol. 12, pp. 423-436.
- Lanir, Y., 1978, "Structure--strength relations in mammalian tendon," *Biophysical J.*, Vol. 24, pp. 541-554.
- Lanir, Y., Saland, E. L., and Foux, A., 1988, "Physico-chemical and microstructural changes in collagen fiber bundles following stretch in-vitro," *Biorheology* J., Vol. 25(4), pp. 591-604.
- Malaviya, P., Butler, D.L., Smith, F.N.L., and Boivin, G.P., 1995, "Mechanical and morphometric properties of the fibrocartilage-rich contact zone in the rabbit flexor tendon," In *Trans. 41 Annual Meeting of the Orthop. Res. Soc.*, Orlando, Florida, pp.133.
- McFarland, E.G., Morrey, B.F., An K.N., and Wood M.B., 1986, "The relationship of vascularity and water content to tendile strength in a patellar tendon replacement of the anterior cruciate ligament in dogs," *Am. J. Sports Med.*, Vol. 14(6): pp. 436-448.
- Mow, V. C., and Hayes, W. C., 1991, *Basic Orthopaedic Biomechanics*, Raven Press, Ltd., New York, New York, pp. 143-243.
- Quapp, K.M., and Weiss, J.A., 1998, "Material characterization of human medial collateral ligament," In *Trans. 44th Annual Meeting of the Orthop. Res. Soc.*, New Orleans, Louisiana, pp. 614.
- Stouffer, DC, Butler, DL, and Hosny, D., 1985, "The relationship between crimp pattern and mechanical response of human patellar tendon-bone units," *J. of Biomech. Eng.*, Vol. 107, pp. 158-165.
- Strocchi, R., DePasquale, V., Gubellini, P., Facchini, A., Marcacci, M., Buda, R., Zaffagrini, S., and Rugger, A., 1992, "The human anterior cruciate ligament: histological and ultrastructural observations," *J. Anat.*, Vol 180, pp. 515-519.
- Thielke, R.J., Vanderby, R. Jr., and Grood, E. S., 1995, "Volumetric changes in ligaments under tension," *Bioengineering Conference. ASME*, Breckenridge, Colorado. pp.197-198.
- Thornton, G.A., Oliynyk, A., Frank, C.B., and Shrive, N.G., 1997, "Ligament creep cannot be predicted from stress relaxation at low stress: A biomechanical study of the rabbit medial collateral ligament," *J. Orthop. Res.*, Vol. 15, pp. 652-656.

- Viidik, A. 1990, "Structure and function of normal and healing tendons and ligaments" in *Biomechanics of Diarthrodial Joints Vol I*, (Edited by Mow, V.C., Ratcliffe, A., and Woo, S. L-Y.), pp. 3-12, Springer-Verlag, N.Y.
- Wilson, A. N., Frank, C. B., Shrive, N. G., 1994, "The behaviour of water in the rabbit medial collateral ligament," *Second World Congress of Biomechanics*, (Edited by Blankevoort, L., and Kooloos, J. G. M.), p. 226b, Amsterdam, The Netherlands.
- Yahia, L.H., Hagemeister, N., Drouin, G., Sati, M., and Rivard, C.H., 1994, "Conceptual Design of Prosthetic ACL: The need for a biomimetical approach," *Biomimetics*, Vol 2(4), pp. 309-330.
- Yahia, L. H., and Drouin, G., 1989, "Microscopical investigation of canine anterior cruciate ligament and patellar tendon: collagen fascicle morphology and architecture," *J. Orthop. Res.*, Vol. 7, pp. 243-251.
- Yahia, L. H., and Drouin, G., 1988, "Collagen structure in human anterior cruciate ligament and patellar tendon," J. Mat. Sci., Vol. 23, pp. 3750-3755.

Table 1: Material Coefficients for Subfascicle FEM

Moduli	Value	
fiber: E1, E3	3350 MPa	
fiber: E2	6700 <b>MPa</b>	
fiber: v23	0.00	
fiber: v12,v13	0.49	
fiber: G1,G2,G3	105 MPa	
fiber: k	$5.1e-19m^4/Ns$	
matrix: E	105 MPa	
matrix: v	0.20	
matrix: k	5.1e-19m <sup>4</sup> /Ns	

Table 2: Fascicle FEM Model Relaxation Response to 2% Strain

collagen fiber angle in	internal pressure in	rate of relaxation	amount of relaxation
epitenon	subfascicle		
degrees	MPa	N/ln(s)	(1-F <sup>f</sup> /F°)%
0	10.6	.0170	16.5
-5	7.0	.0167	21.6
-10	7.6	.0165	20.7
-20	7.9	.0164	17.3
-30	7.3	.0160	16.3
-40	6.0	.0143	14.5
-50	5.2	.0122	12.8
-60	4.4	.0102	10.8
isotropic	3.8	.0045	5.3
no epitenon	6.5	.0141	15.5

# Figures:

Figure 1: Normalized force (F(t)/F<sub>peak</sub>) data from Atkinson et al. (1998) showing a reduced rate and amount of relaxation exhibited by a subfascicular bundle with a cross sectional area of 0.04 mm<sup>2</sup> vs. a larger specimen with a cross section of 16.2 mm<sup>2</sup>.

Figure 2: The subfascicle structure was idealized with a layer of helically oriented collagen and a central region of matrix.

Figure 3: A simple fascicle model was created where two subfascicles were joined together and bound by an oriented epitenon layer.

Figure 4: The relaxation response of the subfascicle model compared favorably to experimental data for a subfascicle (as defined by 1/7 th of the response of a specimen which was likely composed of 7 subfascicles) obtained in a previous study.

Figure 5: The tensile response of the subfascicle model was similar to experimental data obtained in a previous study.

Figure 8: The increased water content simulated in the subfascicle model by: increasing the model permeability, decreasing the Poisson's ratio of the matrix, and by varying the elastic modulus of the matrix portion of the model. The arrows on the plot describe the

time at which a steady state condition was achieved in the fitted model and in the fitted model with the permeability increased to twice the initial permeability. Decreasing the elastic modulus of the matrix resulted in a faster rate of relaxation and more relaxation, consistent with the trend observed in the previous experimental study.

Figure 7: SEM images of human patellar tendon in coronal section: (a) epitenon layers surrounding fasciculi (X60), (b) transverse collagen fibers in epitenon sheath (X13,000).

Figure 8: A representative pressure profile in a subfascicle contained in a fascicle where the epitenon fibers were oriented at -20 degrees.

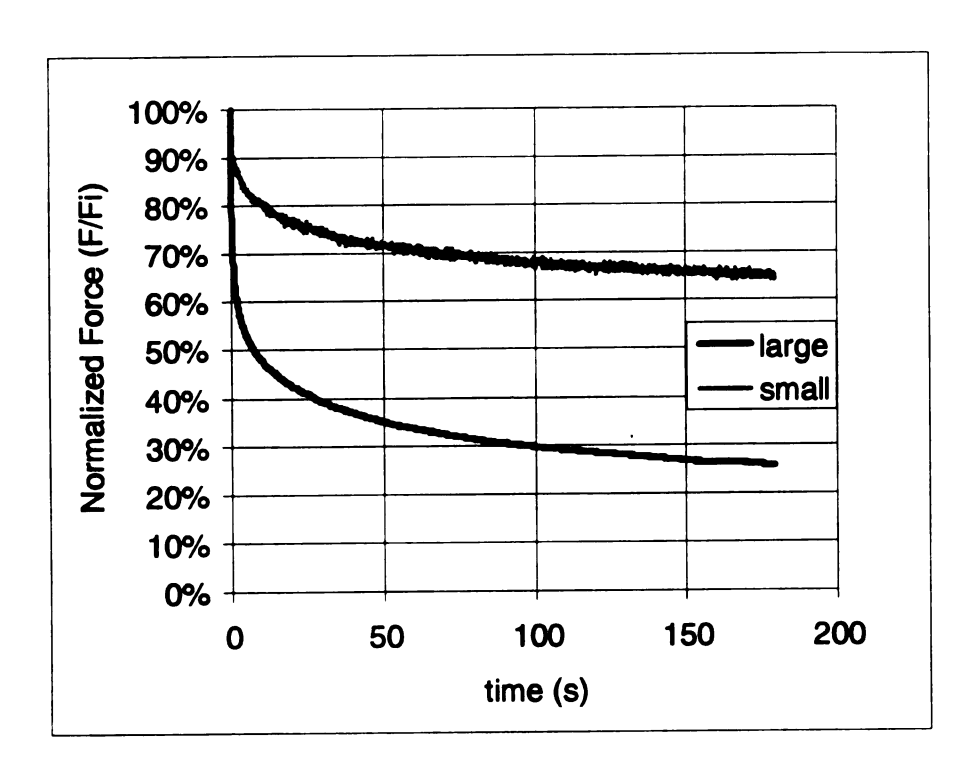


Figure 1

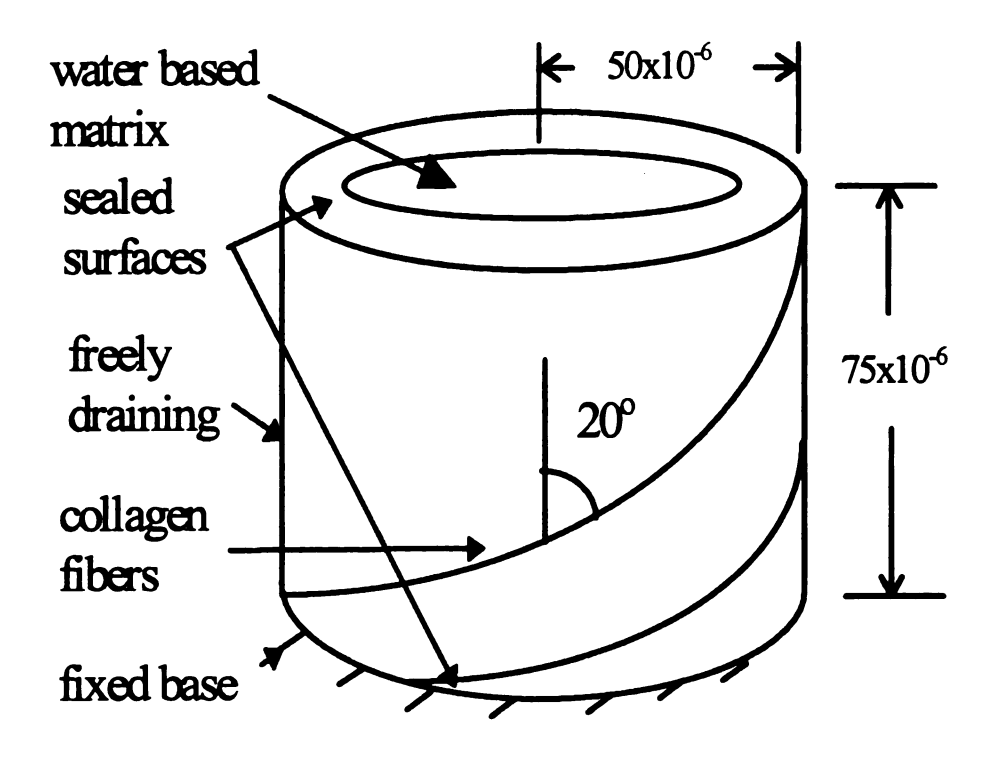


Figure 2

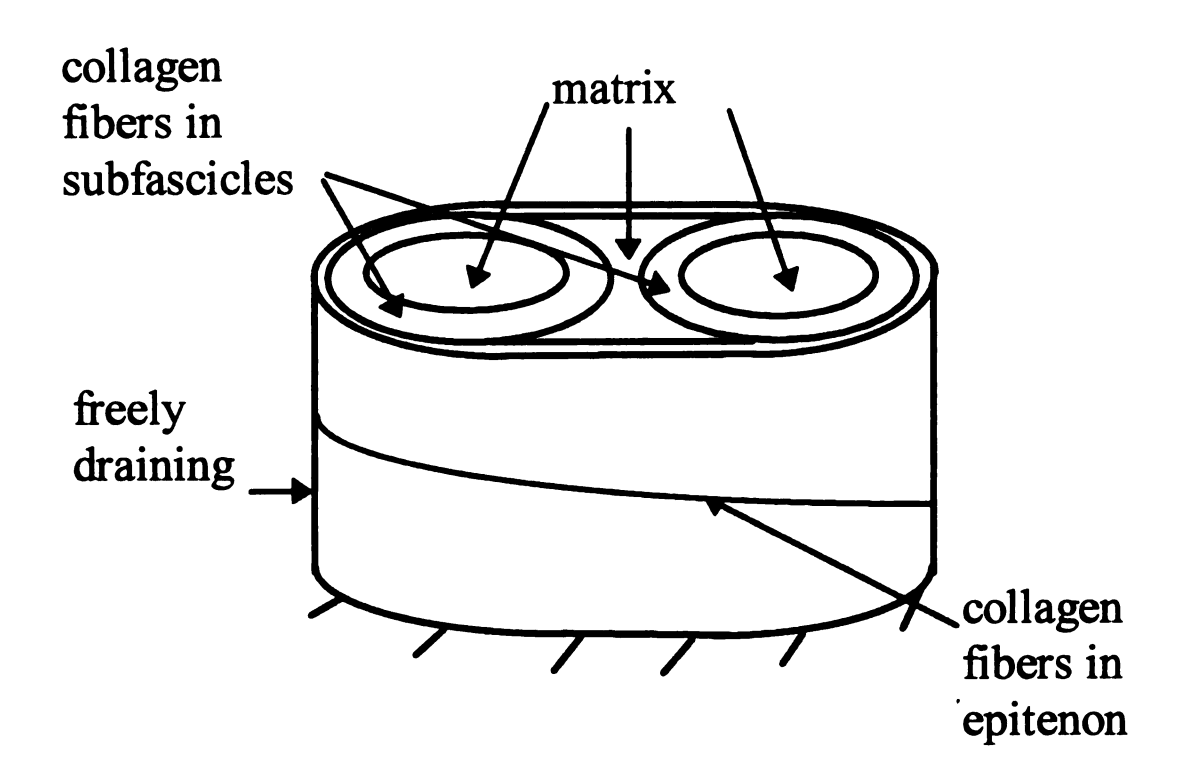


Figure 3

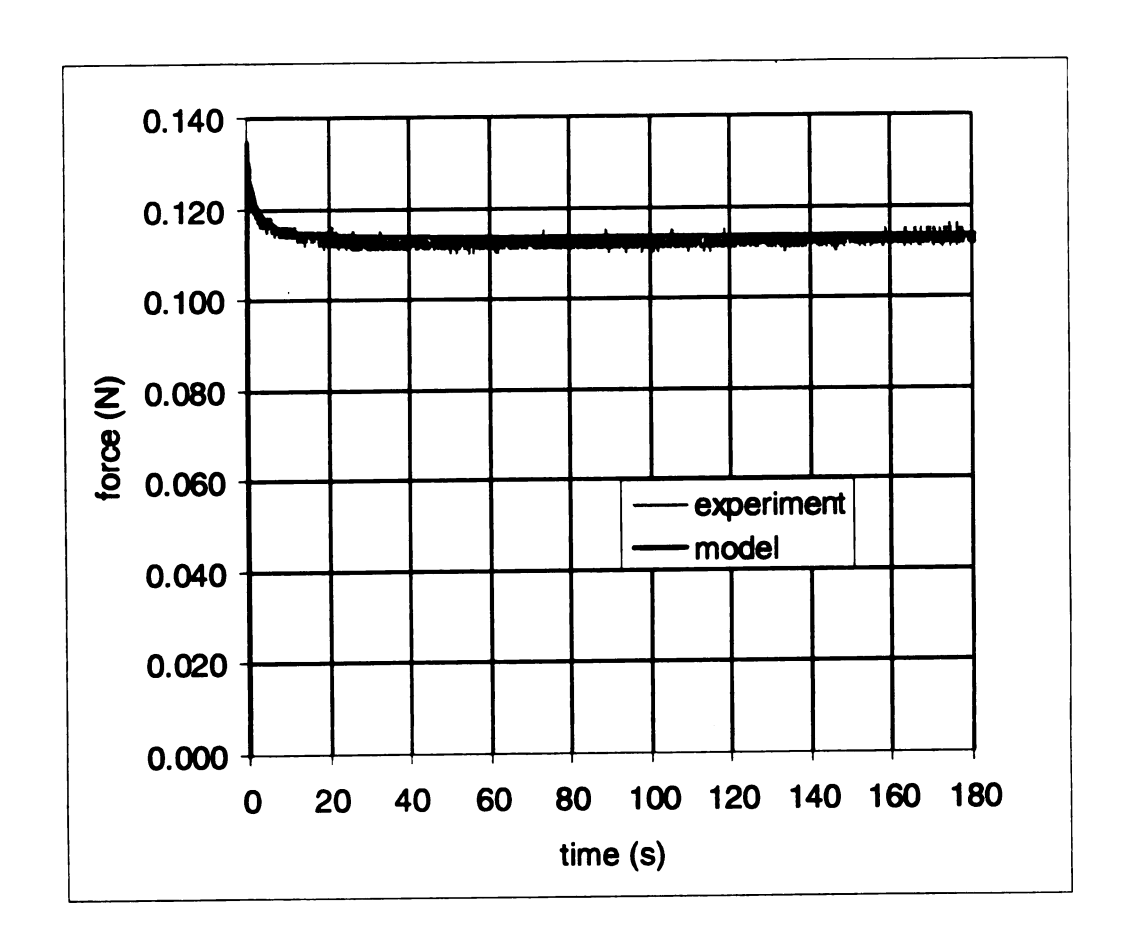


Figure 4

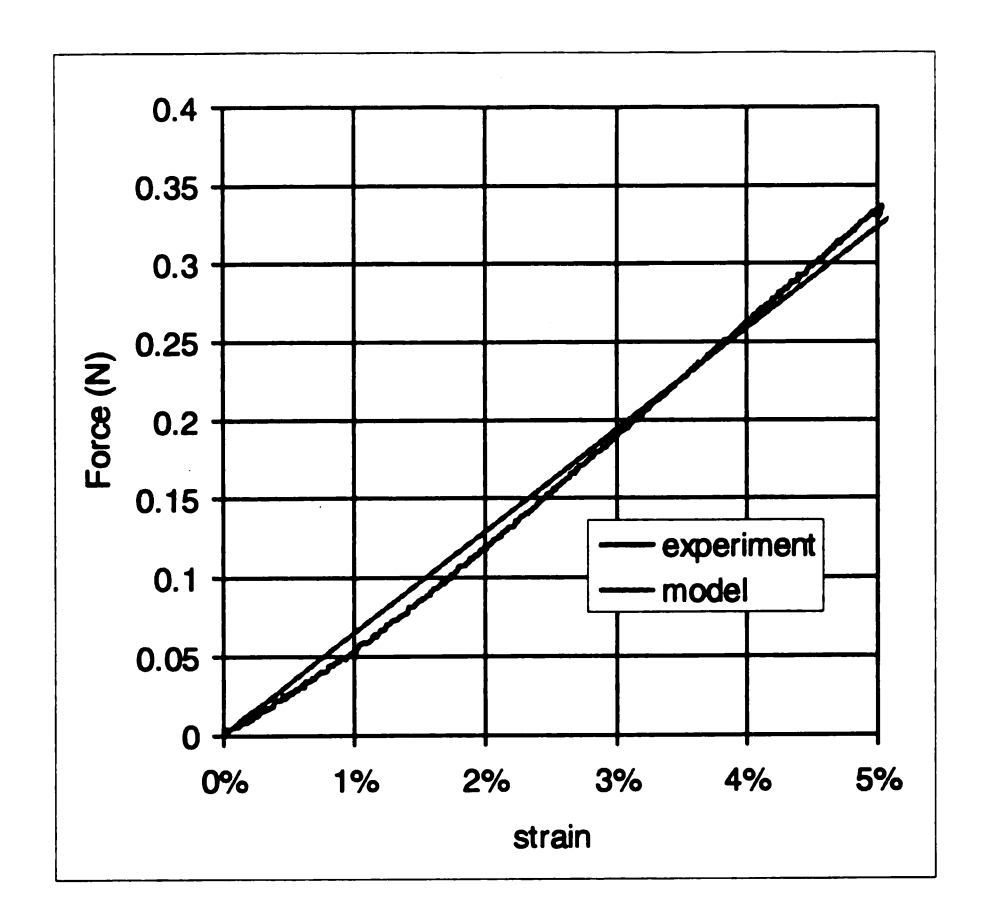


Figure 5

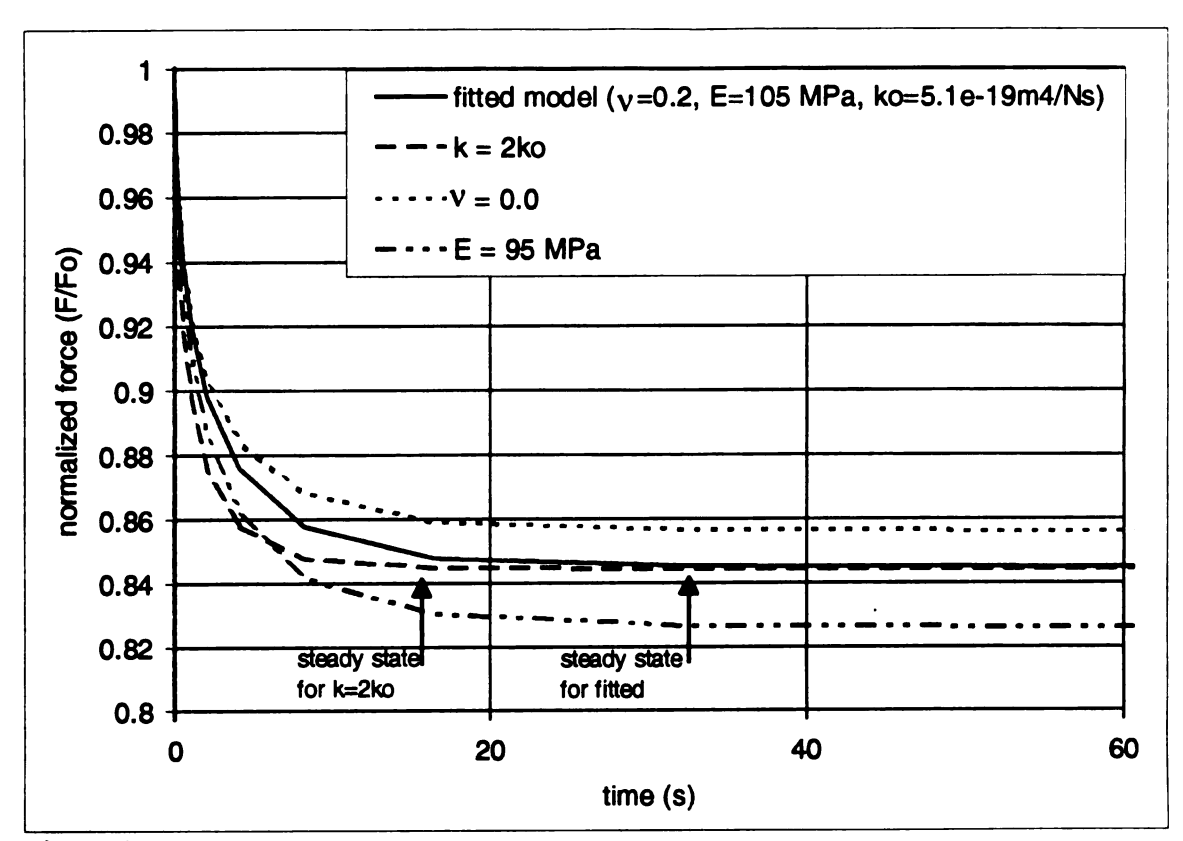


Figure 6

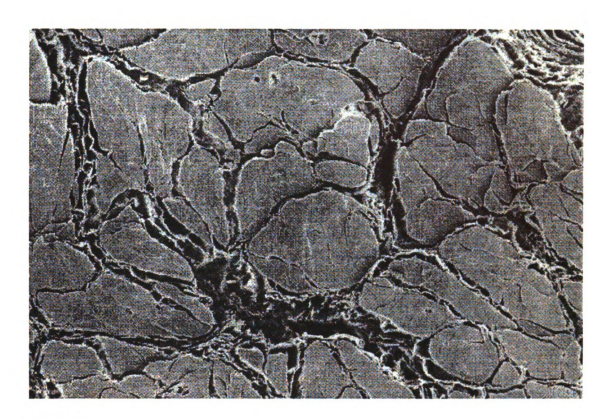


Figure 7a

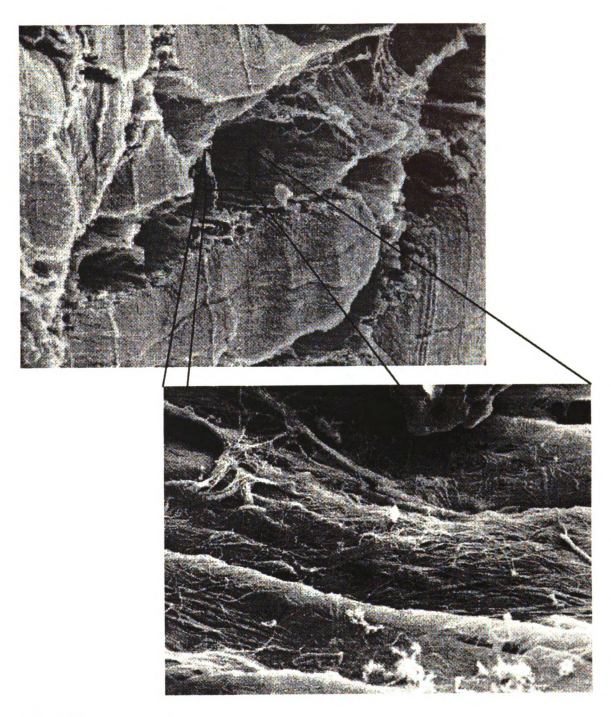


Figure 7 b

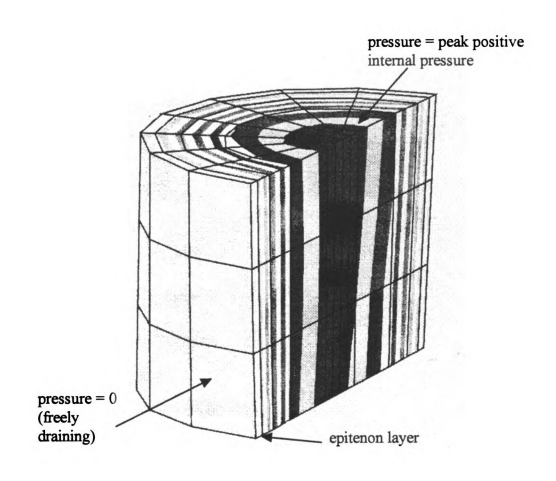


Figure 8

# Chapter 6:

# A Subfascicle Recruitment Model for Tendon

Theresa S. Atkinson

# ABSTRACT:

The tensile strength of tendon and ligament has been attributed to their collagen fasciculi. These fasciculi are composed of subfascicles. Previous finite element modeling of subfascicles suggested that these structures may be responsible for the time varying response exhibited by tendon. An analytic model for tendon, wherein subfascicles are sequentially recruited during tensile extension, was formulated in the current study. Relationships derived from the subfascicle finite element model described in Chapter 5 and from the experimental studies described in Chapter 4 were utilized to define the rate of subfascicle relaxation within the model. This model was able to fit experimental data obtained in a previous study. This fit suggested tissue hydration and subfascicular organization influence the relaxation response. The fitted model was also used to simulate creep. The creep simulation indicated that the experimentally observed difference in creep and relaxation (% creep < % relax) was possible if the rate of relaxation rapidly decreased with increasing strain.

### INTRODUCTION:

Analytic models for tendon and ligament have been developed to describe collagen fiber recruitment during elongation. These models, however, are incapable of predicting the time varying response. Quasi-linear viscoelastic theory has been successfully utilized to characterize the viscous response of the tissue (Kwan et al., 1993, Huang et al., 1997), however this model does not provide a characterization of the collagen structure.

Recently new models for tendon and ligament have been proposed which utilize poroelastic descriptions of the tissue, thereby including the fluid portion of the tissue

(Chen and Vanderby 1997, Atkinson et al, 1997). Chen and Vanderby's model treats the tendon as a continuum, neglecting structural influences. Atkinson et al's model of a collagen subfascicle (1997) provides a description of collagen fibers interacting with a hydrated matrix to produce the time varying response characteristic of tendon. While this model provides a useful interpretive tool, an extension of this model to describe whole tendon remains largely unattainable due to the computational complexity of such a model.

In the current study an analytic model for tendon was developed based on Belkoff and Haut's (1992) fiber recruitment model and on Atkinson et al's (1997) subfascicle finite element model. In this way the phenomenological response of the subfascicle was extended to describe whole tendon. In this model subfascicles are sequentially tensioned to produce the mechanical response of portions of tendon of arbitrary size. The model was fit to experimental data obtained in the study described in Chapter 4. The errors associated with the model's fit to the data were then assessed in order to examine the appropriateness of the model.

## **METHODS:**

The analytic model was based on an earlier model (Belkoff and Haut, 1992). In the current model it was assumed that the responses of tendon, or portions thereof, to elongation loads may be described by sequentially tensioned subfascicles. When the subfascicle finite element model was tensioned, water contained in the matrix was pressurized by the lateral compression of twisted collagen fibers. This caused fluid to move out of the subfascicle and the force generated by the subfascicle decreased. A similar force response was observed for tendon specimens with small cross sections tested

in the experimental study described in Chapter 4 (Figure 1). During a constant strain, stress relaxation test the normalized force, time response can be described by the function:  $F(t)/F_{peak} = -\alpha \ln(t/t_0) + \beta,$ 

where t is the time following subfascicle deformation,  $t_0$  is 1 second,  $\alpha$  is the dimensionless rate of relaxation, and the amount of relaxation (percentage) was characterized by  $\beta$ .

In simulated stress relaxation in the subfascicle FEM, the rate of relaxation was influenced by the peak strain level. This sensitivity was a result of the fiber geometry incorporated in the model, i.e. as the subfascicle finite element model was stretched, collagen fibers rotated and aligned with the applied load. The fibers therefore offered less lateral compression to the matrix. This reduced lateral compression resulted in a matrix which was less pressurized at the peak deformation and, as the fluid flow rate in the model is directly related to fluid pressure by Darcy's law, the relaxation rate decreased. A functional relationship between subfascicle strain and the rate of relaxation was derived by fitting a function through normalized relaxation rates obtained using the subfascicle model described in Chapter 2 to simulate relaxation at strain levels ranging from 1-12%:

$$\alpha' = \alpha \bullet (66.3\epsilon^2 + 1.7\epsilon + .99)$$
  $\delta/L \le 12\%$   
 $\alpha' = 0$   $\delta/L > 12\%.$ 

where  $\alpha$  is the rate of relaxation for small strains ( $\epsilon$ <1%),  $\alpha'$  is the modified rate of relaxation, and  $\epsilon$  is strain.

In the previous experimental study (Chapter 4) the amount a specimen relaxed (β) was found to be directly related to its rate of relaxation (Figure 2, reprinted from Chapter 4). This experimentally derived relationship was included in the analytic model:

$$\beta = 7.12\alpha' + .9903$$
.

where  $\varepsilon$  is the subfascicle strain and L is the initial specimen length.

In the analytic model each subfascicle was assumed to begin to relax as soon as it was recruited, thus the force generated by the subfascicle was described by the function:

$$F = k \bullet [\alpha' \ln(t/t_o) + \beta] \bullet \delta = k \bullet [\alpha' \ln(t/t_o) + 7.12 \alpha' + .9903] \bullet \delta,$$

where F [units: N] was the force generated by the subfascicle, k [N/mm] was the subfascicle stiffness and  $\delta$  [mm] was its elongation.

A Gaussian function was assumed to describe the recruitment of subfascicles during an extension  $\delta$ :

$$R(\delta) = \exp[(\delta - \mu)^2 / 2\sigma^2] / [\sigma \sqrt{2\pi}].$$

The μ parameter described the amount of deformation required to tension 50% of the subfascicles in the tissue. Sigma (σ) was the standard deviation of subfascicle recruitment lengths about that mean. This recruitment function multiplied by the increment of displacement yields the percentage of the total number of subfascicles present in the specimen which are recruited at any given extension. This percentage, multiplied by the total number of subfascicles tensioned for a given displacement. As the total number of subfascicles present in a sample of tendon may not be known (although it might be possible to estimate), the number of subfascicles and the subfascicle stiffness were combined. Given the total number of subfascicles in a specimen, the model would yield the average subfascicle stiffness.

The complete analytic model was therefore:

$$F(\delta,t) = k^{total} \sum_{i=\delta_o}^{\delta} \sum_{j=\delta_o}^{i} (\delta_i - \delta_j) (\delta_{j+1} - \delta_j) R(\delta_{j+1}) T(\delta_i - \delta_j, t_i - t_j),$$

where  $t_i$  -  $t_j$  is the time following the tensioning of a recruited group of subfascicles defined by  $R(\delta_j)(\delta_{j+1} - \delta_j)$ ,  $\delta_i$  -  $\delta_j$  is the elongation of the group,  $\delta_0$  is the initial deformation (generally zero),  $\delta$  is the current deformation, and F is the total force in the specimen at any time and displacement.

The modified sensitivity coefficients ( $\beta * dF/d\beta$ , where  $\beta = k$ ,  $\mu$ ,  $\sigma$ , and  $\alpha$ ) for the model parameters were plotted for both tensile extension and stress relaxation (Figure 3). These plots indicated that the  $\alpha$  and k terms were related (they exhibited similarly shaped sensitivity curves) during tensile extension, therefore the rate term ( $\alpha$ ) could not be distinguished from the stiffness term (k) using the tensile response. However, during relaxation the parameters were distinguishable. Therefore the parameters  $\mu$ ,  $\sigma$ , and k were obtained by fitting tensile experimental data using a nonlinear curve fitting procedure (Marquardt's method, Press, et al, 1988). The fitted  $\mu$ ,  $\sigma$ , and k values were then held constant and the relaxation response was simulated. If the relaxation response was too fast or too slow, a new rate of relaxation was assumed. This new rate was then utilized in a subsequent fitting of the  $\mu$ ,  $\sigma$ , and k values using the tensile test data. The iterative fitting process continued until the parameters converged and a fit to both tensile and relaxation responses was obtained.

The analytic model was fit to data obtained in previous testing of tendon as described in Chapter 4: the largest and smallest dissections of patellar tendons from the first series of tests and all specimens from the second series of tests. The fitted models

were used to obtain a simulated creep response for each specimen. The creep response was compared to the relaxation response.

Several further numerical exercises were performed in order to assess the ability of the model to reproduce the experimentally observed tensile and relaxation responses. The differences between the experimental data and the model (the residuals) were plotted for both relaxation and tensile tests so that any trends in the residuals might be identified.

Trends in the residuals signify systematic errors in the model. A sequential parameter estimation scheme was also utilized to obtain the model parameters for one specimen.

Here the model was initially fit using the first 490 data points, then 491 data points were considered and the parameter values obtained from the previous iteration were used as the initial "guess". This process continued until 500 data points were considered. The variation in each parameter was plotted versus the number of data points considered.

Trends in this plot also indicate systematic inadequacies in the model.

# **RESULTS:**

The analytic model was able to fit the tensile and relaxation responses exhibited by both small and large specimen (Figure 4). The fit was best in cases where the peak force in the relaxation experiment was similar to or less than that for the same deformation in the tensile tests. The specimen stiffness obtained from the model increased linearly with specimen cross sectional area (Figure 5). The rate of subfascicle relaxation increased nonlinearly with specimen cross sectional area (Figure 6). The deformation required to recruit 50% of the subfascicles ( $\mu$ ) of the smallest portions of tendon were much smaller than those of largest specimen, but there was no significant difference for the small and

large groups. There was a significant positive correlation between the model parameter  $\mu$  and the rate of relaxation (Figure 7). There was not a significant correlation between  $\mu$  and the percentage of fluid present in the specimen (the percentage of fluid was obtained in the experimental study described in Chapter 4).

When the creep was simulated with a fitted model the response was similar to the relaxation response (Figure 8). A reduced creep response, consistent with Thornton et al's (1997) observation, was obtained when a more rapid rate of change of the rate of relaxation ( $\alpha$ ) with respect to strain was assumed (a linear relationship:  $\alpha^{i} = \alpha^{i-1}(1-20*\epsilon,$  note  $\epsilon$  <5% for all simulations) (Figure 9).

The residual plots for all of the tensile tests exhibited a characteristic sinusoidal shape (Figure 10). The percent error in the fit was initially large, when the forces were small, but diminished with time and deformation (Figure 11). The signal error due to electrical noise was measured during a test where no specimen was in place. This error was similar in magnitude to the residuals from the model, however, there was no apparent pattern to this signal (Figure 12). The residual plots for all of the relaxation tests also exhibited a characteristic shape (Figure 13), and again the percent error in the fit diminished with time (Figure 14).

The parameters identified in the sequential estimation scheme tended to increase with increasing numbers of observations (Figure 15). This change was most significant for k and  $\mu$  which increased by 8% with the addition of 10 observations and was least significant for  $\alpha$  (not plotted) which did not change.

## **DISCUSSION:**

In the analytic model, the average subfascicle rate of relaxation was greater in specimens of larger cross section, similar to the gross rate of relaxation observed experimentally. This implies that each constituent subfascicle in a large specimen tended to relax at a faster rate than in a small specimen. A similar trend was observed when Atkinson et al. (1998) compared the response of a fascicle finite element model to that of a single subfascicle. The fascicle model suggested that the presence of connective tissue sheaths surrounding the fascicles in the large specimen might produce enhanced relaxation. As the specimen cross sectional area increases the amount of connective tissue present in the specimen increases (Figure 4, Chapter 5). This increased presence of connective tissue may explain the nonlinear increase in the relaxation response as specimen cross sectional area increased. The analytic model suggested that the increased rate was correlated with increased tissue disorganization as described by the  $\mu$  term in the model. An increased level of disorganization and structural variation might increase interaction between subfascicles and thereby increase the rate and amount of relaxation. As  $\mu$  and the percentage of fluid in the specimens were not correlated, it appears that both water content and the organization of subfascicles may increase the rate of relaxation.

The model also suggested that the stiffness of the specimen increased approximately linearly with increasing cross sectional area. The stiffness provided by the model is a steady state property, as the time varying character of the response is accounted for in  $\alpha$ . This linear trend suggests that the steady state modulus of tendon is nearly constant, not dependent on the cross section. This appears reasonable as this modulus

may be attributed to the collagen fibers within the specimen. The cross sectional areas of the specimens were measured using a constant pressure area micrometer which displaces fluid from the specimen. The cross sections measured might therefore be described as the "solid" or steady state cross sections, predominantly composed of collagen.

When the fitted model was used to examine the creep response, the creep and relaxation responses were similar. However when the rate ( $\alpha$ ) was assumed to decrease rapidly with increasing strain, the model predicted less creep than relaxation. This is essentially the mechanism proposed by Thornton et al. (1997), however the analytic model provides a tool with which the strain sensitivity of the time varying responses of the tissue might be described. Further experimental studies are required to investigate the influence of strain on the relaxation response, however pilot studies suggest a decreased relaxation response as the strain level increases.

The residuals plotted for the tensile simulation exhibit a sinusoidal nature (Figure 10). This error might be due to excitation of the natural frequency of the testing system. During this experiment the testing machine had to accelerate very quickly to achieve the constant rate of deformation desired in the test. Accelerations in the range of 80,000 m/s<sup>2</sup> were calculated using the experimental displacement data and sample rate. This sudden acceleration likely excited the natural frequency of the testing system causing a resonance to be superposed on the signal. A similar pattern of residuals was observed when Belkoff and Haut's (1992) model was fit to tensile test data for a rabbit patellar tendon tested at a similar displacement rate. This suggests that this error was an undesirable product of the test fixture and was not related to the modifications made to the model in the current

study. As the current model was able to describe the character of the tensile response and as the largest errors were close in magnitude to the signal error from the load cell, these errors likely do not present a serious problem for most applications.

When the residuals were examined in the stress relaxation simulation a large degree of error was again noted in the early portion of the response. This is consistent with the use of the natural logarithm - linear function to simulate the time rate of decay of the force. This function tends to positive infinity as time approaches zero. The function can therefore introduce significant error in the early response of the model. In previous studies (Fung et al., 1972) a series of exponentials was used to describe this time change. These functions are well behaved, equal to 1 at zero and tending to zero for longer times. It was demonstrated, however, that the coefficients in these series were not unique. In the future other relaxation functions should be evaluated to address this problem. However, the ability of the current function to fit the remainder of the data and it's relative simplicity have caused others to recommend it's use (Kwan et al., 1983).

In the sequential estimation scheme the stiffness and  $\mu$  parameters were found to increase with increasing numbers of observations, suggesting an inadequacy in the model. It is possible that the stiffening function used in the model (the equation used to decrease the rate as the deformation increases) was not sufficiently steep. The model thus requires a higher stiffness as more long term data is considered in order to maintain the linear force-elongation response at later time points. The need for a steeper function was also suggested by the creep simulations which showed creep equal to relaxation with the current model, contrary to experimental data (Thornton, et al., 1997). When a more

aggressive relaxation rate/ strain relationship was employed the creep response was surpressed and the model predicted less creep, consistent with Thornton et al.'s (1997) data. Further experimental studies are required to determine the appropriate peak strain-relaxation rate relationship.

While the present model was able to fit the experimental tensile and relaxation responses, several limitations exist within its development. The most important limitation was that the average rate of subfascicle relaxation was noted to vary with specimen cross section, but no explicit relationship was incorporated into the model. The model and Atkinson et al's previous experimental study (1998) suggest that the rate of relaxation increases with specimen cross section according to a natural logarithmic relationship. While the physical basis for this relationship is currently unknown, it appears reasonable to suggest that small increases in a specimen cross section at the "fascicular" level present a more significant increase in the complexity of the potential subfascicle interactions than similar increases at the "whole tendon" level. Further ultrastructural visualization and structural modeling may provide a more detailed understanding of this observed relation. In addition the model incorporates a rate of relaxation/amount of relaxation relationship, derived from experimental studies, which was attributed to the tissue hydration. Further experimental studies are required to confirm the source of this relationship and to further explore the influence of hydration.

In conclusion, the model was able to fit the available experimental data and may be used to simulate the creep response. Additional studies are required to develop explicit

relationships between trends observed in the model and the subfascicle morphology of the tested specimen.

## **REFERENCES:**

- Atkinson, T.S., Ewers, B. and Haut, R.C., 1998, The Tensile and Stress Relaxation Responses of Human Patellar Tendon Varies with Specimen Cross Sectional Area, submitted to *J. Biomechanics*, April 1998.
- Atkinson, T.S., Haut, R.C. and Altiero, N.J. (1997) A poroelastic model that predicts some phenomenological responses of ligaments and tendons. *J. Biomech. Eng.* 119, 400-405.
- Atkinson, T.S., Haut, R.C. and Altiero, N.J. (1996) A microstructural poroelastic model for patellar tendon. In *Proceedings of the 1997 Bioengineering Conference*, Sunriver, Oregon.
- Belkoff, S. M. and Haut, R.C., 1992, "Microstructurally based model analysis of  $\gamma$  irradiated tendon allografts", J. Othop. Res., Vol. 10, pp. 461-464.
- Chen, C., and Vanderby, R., 1997, A poroelastic model of streaming potential and interstitial fluid flow in ligament and tendon, In *Proceedings of the 1997 Bioengineering Conference*. Sun River, Oregon, pp. 185-186.
- Danylchuk, K.D., Finlay, J.B. and Krcek, J.P., 1978, "Microstructural organization of human and bovine cruciate ligaments", Clinical Orthopaedics and Related Research, No. 131, pp. 294-298.
- Elliott, D.H., 1965, Structure and function of mammalian tendons, *Biol. Rev.*, Vol. 40, pp. 394-421.
- Fung, Y.C., Perrone, N, and Anliker, M., editors, 1972, Biomechanics: Its Foundations and Objectives, Prentice-Hall, Inc.
- Huang, C., Wang, V.M., Cohen, N.P., Bucchieri, J.S., Pawluk, R.J., Pollock, R.G., and Mow, V.C., 1997, Nonlinear viscoelastic properties of the inferior glenohumeral ligament, In *Proceedings of the 1997 Bioengineering Conference*, Sunriver, Oregon.
- Kwan, M.K., Lin, T.H-C., and Woo, S. L-Y, 1993, "On the viscoelastic properties of the anteromedial bundle of the anterior cruciate ligament," *J. Biomechanics*, Vol. 26(4), pp. 447-452.
- Press, W.H., Flannery, B.P., Tevolsky, S.A., and Vetterling, W.T., 1988, "Modeling of Data" in *Numerical Recipes: The Art of Scientific Computing*, Cambridge Unversity Press, N.Y., pp. 498-525.

Strocchi, R., DePasquale, V., Gubellini, P., Facchini, A., Marcacci, M., Buda, R., Zaffagrini, S., and Rugger, A., 1992, The human anterior cruciate ligament: histological and ultrastructural observations, *J. Anat.*, Vol 180, pp. 515-519.

Thornton, G.A., Oliynyk, A., Frank, C.B., and Shrive, N.G., 1997, Ligament creep cannot be predicted from stress relaxation at low stress: A biomechanical study of the rabbit medial collateral ligament, *J. Orthop. Res.*, 15: 652-656.

#### FIGURES LEGENDS:

- Figure 1: Stress relaxation of a specimen tested in the study described in Chapter 4. The time rate of change of the force is fitted well by a natural logarithm function.
- Figure 2: The rate of relaxation and the percent relaxation of the specimen tested in Chapter 4 were linearly related.
- Figure 3: Modified sensitivity coefficients for the model parameters. The similarity between the  $\alpha$  and k curves for extension indicates that these parameters have a similar influence on the tensile response. The relaxation response was therefore used to obtain  $\alpha$ .
- Figure 4: Representative examples of the model's ability to fit experimentally obtained tensile and relaxation responses in specimens of both large and small cross sectional areas.
- Figure 5: The stiffness derived from the model increased linearly with cross sectional area.
- Figure 6: The average subfascicle rate of relaxation decreased with decreasing specimen cross sectional area.
- Figure 7: The average subfascicle rate of relaxation increased with increasing  $\mu$ , suggesting more disorganization (a longer toe region) led to faster rates of relaxation.
- Figure 8: The model predicted slightly less creep than relaxation for a typical tendon specimen.
- Figure 9: The model predicted significantly less creep than relaxation when the rate of relaxation was assumed to decay rapidly with increasing strain.
- Figure 10: The error in the model's fit to the tensile data exhibited a sinusoidal shape
- Figure 11: The error constituted a large percentage of the measurement initially, but at longer times and larger elongations it constituted a small percentage.
- Figure 12: Signal noise from the load cell used in the experiments during a tensile test when no specimen was in place.
- Figure 13: The error in the model's fit to the relaxation data decayed with time.
- Figure 14: The error was a large percentage of the measurement initially, then a smaller percentage later.
- Figure 15: The estimated parameter values increased with increasing numbers of observations.

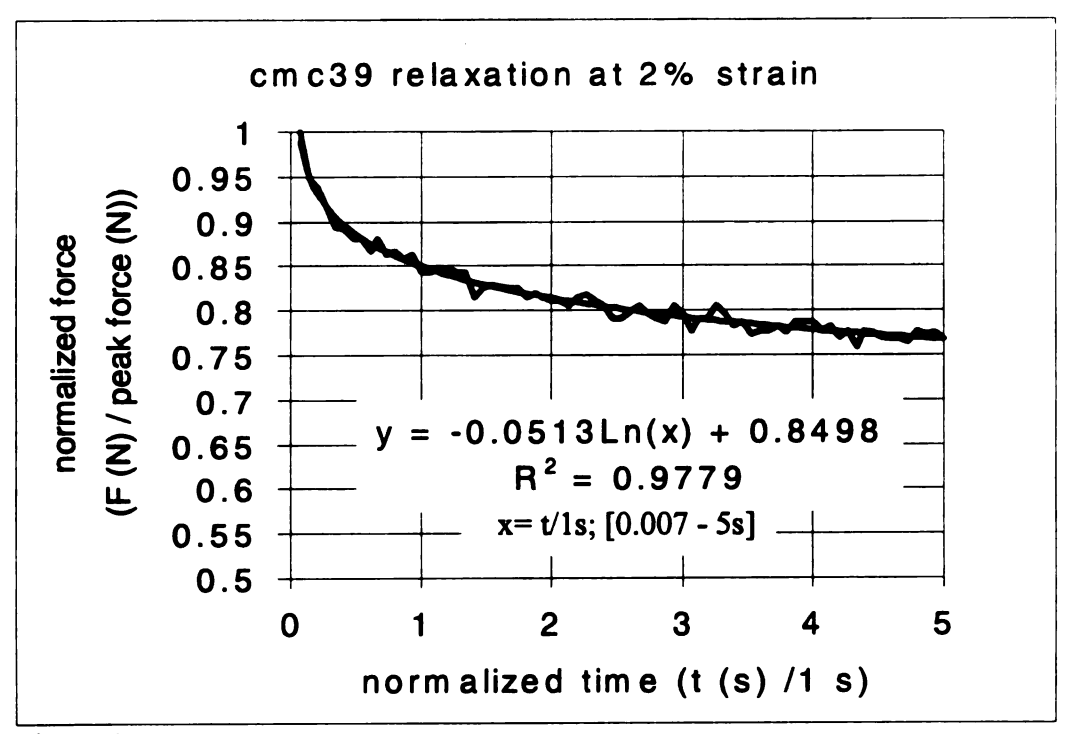


Figure 1

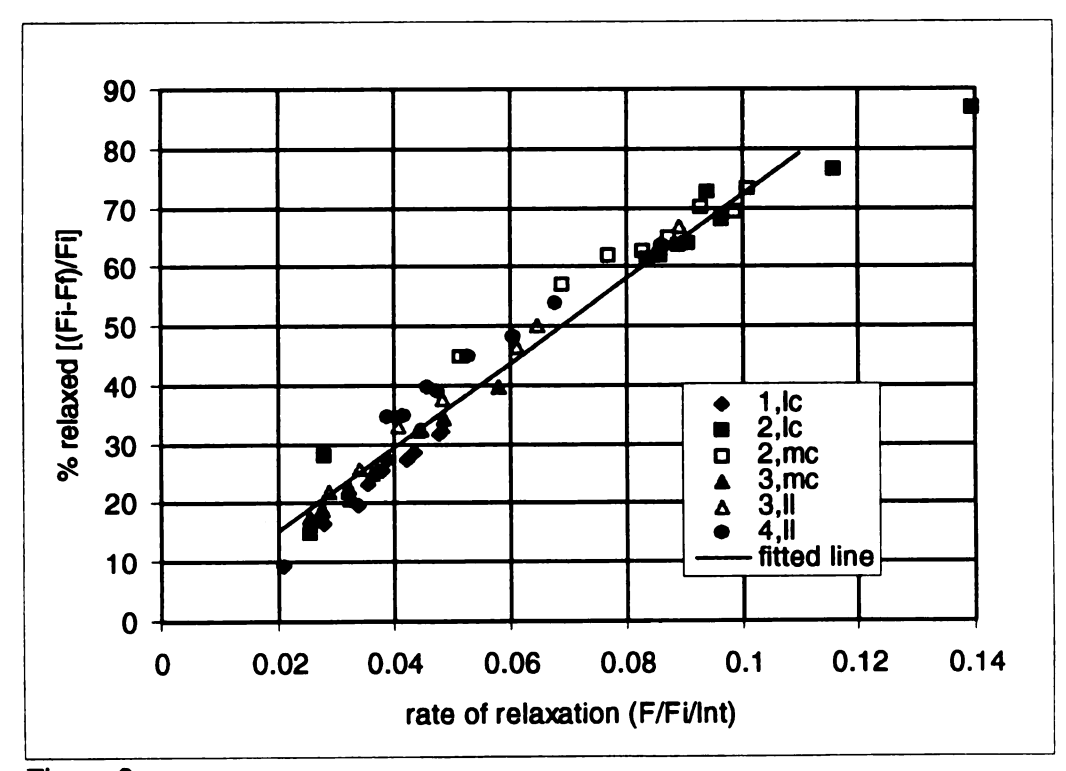


Figure 2

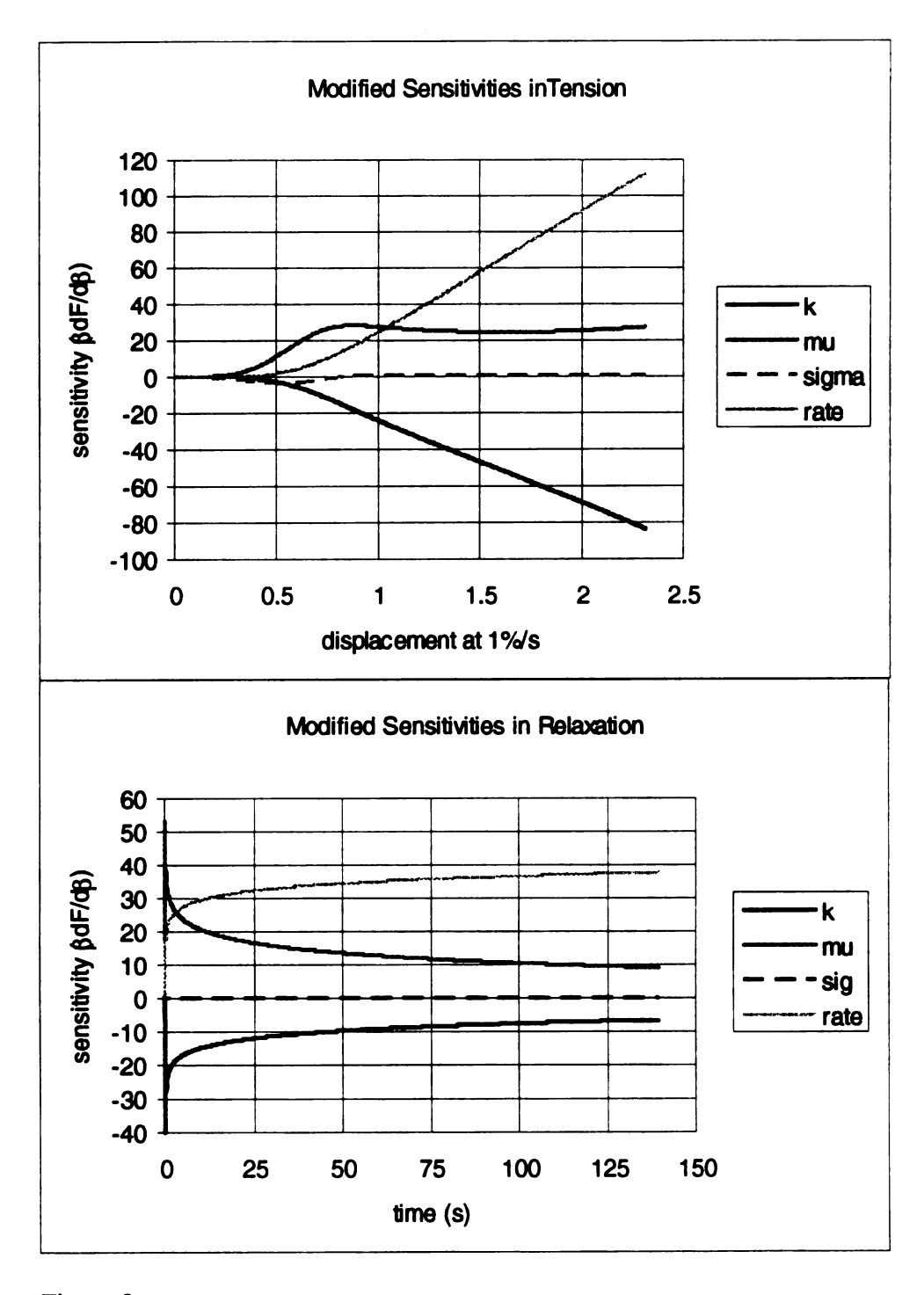


Figure 3

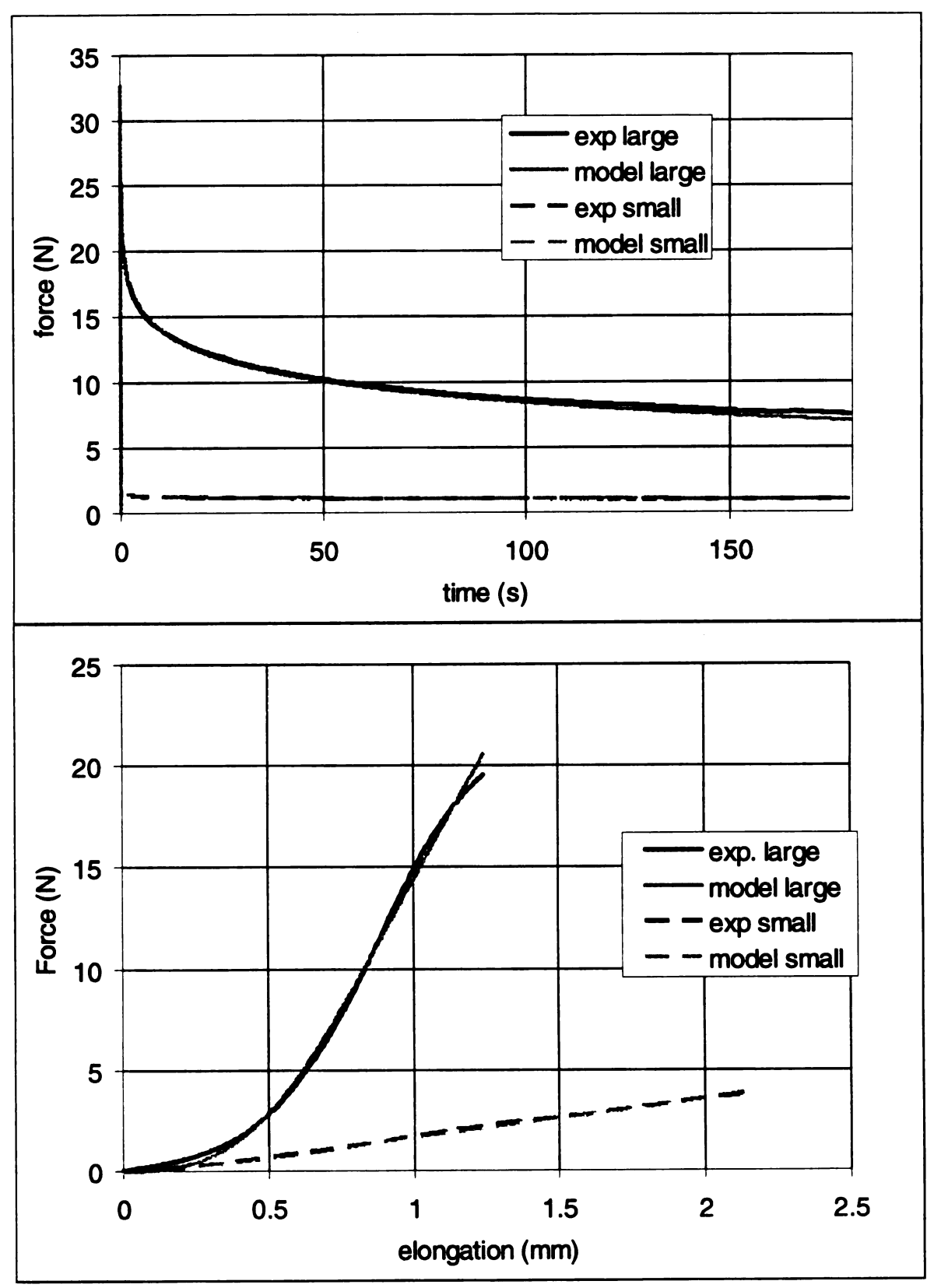
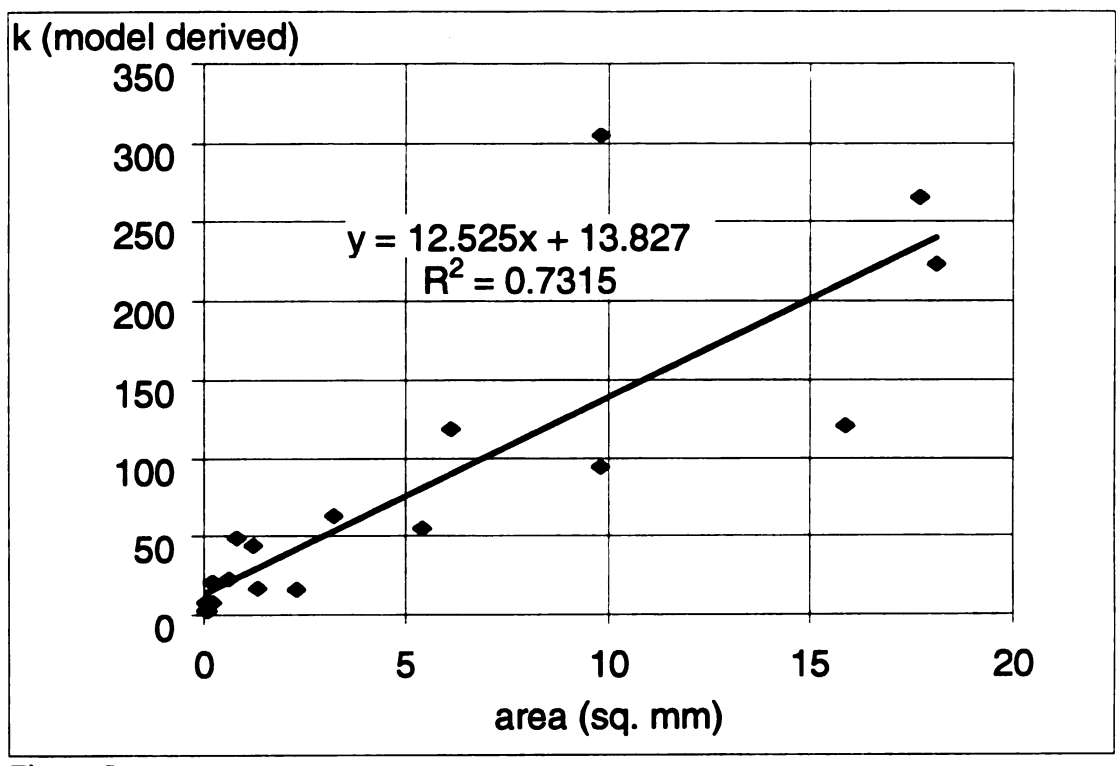


Figure 4



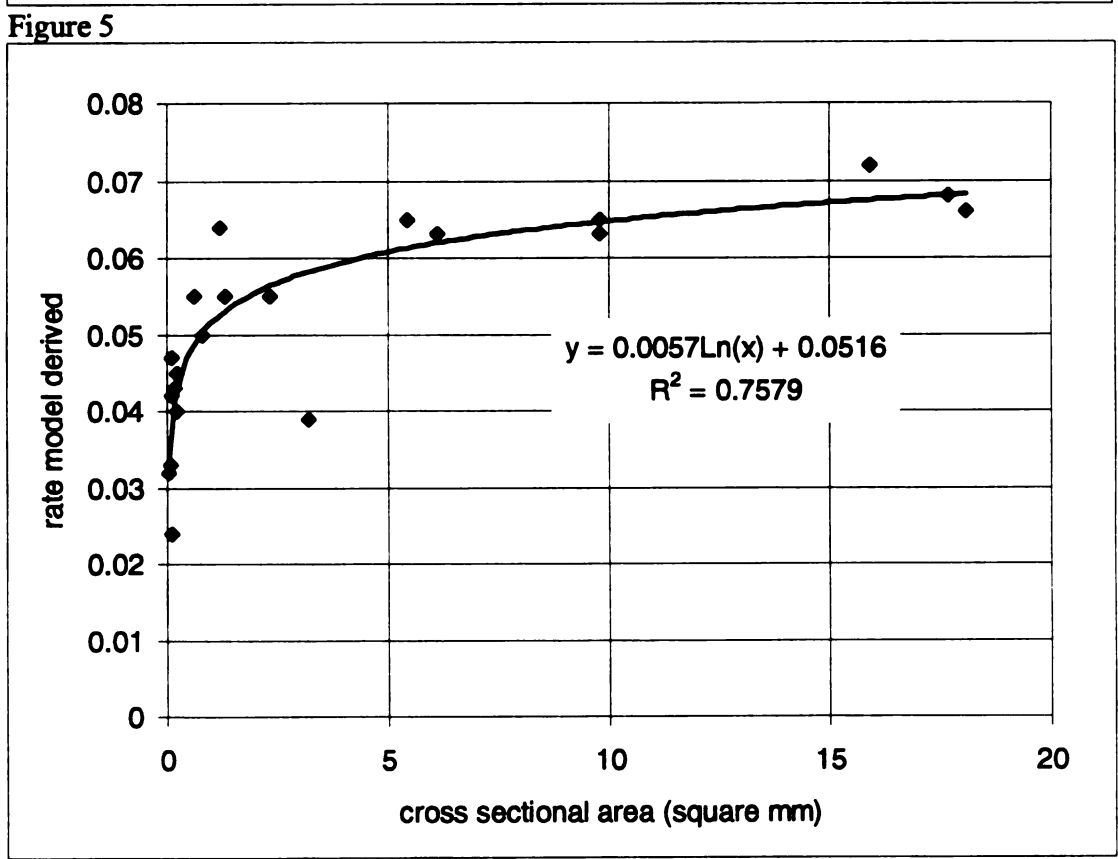


Figure 6

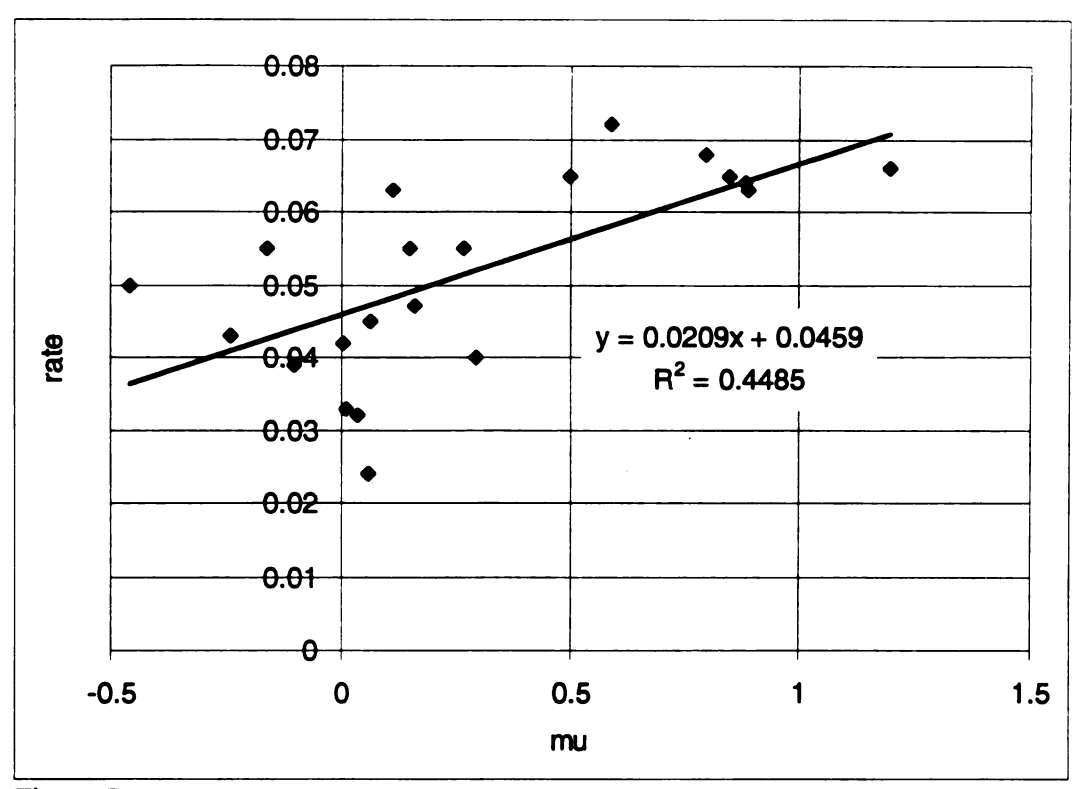


Figure 7

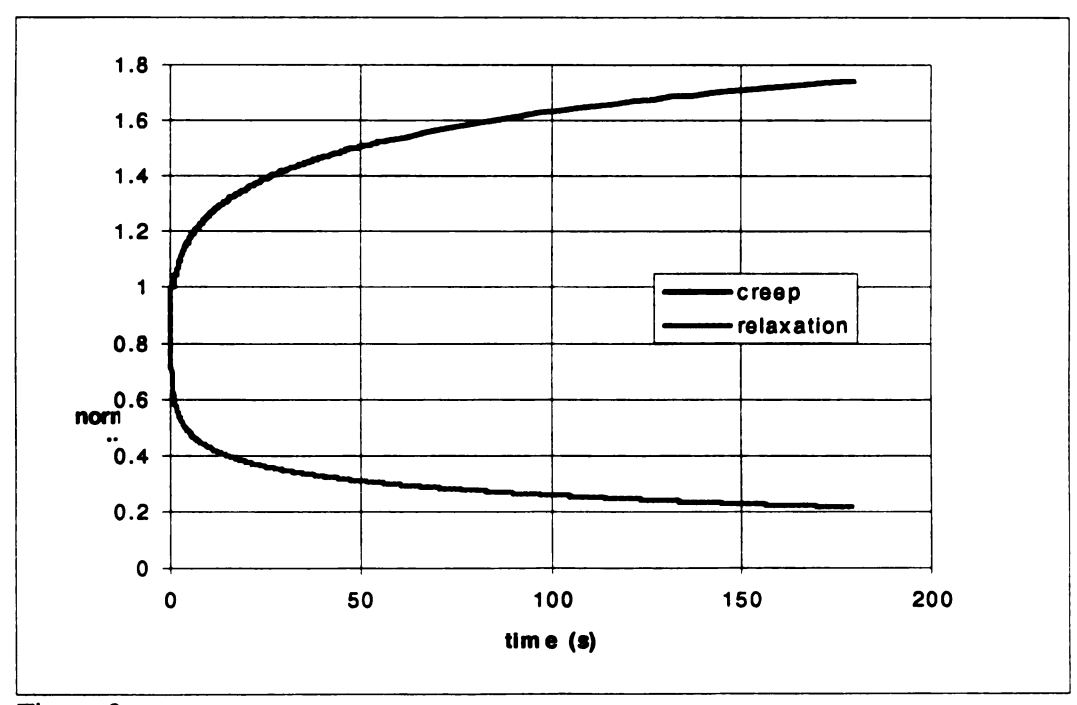


Figure 8

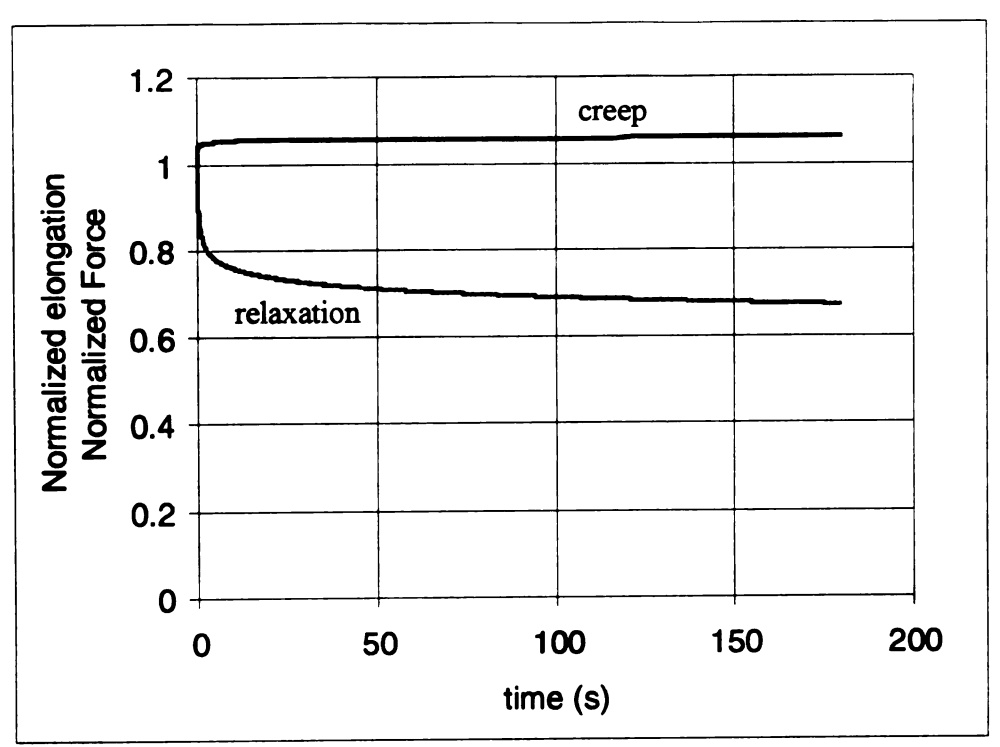


Figure 9

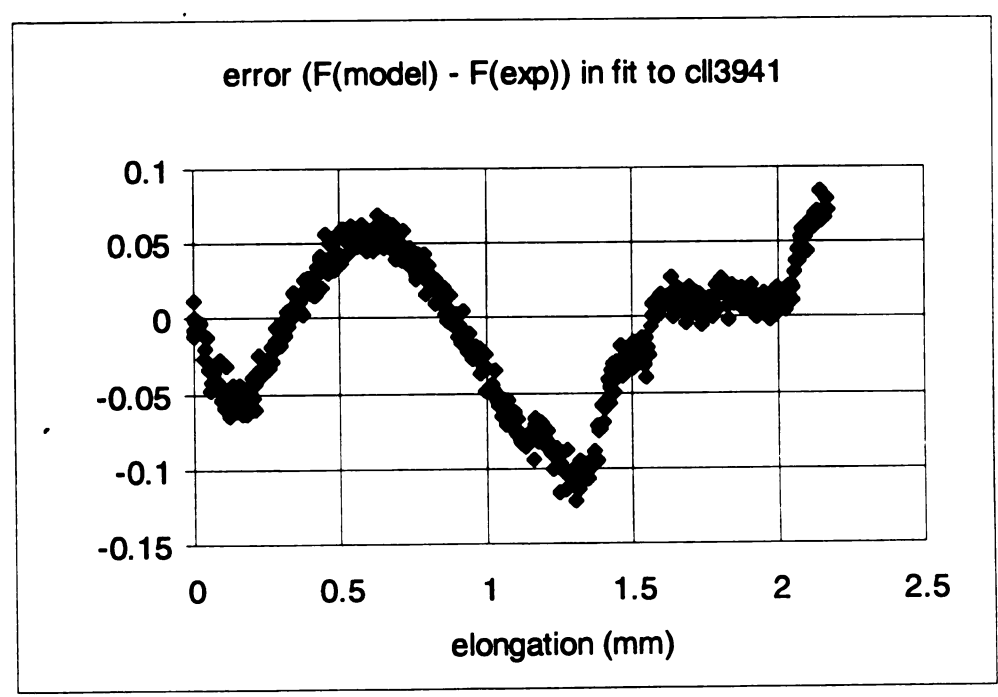
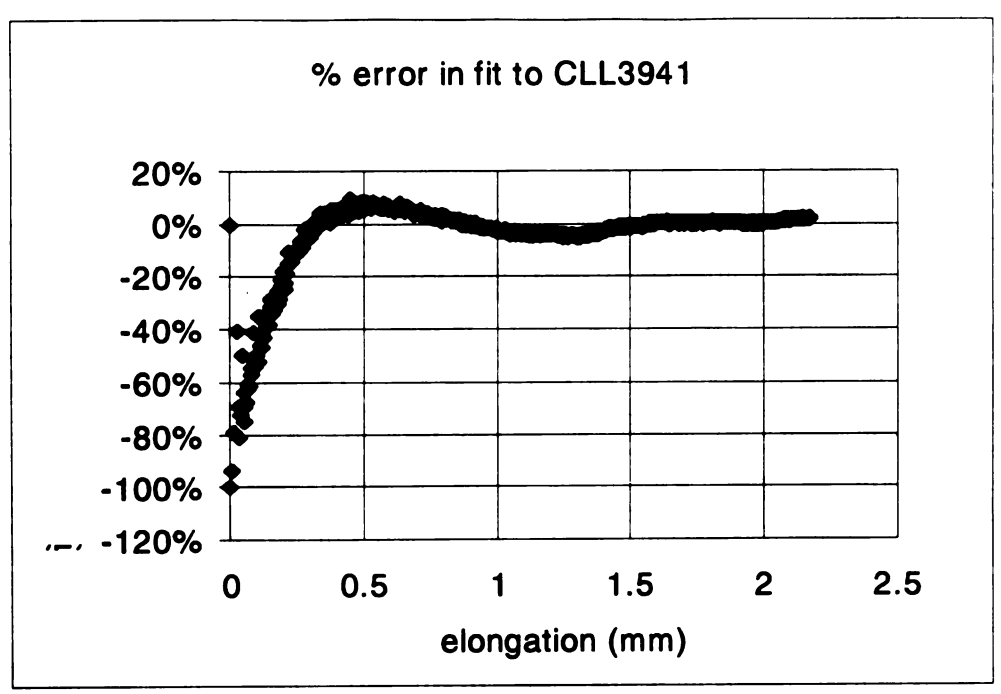


Figure 10



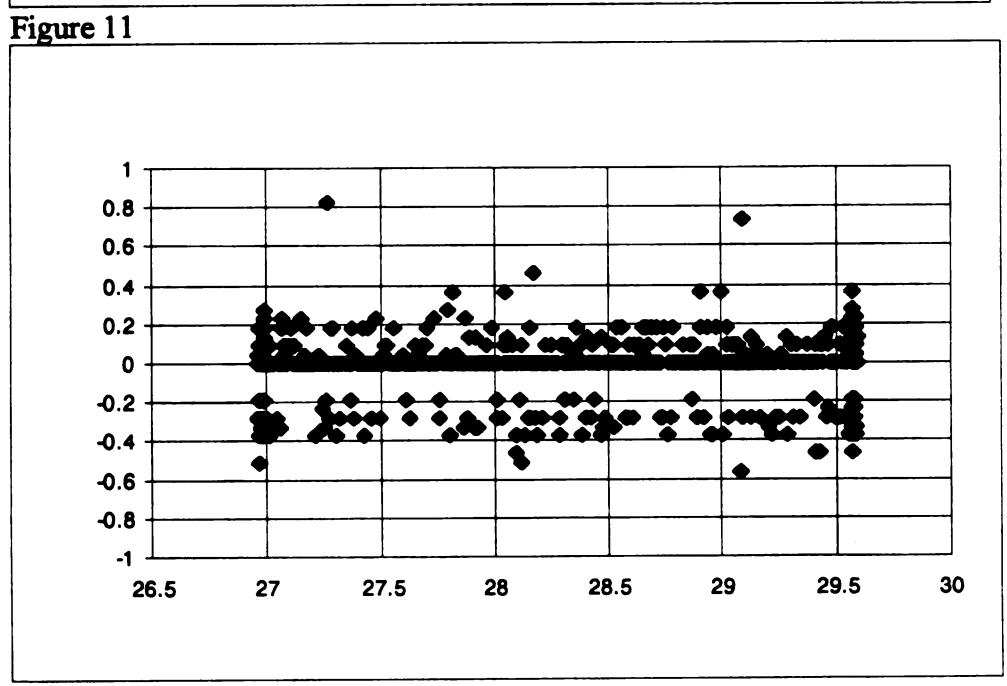


Figure 12

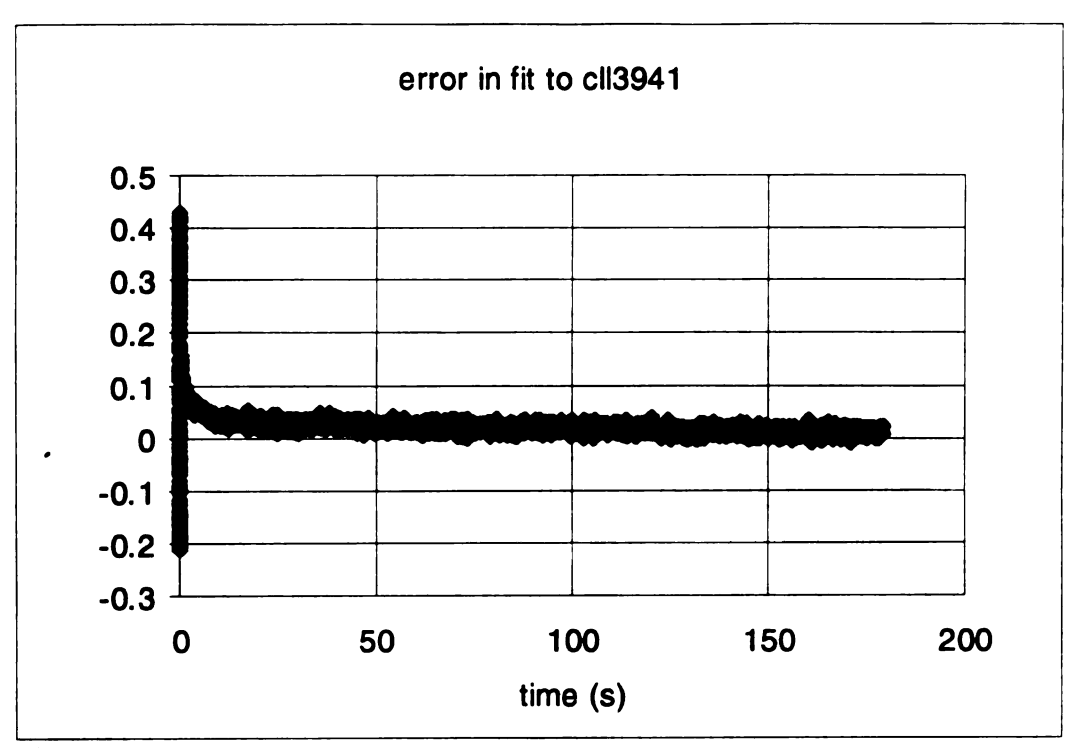


Figure 13

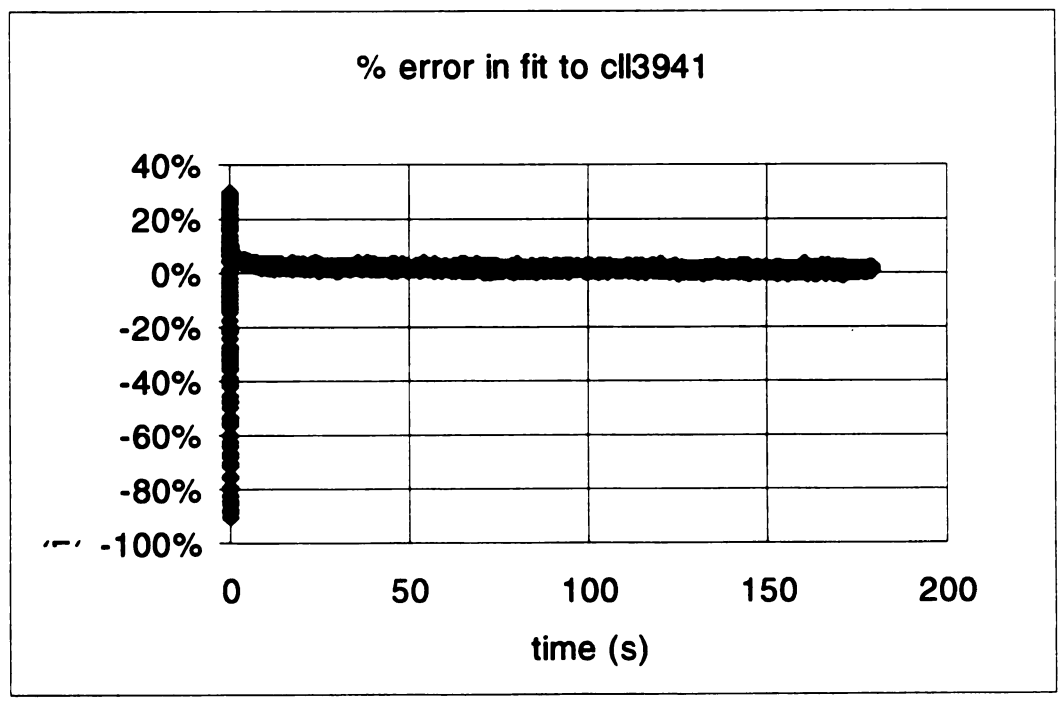


Figure 14

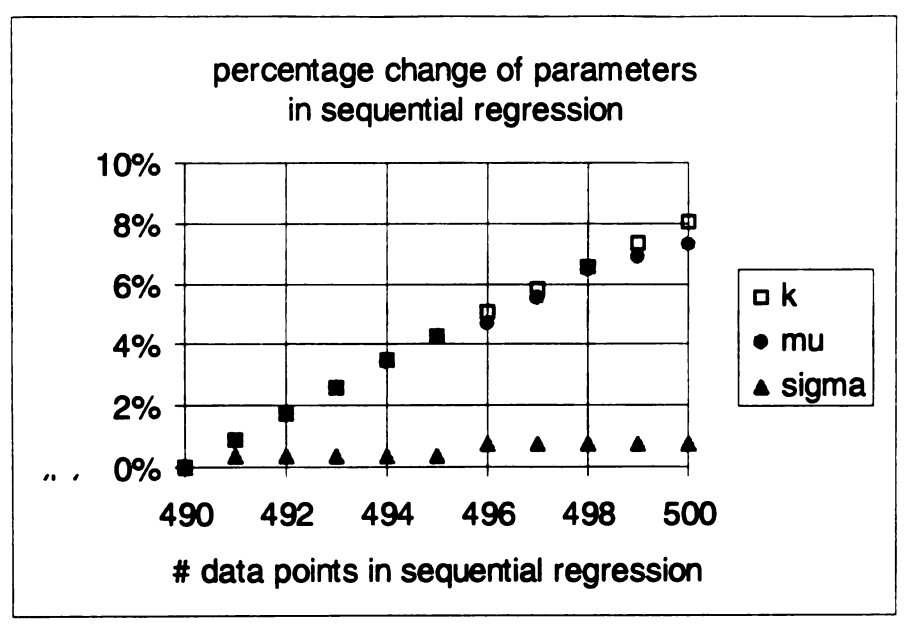


Figure 15

# Chapter 7:

# Conclusions and Recommendations for Future Work

Theresa S. Atkinson

The studies described in this dissertation represent a continuing effort to develop a structurally realistic model for tendon. Earlier efforts by other researchers focused on structural modeling of the collagen portion of the tissue without regard for the fluid portion. While these models were capable of reproducing the characteristic nonlinear tensile response of the tissue, they could not be used to quantify the influence of fluid in the tissue. The models described in this dissertation were based upon the concept that fluid motion in the tissue arises when the collagen fibers in the tissue to compress the fluid filled interstitial matrix. These models demonstrate that fluid motion at the subfascicular and fascicular level is likely important in the production of the observed time varying mechanical responses of tendon.

While the finite element models in Chapters 3 and 5 provided a reasonable description of a single fascicle or a simple fascicle, they remain far from a model of a whole tendon. At this time the computational power required to create a whole tendon model composed of hundreds of fascicle models poses a significant challenge. The finite element models described in this dissertation do, however, provide a tool which can be used to explore the mechanical responses associated with these microstructural elements. This type of information was used as the basis for the subfascicle recruitment model for tendon described in Chapter 6. Similar to previously posed collagen recruitment models, the analytic model provided a phenomenologic description of tendon and ligament. While the analytic model has the advantage of being relatively easy to apply to a variety of tissues, it requires validation and further development to provide a more explicit expression of the collagen/interstitial fluid interaction.

Although the studies contained in this dissertation shed light on the possible mechanical interactions of the fluid and solid portions of tendon, many issues remain to be explored. One issue raised in the course of this research was the potential importance of the connective tissues surrounding the fascicles in the production of the relaxation response. In order to investigate whether the continuous network of connective tissue in tendon (the epitenon) enhances the relaxation response, a set of pilot experiments were performed. The medial and lateral halves of a single human patellar tendon (78 year old male, congestive heart failure) were tested in distilled water. The test protocol was similar to that used in the experiments described in Chapter 4. Briefly, specimens were held at a constant strain of 2% for 180s in a relaxation test. Immediately following the relaxation test a tensile test was performed at a strain rate of 1% strain/second. Following the initial test, several slits were made along the length of the specimens such that each specimen was divided into eighths which remained connected to the bone blocks at each end. These slits in the tendon were intended to disturb the connective tissue network surrounding the subfascicles and thereby decrease the rate and amount of relaxation produced. The specimens were re-equilibrated in distilled water for 1 hour, then retested.

This protocol resulted in a reduced rate and amount of relaxation in the sectioned tendon in comparison with its intact response. The amount of relaxation was reduced by 14% in one case and 13% in the other. The rates of relaxation were reduced by 11% and 13%.

These results support the hypothesis that the system of connective tissue in tendon plays a role in the production of the relaxation response. However, further testing is

required. In these tests the pieces of the subdivided tendon were relatively large compared to the smallest specimen tested in Chapter 4. Further subdividing might produce larger differences in the relaxation response. The structure of the tested specimen should also be verified using microscopic or scanning electronic microscopic techniques.

Another area where further investigation is warranted is in the simulation of the creep response of the tissue. Thornton et al. (1997) found that the rabbit medial collateral ligament creeped less than it relaxed. They suggested that the mechanisms of creep and relaxation differ, with fiber reorientation limiting the creep response. In Chapter 6 of this dissertation the analytic model was used to examine creep. This work suggested that the tissue would creep less than it relaxed if the rate of relaxation decreased rapidly with increasing strain. In other words, if the decay of the stiffness of the tissue was limited as the strain increased, the creep would also be limited. A similar trend was identified in the subfascicle finite element model in a series of simulated experiments.

The simulated experiments were performed as follows. A relaxation test was simulated with a peak strain of 4% imposed. The peak force from this simulation was then imposed on the model in a separate simulated creep test.

Experiments with the model indicated that the subfascicle creeped *more* than it relaxed for smaller fiber orientation angles (more transverse orientations) (Table 1). At larger fiber angles (more axially aligned) the subfascicle creeped *less* than it relaxed. At a 75 degree fiber orientation, there was 75% more relaxation than creep. In this case, and in each case where the model creeped less than it relaxed, the rate of change of the rate of relaxation with strain was greater than that in cases with more creep (Figure 1). In the

cases with reduced creep, the rate of relaxation was slower than for cases where there was more creep (Figure 1). In order to examine whether the reduced creep response was a result of the relatively low amounts of relaxation noted in the 73-80 degree cases, another simulation was performed. The matrix modulus was decreased (for the 75 degree fiber angle case) to achieve an increased amount of relaxation. This increased relaxation did not result in increased creep (Table 1), suggesting that the creep response was more sensitive to the fiber orientation than to the relaxation response. The internal pressure in the model, which governs the rate of relaxation, was also lower in cases where less creep was noted (Figure 2). The pressure increased more slowly with increasing strain in cases with less creep.

The simulated experiments demonstrated that when the helical wrapping of the model's fibers about the matrix was reduced, the time variation of the axial force in the model was also reduced. This mechanism was similar to that suggested by Thornton et al.'s (1998) who found that the crimping of collagen was reduced following creep. This reduced crimp results in a more axially aligned collagen fibers which likely have limited interaction with the fluid filled matrix. The time variation of the force generated by the collagen was therefore reduced. In the future the creep and relaxation responses for human tendon should be examined. It will be important to examine the responses of specimens with both small and large cross sectional areas to determine whether the creep response originates in the subfascicle, or whether it varies with specimen cross sectional area similar to the relaxation response. It would also be valuable to examine the collagen fiber organization in specimens at the conclusion of relaxation and creep tests. This

information might shed further light on the role of the collagen morphology in the production of mechanical responses.

In addition to the efforts outlined above, further experimentation is required to expand the basis for the analytic model described in Chapter 6 and provide for its validation. Experimental development of a functional relationship between the rate of relaxation and the water content of the tissue is required. This work might involve measuring the permeability of the tendon via a confined compression creep test. Future validation of the analytic model might involve prediction of the creep response of a specimen using a model fit to its relaxation and tensile responses.

In conclusion, it is clear that further ultrastructural study and modeling of human and animal tendon microstructure is required. The studies contained in this dissertation provide a step in this process, but future studies will enhance our understanding of these tissues. As indicated throughout this final chapter, future research efforts should continue to focus the roles of fluid and collagen structure in the production of the mechanical responses of tendon and ligament. These efforts promise to continue to provide insights which will assist in the development of techniques and devices to maintain the optimal function of tendon and ligament.

#### References:

Thornton, G.A., Oliynyk, A., Frank, C.B., and Shrive, N.G., 1997, Ligament creep cannot be predicted from stress relaxation at low stress: A biomechanical study of the rabbit medial collateral ligament, *J. Orthop. Res.*, 15: 652-656.

Thornton, GM, Sutherland, CA, Barclay, LD, Leask, GP, Marchuk, LL, Frank, CB, Shrive, NG, 1998, Creep is resisted by fibre recruitement in ligament: Evidence from altered crimp patterns, *Trans. 44th An. Meeting Orthop. Res. Soc.*, pp. 45.

# Figure Legends:

Figure 1: The rate of relaxation decreased with increasing strain in the subfascicle model (with material properties as defined in Chapter 5 and with fiber angles of 70 and 75 degrees). Note that slower rates of relaxation occur with the 75 degree fiber angle. Also note that the rate of relaxation decreases more rapidly with increasing strain in the 75 degree case as compared to the 70 degree case.

Figure 2: The peak internal pressure in the subfascicle model (at the start of the creep test) increased with increasing peak strain (the point where the creep load was fully applied).

The internal pressure in the 75 degree case was lower than that in the 70 degree case. The rate of change of the peak internal pressure with increasing strain in the 75 degree case was less than in the 70 degree case.

# **TABLES:**

TABLE 1: Comparison of Relaxation and Creep

Δ <sub>θ</sub>	% relax	% creep
80 degrees	1.4%	1.2%
75 degrees	6.5%	1.6%
75 degrees, reduced $E_{\text{matrix}} = .8E_{\text{matrix}}$	7.5%	1.6%
73 degrees	9.7%	9.3%
70 degrees	13.4%	15.0%
60 degrees	24.1%	37.8%

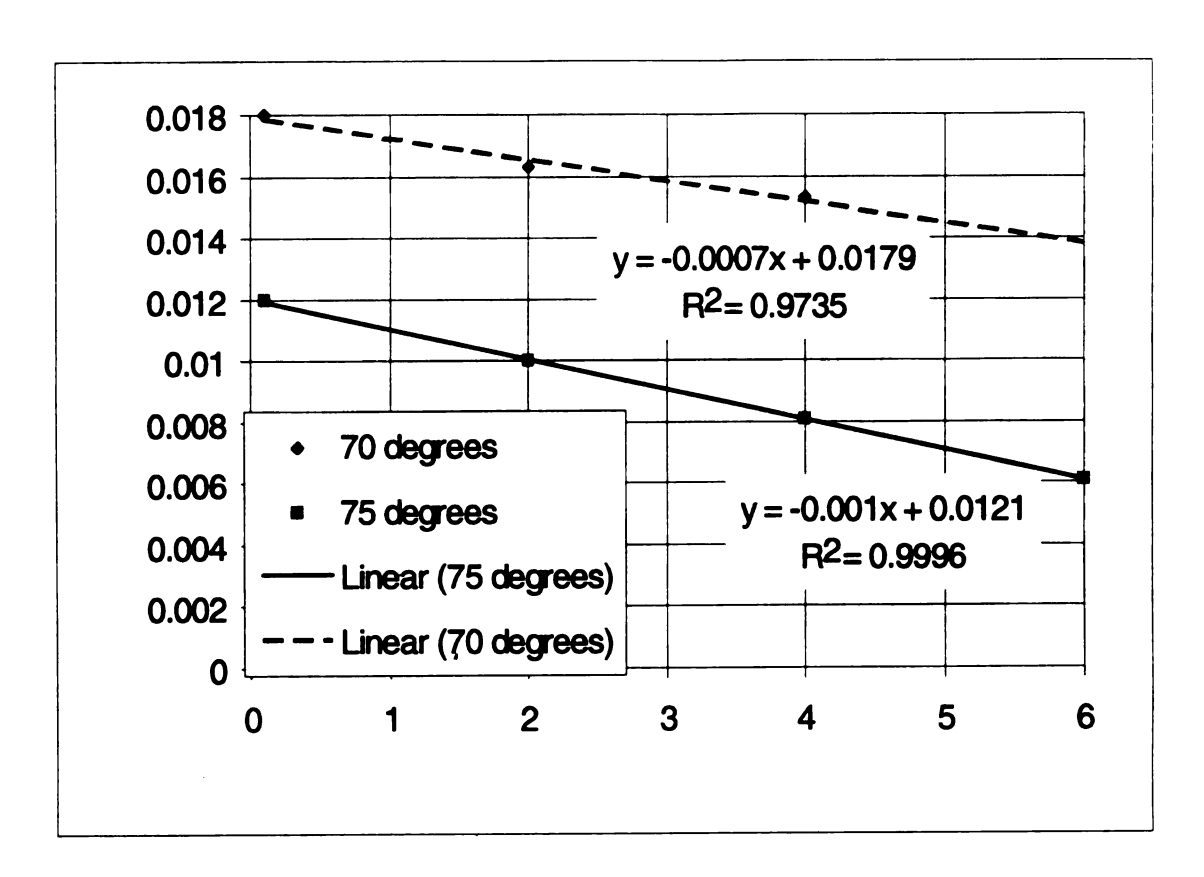


Figure 1

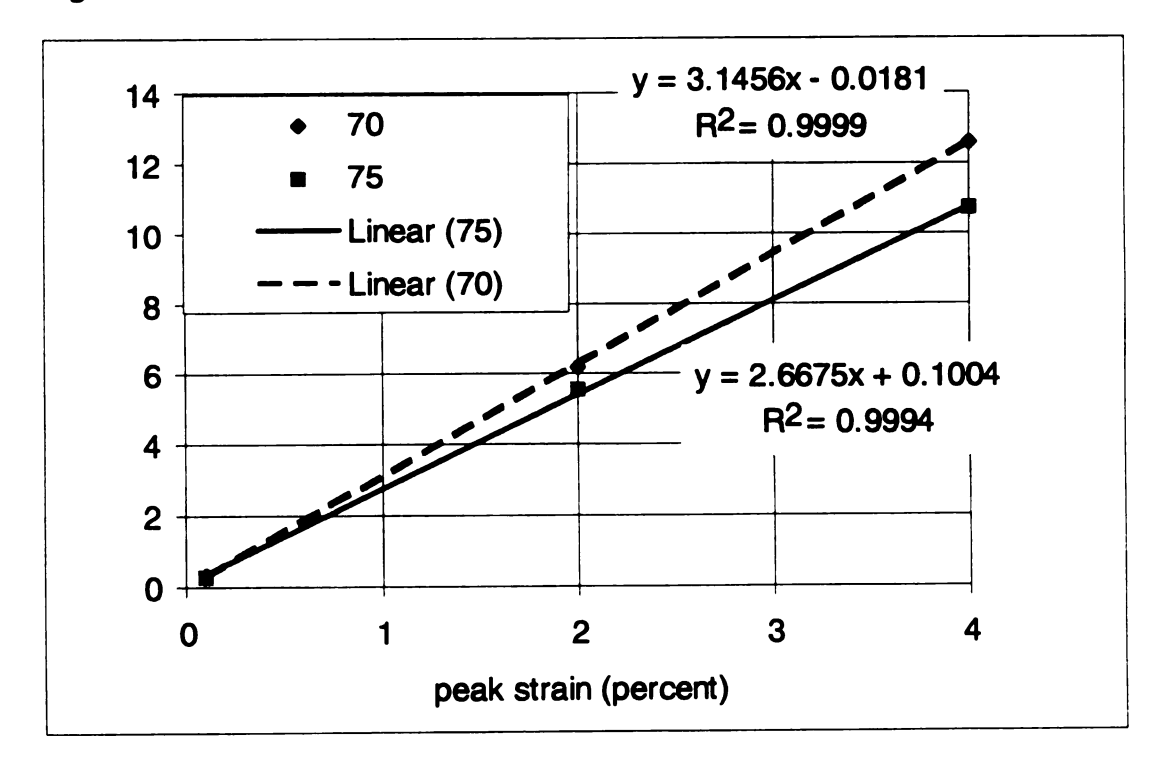


Figure 2

# APPENDIX A

Porous Elastic Material Behavior

The porous elastic material model was utilized in the original version of the subfasicle finite element model. This model was created to describe the behavior of certain clays which are highly compressible.

(1) de = -\kappad(lnp)

e = voids ratio
volume holes (fluid)/volume solid
p = fluid pressure

(2) 
$$\epsilon = \text{volumetric strain} = \epsilon_1 + \epsilon_2 + \epsilon_3 = -(e_0 - e)/(1 + e_0)$$

(3) 
$$d \in = -(\kappa/(1+e_0))d(\ln p)$$

integrate (3)

(4) 
$$\epsilon = -\kappa(\ln p)/(1+e_o)$$
  $e \qquad \qquad \kappa$ 

(5) 
$$\epsilon = \Delta V/V_0 = (V-V_0)/V_0 = V/V_0 - 1 = \ln p$$

(6) 
$$-\kappa(\ln p)/(1+e_o) = J - 1$$

(7) 
$$(\ln(1/p))\kappa/(1+e_0) = J-1$$

(8) 
$$1/p = (p_o + p_t)/(p + p_t)$$
 note:  $p_o$  is the initial stress, so that when  $p=0$  you get some stress, i.e.:  $lnp_o - ln0$   $ln(p_o + p_t) - ln(p_t)$ 

 $p_t$  is the tensile strength such that as p goes to  $-p_t$  (-p because you are pulling)  $V/V_o = \infty$ ,

The shear modulus of the materials is derived:

(9) 
$$de = -\kappa d(lnp) = -\kappa d\sigma_{mean}/\sigma_{mean}$$

(10) 
$$p = -\sigma_{mean}$$

(11) 
$$d(lnp) = dp/p = -d\sigma_{mean}/\sigma_{mean}$$

(12) 
$$d\sigma_{mean}/d\epsilon = K = = tangent bulk modulus$$

(13) recall 
$$d \in -(\kappa/(1 + e_o))d d\sigma_{mean}/\sigma_{mean}$$
 combine the derivative of (4) above with equation (11)

(14) 
$$K = \sigma_{mean}(1 + e_o) / - \kappa$$

(15) recall: 
$$K = E/(3(1-2v))$$
  $G=E/(2(1+v))$   
 $K = G2(1+v)/(3(1-2v))$ 

(17) 
$$G2(1+\upsilon)/(3(1-2\upsilon)) = \sigma_{mean}(1+e_o)/-\kappa$$
  
 $G = 3\sigma_{mean}(1+e_o)(1-2\upsilon)/(-2(1+\upsilon)\kappa)$   
recall:  $-\sigma_{mean} = p$ 

(18) 
$$G = 3(1+e_o)(1-2v)p/(2(1+v)\kappa)$$

In Abaqus p=p+p<sub>t</sub> as explained above and an additional term  $\exp(\epsilon^e_{vol})$  is added on,  $\epsilon^e_{vol} = \ln J^e$ 

therefore: 
$$G = \frac{3(1-2\upsilon)(1+e_o) \quad (p+p_t) \ J}{2(1+\upsilon)\kappa}$$

This was utilized in the first model because it provided a non-linear stiffening like tendon. The nonlinear poroelastic material stiffens upon compression. This is accomplished through moderation of the shear modulus in the following way:

$$G = \left[ \frac{3(1-2\nu)(1+e_o)}{2(1+\nu)\kappa} \right] \left( P + P_t \right) \exp\left(\varepsilon_{vol}^{el}\right)$$

where  $e_o$  is the initial voids ratio (volume fraction of fluid/volume fraction of solid), P is the internal pressure,  $P_t$  is the elastic ultimate strength,  $\epsilon^{el}_{vol} = \ln J^{el}$  is the elastic portion of volume change, v is Poisson's ratio, and  $\kappa$  is the log bulk modulus (relating the logarithm of pressure to the dilatation) (Abaqus Theory Manual, Zienkiewicz and Naylor, 1972). Thus, G increases with compaction and pressure. Assuming that the volume fraction of water in tendon is similar to the weight fraction (70% of the wet weight is water), an initial voids ratio of 2.33 (=.7/.3) was used for the nonlinear poroelastic portion of the model (Haut, 1993; Mow and Hayes 1991), however,  $e_0$ =1.0 (50%) was also investigated. Based on the assumption that fluid in tendon is similar to that in other tissues, the log bulk modulus of the nonlinear poroelastic core was obtained from data for fluid in the human annulus fibrosis (Best et al., 1984). Poisson's ratio was assumed to be 0.49. The tensile modulus of the material was then derived such that the initial shear modulus of the inner core approximately matched the shear moduli of the outer poroelastic ring.

## References:

Best, B. A., Setton, L. A., Guilak, A., Ratcliffe, A., Weidenbaum, M. and Mow, V. C., 1989, "Permeability and compressive stiffness of annulus fibrosus: variation with site and composition," *Trans. Orthop. Res. Soc.*, Vol. 14, p. 354.

Haut, R. C., 1993, "The mechanical and viscoelastic properties of the anterior cruciate ligament and of ACL fascicles," *The Anterior Cruciate Ligament: Current and Future Concepts*, (Edited by Jackson, D. W., et al.), Raven Press, Ltd., New York.

Mow, V. C., and Hayes, W. C., 1991, *Basic Orthopaedic Biomechanics*, Raven Press, Ltd., New York, New York, pp. 143-243.

Zienkiewicz, O.C. and Naylor, D.J., 1972, "The adaptation of critical state solid mechanics theory for use in finite elements", **Stress-Strain Behavior of Soils**, Parry, R.H.G. ed., Foulis and Co, , pp. 537-543.

## APPENDIX B

Subfascicle model Abaqus code

```
*heading.unsymm
**single tall fascicle
*node
9,-10e-6,-10e-6
81,10e-6,-10e-6
153,10e-6,10e-6
225,-10e-6,10e-6
288,-10e-6,-7.5e-6
*ngen
9,81,9
153,225,9
81,153,9
225,288,9
*node
289,-7.5e-6,-7.5e-6
295,7.5e-6,-7.5e-6
331,-7.5e-6,7.5e-6
337,7.5e-6,7.5e-6
*ngen
289,295,1
331,337,1
*nset,nset=cl,generate
289,295,1
*nset,nset=c2,generate
331,337,1
*nfill
c1, c2, 6, 7
*nset, nset=center,generate
9,288,9
*node
1,-42.4264e-6,-42.4264e-6
109,60e-6,0
181,0,60e-6
280,-49.88818e-6,-33.33421e-6
*ngen.line=c
1,109,9,313
109,181,9,313
181,280,9,313
*nset, nset=outer,generate
1,280,9
*nfill,bias=.95
outer, center, 8,1
*nset, nset=bottom,generate
1,337
**
```

```
*node
2409,-10e-6,-10e-6,75e-6
2481,10e-6,-10e-6,75e-6
2553,10e-6,10e-6,75e-6
2625,-10e-6,10e-6,75e-6
2688,-10e-6,-7.5e-6,75e-6
*ngen
2409,2481,9
2553,2625,9
2481,2553,9
2625,2688,9
*node
2689,-7.5e-6,-7.5e-6,75e-6
2695,7.5e-6,-7.5e-6,75e-6
2731,-7.5e-6,7.5e-6,75e-6
2737,7.5e-6,7.5e-6,75e-6
*ngen
2689,2695,1
2731,2737,1
*nset,nset=clt,generate
2689,2695,1
*nset,nset=c2t,generate
2731,2737,1
*nfill
c1t,c2t,6,7
*nset, nset=centert,generate
2409,2688,9
*node
2401,-42.4264e-6,-42.4264e-6,75e-6
2509,60e-6,0,75e-6
2581,0,60e-6,75e-6
2680,-49.88818e-6,-33.33421e-6,75e-6
*ngen,line=c
2401,2509,9,2713
2509,2581,9,2713
2581,2680,9,2713
*nset, nset=outert,generate
2401,2680,9
*nfill,bias=.95
outert, centert, 8,1
*nset,nset=top,generate
2401,2737,1
*nfill
bottom,top,6,400
```

## \*element,type=C3d20RP 1,297,299,313,311,1097,1099,1113,1111,298,306,312,304, 1098.1106.1112.1104.697.699.713.711 2,299,301,315,313,1099,1101,1115,1113,300,308,314,306, 1100,1108,1114,1106,699,701,715,713 3,313,315,329,327,1113,1115,1129,1127,314,322,328,320, 1114,1122,1128,1120,713,715,729,727 4,311,313,327,325,1111,1113,1127,1125,312,320,326,318, 1112,1120,1126,1118,711,713,727,725 5,9,27,297,279,809,827,1097,1079,18,290,296,288, 818,1090,1096,1088,409,427,697,679 6,27,45,299,297,827,845,1099,1097,36,292,298,290, 836,1092,1098,1090,427,445,699,697 7,45,63,301,299,845,863,1101,1099,54,294,300,292, 854,1094,1100,1092,445,463,701,699 8,63,81,99,301,863,881,899,1101,72,90,302,294, 872,890,1102,1094,463,481,499,701 9,279,297,311,261,1079,1097,1111,1061,296,304,310,270, 1096,1104,1110,1070,679,697,711,661 10,301,99,117,315,1101,899,917,1115,302,108,316,308, 1102,908,1116,1108,701,499,517,715 11,261,311,325,243,1061,1111,1125,1043,310,318,324,252, 1110,1118,1124,1052,661,711,725,643 12,315,117,135,329,1115,917,935,1129,316,126,330,322, 1116,926,1130,1122,715,517,535,729 13,243,325,207,225,1043,1125,1007,1025,324,332,216,234, 1124,1132,1016,1034,643,725,607,625 14.325.327.189.207.1125.1127.989.1007.326.334.198.332. 1126,1134,998,1132,725,727,589,607 15,327,329,171,189,1127,1129,971,989,328,336,180,334, 1128,1136,980,1134,727,729,571,589 16,329,135,153,171,1129,935,953,971,330,144,162,336, 1130,944,962,1136,729,535,553,571 \*element,type=c3d20rp 17,7,25,27,9,807,825,827,809,16,26,18,8,816,826,818,808, 407,425,427,409 32,277,7,9,279,1077,807,809,1079,286,8,288,278, 1086,808,1088,1078,677,407,409,679 33,5,23,25,7,805,823,825,807,14,24,16,6, 814,824,816,806,405,423,425,407 48,275,5,7,277,1075,805,807,1077,284,6,286,276, 1084,806,1086,1076,675,405,407,677 49,3,21,23,5,803,821,823,805,12,22,14,4,812,822,814,804, 403,421,423,405

64,273,3,5,275,1073,803,805,1075,282,4,284,274,

```
1082,804,1084,1074,673,403,405,675
65,1,19,21,3,801,819,821,803,10,20,12,2,810,820,812,802,
401,419,421,403
80.271.1.3.273.1071.801.803,1073,280,2,282,272,
1080,802,1082,1072,671,401,403,673
*elgen
17,15,18,1,1,1,1,3,800,80
33,15,18,1,1,1,1,3,800,80
49,15,18,1,1,1,1,3,800,80
65,15,18,1,1,1,1,3,800,80
*elgen
1,1,1,1,1,1,3,800,80
2,1,1,1,1,1,3,800,80
3,1,1,1,1,1,3,800,80
4,1,1,1,1,1,3,800,80
5,1,1,1,1,1,3,800,80
6,1,1,1,1,1,3,800,80
7,1,1,1,1,1,3,800,80
8,1,1,1,1,1,3,800,80
9,1,1,1,1,1,3,800,80
10,1,1,1,1,1,3,800,80
11,1,1,1,1,1,3,800,80
12,1,1,1,1,1,3,800,80
13,1,1,1,1,1,3,800,80
14,1,1,1,1,1,3,800,80
15,1,1,1,1,1,3,800,80
16,1,1,1,1,1,3,800,80
32,1,1,1,1,1,1,3,800,80
48,1,1,1,1,1,3,800,80
64,1,1,1,1,1,3,800,80
80,1,1,1,1,1,3,800,80
*elset,elset=matrix,generate
1,48
65,80
81,128
145,160
161,208
225,240
*elset,elset=fibers,generate
49.64
129,144
209,224
 *nset, nset=drain,generate
 1,271,18
 801,1071,18
```

```
1601,1871,18
2401,2671,18
*nset,nset=top2,generate
2403,2409
2689,2737
2412,2418
2422,2427
2430,2436
2439,2445
2448,2454
2457,2463
2466,2472
2475,2481
2484,2490
2493,2499
2502,2508
2511,2517
2520,2526
2529,2535
2538,2544
2547,2553
2556,2562
2565,2571
2574,2580
2583,2589
2592,2598
2601,2607
2610,2616
2619,2625
2628,2634
2637,2643
2646,2652
2655,2661
2664,2670
2673,2679
2682,2688
*nset,nset=rside,generate
73,145,9
473,545,9
873,945,9
1273,1345,9
1673,1745,9
2073,2145,9
2473,2545,9
*orientation,name=orient1,definition=nodes,system=cylindrical
```

```
313,713
1,70
*nset,nset=alln,generate
1,337
401,737
801,1137
1201,1537
1601,1937
2001,2337
2401,2737
*initial conditions, type=saturation
alln.1
*initial conditions,type=ratio
alln.2.3
**
**oriented collagen properties (ring)
*solid section, elset=fibers, material=collagen, orientation=orient1
*material.name=collagen
*elastic,type=engineering constants
3350,6700,3350,.49,0,.49,105,105,
*permeability,specific weight=1
5.1e-13
**
**matrix core properties:
*solid section, elset=matrix, material=water
*material.name=water
*elastic,type=isotropic
105,.2
*permeability,specific weight=1
5.1e-13
*boundary
bottom,3
253,2
37,1
109,2
181,1
drain,8
*restart, write, frequency=1
*step,nlgeom,inc=200
*soils,consolidation,utol=5e5
1e-6,.001
*boundary,type=displacement
```

```
top,3,3,1.5e-6
*endstep
*step,inc=200
*soils,consolidation,utol=5e5,end=ss
.001,180,.06,100,.001
*endstep
**
**
**note ** = a comment line
**in order to run a creep simulation
**comment out the above load case
**and uncomment out the below load
**case (i.e. add ** before the lines
**above starting at *step and ending at
** *endstep, then delete ** from the
**lines below)
**
**
***step,nlgeom,inc=200,amplitude=ramp
***soils,consolidation,utol=5e5
**1e-10.0.001
****enter the peak force from the relaxation
****test divided by 257 (the number of nodes)
****as the load here (i.e. top,3,load)
***cload
**top,3,0.01033e-7
***endstep
***step,inc=200
***soils,consolidation,utol=5e5,end=ss
**1e-20,180,.06,100,.001
***endstep
```

## APPENDIX C

Fascicle model Abaqus code

```
*heading,unsymm
**tall 2 fascicle model
*node
9,-10e-6,-10e-6
81,10e-6,-10e-6
153,10e-6,10e-6
225,-10e-6,10e-6
288,-10e-6,-7.5e-6
*ngen
9,81,9
153,225,9
81,153,9
225,288,9
*node
289,-7.5e-6,-7.5e-6
295,7.5e-6,-7.5e-6
331,-7.5e-6,7.5e-6
337,7.5e-6,7.5e-6
*ngen
289,295,1
331,337,1
*nset,nset=c1,generate
289,295,1
*nset,nset=c2,generate
331,337,1
*nfill
c1, c2, 6, 7
*nset, nset=center,generate
9,288,9
*node
1,-42.4264e-6,-42.4264e-6
109,60e-6,0
181,0,60e-6
280,-49.88818e-6,-33.33421e-6
*ngen,line=c
1,109,9,313
109,181,9,313
181,280,9,313
*nset,nset=outer,generate
1,280,9
*nfill,bias=.75
outer, center, 8,1
*nset,nset=bottom,generate
1,337
```

\*\*

```
*node
2409,-10e-6,-10e-6,75e-6
2481,10e-6,-10e-6,75e-6
2553,10e-6,10e-6,75e-6
2625,-10e-6,10e-6,75e-6
2688,-10e-6,-7.5e-6,75e-6
*ngen
2409,2481,9
2553,2625,9
2481,2553,9
2625,2688,9
*node
2689,-7.5e-6,-7.5e-6,75e-6
2695,7.5e-6,-7.5e-6,75e-6
2731,-7.5e-6,7.5e-6,75e-6
2737,7.5e-6,7.5e-6,75e-6
*ngen
2689,2695,1
2731,2737,1
*nset,nset=clt,generate
2689,2695,1
*nset,nset=c2t,generate
2731,2737,1
*nfill
c1t,c2t,6,7
*nset, nset=centert,generate
2409,2688,9
*node
2401,-42.4264e-6,-42.4264e-6,75e-6
2509,60e-6,0,75e-6
2581,0,60e-6,75e-6
2680,-49.88818e-6,-33.33421e-6,75e-6
*ngen,line=c
2401,2509,9,2713
2509,2581,9,2713
2581,2680,9,2713
*nset, nset=outert,generate
2401,2680,9
*nfill,bias=.75
outert, centert, 8,1
*nset,nset=top,generate
2401,2737,1
*nfill
bottom,top,6,400
**
```

```
*element,type=C3d20RP
1,297,299,313,311,1097,1099,1113,1111,298,306,312,304,
1098,1106,1112,1104,697,699,713,711
2,299,301,315,313,1099,1101,1115,1113,300,308,314,306,
1100,1108,1114,1106,699,701,715,713
3,313,315,329,327,1113,1115,1129,1127,314,322,328,320,
1114,1122,1128,1120,713,715,729,727
4,311,313,327,325,1111,1113,1127,1125,312,320,326,318,
1112,1120,1126,1118,711,713,727,725
5,9,27,297,279,809,827,1097,1079,18,290,296,288,
818,1090,1096,1088,409,427,697,679
6,27,45,299,297,827,845,1099,1097,36,292,298,290,
836,1092,1098,1090,427,445,699,697
7,45,63,301,299,845,863,1101,1099,54,294,300,292,
854,1094,1100,1092,445,463,701,699
8,63,81,99,301,863,881,899,1101,72,90,302,294,
872,890,1102,1094,463,481,499,701
9,279,297,311,261,1079,1097,1111,1061,296,304,310,270,
1096,1104,1110,1070,679,697,711,661
10,301,99,117,315,1101,899,917,1115,302,108,316,308,
1102,908,1116,1108,701,499,517,715
11,261,311,325,243,1061,1111,1125,1043,310,318,324,252,
1110,1118,1124,1052,661,711,725,643
12,315,117,135,329,1115,917,935,1129,316,126,330,322,
1116,926,1130,1122,715,517,535,729
13,243,325,207,225,1043,1125,1007,1025,324,332,216,234,
1124,1132,1016,1034,643,725,607,625
14,325,327,189,207,1125,1127,989,1007,326,334,198,332,
1126,1134,998,1132,725,727,589,607
15,327,329,171,189,1127,1129,971,989,328,336,180,334,
1128,1136,980,1134,727,729,571,589
16,329,135,153,171,1129,935,953,971,330,144,162,336,
1130,944,962,1136,729,535,553,571
*element,type=c3d20rp
17,7,25,27,9,807,825,827,809,16,26,18,8,816,826,818,808,
407,425,427,409
32,277,7,9,279,1077,807,809,1079,286,8,288,278,
1086,808,1088,1078,677,407,409,679
33,5,23,25,7,805,823,825,807,14,24,16,6,
814,824,816,806,405,423,425,407
48,275,5,7,277,1075,805,807,1077,284,6,286,276,
1084,806,1086,1076,675,405,407,677
49,3,21,23,5,803,821,823,805,12,22,14,4,812,822,814,804,
403,421,423,405
64,273,3,5,275,1073,803,805,1075,282,4,284,274,
```

```
1082,804,1084,1074,673,403,405,675
80,271,1,3,273,1071,801,803,1073,280,2,282,272,
1080,802,1082,1072,671,401,403,673
66, 19, 37, 39, 21, 819, 837, 839, 821, 28, 38, 30, 20, 828, 838, 830, 820,
419,437,439,421
65,1,19,21,3,801,819,821,803,10,20,12,2,810,820,812,802,
401,419,421,403
69,73,91,93,75,873,891,893,875,82,92,84,74,882,892,884,874,
473,491,493,475
75,201,183,181,199,1001,983,981,999,192,182,190,200,992,982,990,1000,
601,583,581,599
*elgen
17,15,18,1,1,1,3,800,80
33,15,18,1,1,1,1,3,800,80
49,15,18,1,1,1,1,3,800,80
69,4,18,1,1,1,1,3,800,80
75,5,18,1,1,1,1,3,800,80
*elgen
1,1,1,1,1,1,3,800,80
2,1,1,1,1,1,3,800,80
3,1,1,1,1,1,3,800,80
4,1,1,1,1,1,3,800,80
5,1,1,1,1,1,3,800,80
6,1,1,1,1,1,3,800,80
7,1,1,1,1,1,3,800,80
8,1,1,1,1,1,3,800,80
9,1,1,1,1,1,3,800,80
10,1,1,1,1,1,3,800,80
11,1,1,1,1,1,3,800,80
12,1,1,1,1,1,3,800,80
13,1,1,1,1,1,3,800,80
14,1,1,1,1,1,3,800,80
15,1,1,1,1,1,3,800,80
16,1,1,1,1,1,3,800,80
32,1,1,1,1,1,3,800,80
48,1,1,1,1,1,1,3,800,80
64,1,1,1,1,1,3,800,80
65,1,1,1,1,1,1,3,800,80
66,1,1,1,1,1,1,3,800,80
80,1,1,1,1,1,1,3,800,80
*node
2809,120e-6,-10e-6
2881,140e-6,-10e-6
2953,140e-6,10e-6
3025,120e-6,10e-6
```

```
3088,120e-6,-7.5e-6
*ngen
2809,2881,9
2953,3025,9
2881,2953,9
3025,3088,9
*node
3089,122.5e-6,-7.5e-6
3095,137.5e-6,-7.5e-6
3131,122.5e-6,7.5e-6
3137,137.5e-6,7.5e-6
*ngen
3089,3095,1
3131,3137,1
*nset,nset=c1r,generate
3089,3095,1
*nset,nset=c2r,generate
3131,3137,1
*nfill
c1r,c2r,6,7
*nset,nset=centrr,generate
2809,3088,9
*node
2801,87.5736e-6,-42.4264e-6
2909,190e-6,0
2981,130e-6,60e-6
3080,80.11182e-6,-33.33421e-6
*ngen_line=c
2801,2909,9,3113
2909,2981,9,3113
2981,3080,9,3113
*nset,nset=outerr,generate
2801,3080,9
*nfill,bias=.75
outerr, centrr, 8,1
*nset,nset=bottomr,generate
2801,3137
**
*node
5209,120e-6,-10e-6,75e-6
5281,140e-6,-10e-6,75e-6
5353,140e-6,10e-6,75e-6
5425,120e-6,10e-6,75e-6
5488,120e-6,-7.5e-6,75e-6
*ngen
```

```
5209,5281,9
5353,5425,9
5281,5353,9
5425,5488,9
*node
5489,122.5e-6,-7.5e-6,75e-6
5495,137.5e-6,-7.5e-6,75e-6
5531,122.5e-6,7.5e-6,75e-6
5537,137.5e-6,7.5e-6,75e-6
*ngen
5489,5495,1
5531,5537,1
*nset,nset=cltr,generate
5489,5495.1
*nset,nset=c2tr,generate
5531,5537,1
*nfill
c1tr.c2tr.6.7
*nset,nset=centertr,generate
5209,5488,9
*node
5201,87.5736e-6,-42.4264e-6,75e-6
5309,190e-6,0,75e-6
5381,130e-6,60e-6,75e-6
5480,80.11182e-6,-33.33421e-6,75e-6
*ngen.line=c
5201,5309,9,5513
5309,5381,9,5513
5381,5480,9,5513
*nset,nset=outertr,generate
5201,5480,9
*nfill,bias=.75
outertr, centertr, 8,1
*nset,nset=topr,generate
5201,5537,1
*nfill
bottomr,topr,6,400
*element,type=C3d20RP
241,3097,3099,3113,3111,3897,3899,3913,3911,3098,3106,3112,3104,
3898,3906,3912,3904,3497,3499,3513,3511
242,3099,3101,3115,3113,3899,3901,3915,3913,3100,3108,3114,3106,
3900,3908,3914,3906,3499,3501,3515,3513
243,3113,3115,3129,3127,3913,3915,3929,3927,3114,3122,3128,3120,
3914,3922,3928,3920,3513,3515,3529,3527
```

```
244,3111,3113,3127,3125,3911,3913,3927,3925,3112,3120,3126,3118,
3912,3920,3926,3918,3511,3513,3527,3525
245.2809.2827.3097.3079.3609.3627.3897.3879.2818.3090.3096.3088.
3618,3890,3896,3888,3209,3227,3497,3479
246.2827.2845.3099.3097.3627.3645.3899.3897.2836.3092.3098.3090.
3636,3892,3898,3890,3227,3245,3499,3497
247,2845,2863,3101,3099,3645,3663,3901,3899,2854,3094,3100,3092,
3654,3894,3900,3892,3245,3263,3501,3499
248,2863,2881,2899,3101,3663,3681,3699,3901,2872,2890,3102,3094,
3672,3690,3902,3894,3263,3281,3299,3501
249,3079,3097,3111,3061,3879,3897,3911,3861,3096,3104,3110,3070,
3896,3904,3910,3870,3479,3497,3511,3461
250,3101,2899,2917,3115,3901,3699,3717,3915,3102,2908,3116,3108,
3902,3708,3916,3908,3501,3299,3317,3515
251,3061,3111,3125,3043,3861,3911,3925,3843,3110,3118,3124,3052,
3910,3918,3924,3852,3461,3511,3525,3443
252,3115,2917,2935,3129,3915,3717,3735,3929,3116,2926,3130,3122,
3916,3726,3930,3922,3515,3317,3335,3529
253,3043,3125,3007,3025,3843,3925,3807,3825,3124,3132,3016,3034,
3924.3932.3816.3834.3443.3525.3407.3425
254,3125,3127,2989,3007,3925,3927,3789,3807,3126,3134,2998,3132,
3926,3934,3798,3932,3525,3527,3389,3407
255,3127,3129,2971,2989,3927,3929,3771,3789,3128,3136,2980,3134,
3928,3936,3780,3934,3527,3529,3371,3389
256,3129,2935,2953,2971,3929,3735,3753,3771,3130,2944,2962,3136,
3930,3744,3762,3936,3529,3335,3353,3371
*element.tvpe=c3d20rp
257,2807,2825,2827,2809,3607,3625,3627,3609,2816,2826,2818,2808,
3616,3626,3618,3608,3207,3225,3227,3209
272,3077,2807,2809,3079,3877,3607,3609,3879,3086,2808,3088,3078,
3886,3608,3888,3878,3477,3207,3209,3479
273,2805,2823,2825,2807,3605,3623,3625,3607,2814,2824,2816,2806,
3614,3624,3616,3606,3205,3223,3225,3207
288,3075,2805,2807,3077,3875,3605,3607,3877,3084,2806,3086,3076,
3884,3606,3886,3876,3475,3205,3207,3477
289,2803,2821,2823,2805,3603,3621,3623,3605,2812,2822,2814,2804,
3612,3622,3614,3604,3203,3221,3223,3205
304,3073,2803,2805,3075,3873,3603,3605,3875,3082,2804,3084,3074,
3882,3604,3884,3874,3473,3203,3205,3475
320,3071,2801,2803,3073,3871,3601,3603,3873,3080,2802,3082,3072,
3880,3602,3882,3872,3471,3201,3203,3473
307,2837,2855,2857,2839,3637,3655,3657,3639,2846,2856,2848,2838,
3646,3656,3648,3638,3237,3255,3257,3239
317,3037,3019,3017,3035,3837,3819,3817,3835,3028,3018,3026,3036.
3828,3818,3826,3836,3437,3419,3417,3435
```

```
*elgen
257,15,18,1,1,1,1,3,800,80
273,15,18,1,1,1,1,3,800,80
289,15,18,1,1,1,1,3,800,80
307,8,18,1,1,1,1,3,800,80
317,3,18,1,1,1,1,3,800,80
*elgen
241,1,1,1,1,1,1,3,800,80
242,1,1,1,1,1,1,3,800,80
243,1,1,1,1,1,1,3,800,80
244,1,1,1,1,1,1,3,800,80
245,1,1,1,1,1,3,800,80
246,1,1,1,1,1,1,3,800,80
247,1,1,1,1,1,1,3,800,80
248,1,1,1,1,1,1,3,800,80
249,1,1,1,1,1,3,800,80
250,1,1,1,1,1,1,3,800,80
251,1,1,1,1,1,1,3,800,80
252,1,1,1,1,1,1,3,800,80
253,1,1,1,1,1,1,3,800,80
254,1,1,1,1,1,1,3,800,80
255,1,1,1,1,1,1,3,800,80
256,1,1,1,1,1,1,3,800,80
272,1,1,1,1,1,3,800,80
288,1,1,1,1,1,1,3,800,80
304,1,1,1,1,1,1,3,800,80
320,1,1,1,1,1,3,800,80
*node
5601,62.5e-6,-22.96e-6
5602,65e-6,-22.96e-6
5603,67.5e-6,-22.96e-6
5613,62.5e-6,22.96e-6
5614,65e-6,22.96e-6
5615,67.5e-6,22.96e-6
*nset,nset=join1,generate
5601,5603
*nset,nset=join2,generate
5613,5615
*nfill
join1,join2,4,3
*node
6201,62.5e-6,-22.96e-6,75e-6
6202,65e-6,-22.96e-6,75e-6
6203,67.5e-6,-22.96e-6,75e-6
6213,62.5e-6,22.96e-6,75e-6
```

```
6214,65e-6,22.96e-6,75e-6
6215,67.5e-6,22.96e-6,75e-6
*nset_nset=join1t,generate
6201.6203
*nset,nset=join2t,generate
6213,6215
*nfill
join1t,join2t,4,3
*nset,nset=extrab,generate
5601,5615
*nset,nset=extrat,generate
6201,6215
*nfill
extrab, extrat, 6, 100
*element.tvpe=c3d20rp
481,91,5602,5608,109,891,5802,5808,909,5601,5605,5607,100,
5801.5805.5807.900.491.5702.5708.509
483,109,5608,5614,127,909,5808,5814,927,5607,5611,5613,118,
5807,5811,5813,918,509,5708,5714,527
482,5602,3071,3053,5608,5802,3871,3853,5808,5603,3062,5609,5605,
5803,3862,5809,5805,5702,3471,3453,5708
484,5608,3053,3035,5614,5808,3853,3835,5814,5609,3044,5615,5611,
5809,3844,5815,5811,5708,3453,3435,5714
485,891,5802,5808,909,1691,6002,6008,1709,5801,5805,5807,900,
6001.6005.6007.1700.1291.5902.5908.1309
487,909,5808,5814,927,1709,6008,6014,1727,5807,5811,5813,918,
6007,6011,6013,1718,1309,5908,5914,1327
486,5802,3871,3853,5808,6002,4671,4653,6008,5803,3862,5809,5805,
6003,4662,6009,6005,5902,4271,4253,5908
488,5808,3853,3835,5814,6008,4653,4635,6014,5809,3844,5815,5811.
6009,4644,6015,6011,5908,4253,4235,5914
489,1691,6002,6008,1709,2491,6202,6208,2509,6001,6005,6007,1700.
6201,6205,6207,2500,2091,6102,6108,2109
490,6002,4671,4653,6008,6202,5471,5453,6208,6003,4662,6009,6005,
6203.5462.6209.6205.6102.5071.5053.6108
491,1709,6008,6014,1727,2509,6208,6214,2527,6007,6011,6013,1718,
6207,6211,6213,2518,2109,6108,6114,2127
492,6008,4653,4635,6014,6208,5453,5435,6214,6009,4644,6015,6011,
6209,5444,6215,6211,6108,5053,5035,6114
*node
6302,20e-6,-54.62e-6
6301,20e-6,-56.735e-6
6300,20e-6,-58.85e-6
6326,110e-6,-54.62e-6
6325,110e-6,-56.735e-6
```

6324,110e-6,-58.85e-6 6902,20e-6,-54.62e-6,75e-6 6901,20e-6,-56.735e-6,75e-6 6900,20e-6,-58.85e-6,75e-6 6926,110e-6,-54.62e-6,75e-6 6925,110e-6,-56.735e-6,75e-6 6924,110e-6,-58.85e-6,75e-6 \*nset,nset=leftl,generate 6300,6302 \*nset,nset=rightl,generate 6324,6326 \*nfill leftl,rightl,8,3 \*nset,nset=baseb,generate 6300,6326 \*nset,nset=leftlt,generate 6900,6902 \*nset,nset=rightlt,generate 6924,6926 \*nfill leftlt,rightlt,8,3 \*nset,nset=basebt,generate 6900,6926 \*nfill baseb,basebt,6,100 \*node 6329,20e-6,58.85e-6 6328,20e-6,56.735e-6 6327,20e-6,54.62e-6 6353,110e-6,58.85e-6 6352,110e-6,56.735e-6 6351,110e-6,54.62e-6 6929,20e-6,58.85e-6,75e-6 6928,20e-6,56.735e-6,75e-6 6927,20e-6,54.62e-6,75e-6 6953,110e-6,58.85e-6,75e-6 6952,110e-6,56.735e-6,75e-6 6951,110e-6,54.62e-6,75e-6 \*nset,nset=leftl2,generate 6327,6329 \*nset,nset=rightl2,generate 6351,6353 \*nfill leftl2,rightl2,8,3 \*nset,nset=baseb2,generate

```
6327,6353
*nset_nset=leftlt2,generate
6927,6929
*nset_nset=rightlt2,generate
6951,6953
*nfill
leftlt2,rightlt2,8,3
*nset,nset=basebt2,generate
6927,6953
*nfill
baseb2.basebt2.6.100
*element,type=c3d20rp
600,37,6300,6302,39,837,6500,6502,839,46,6301,48,38,846,6501,848,838,
437,6400,6402,439
606,837,6500,6502,839,1637,6700,6702,1639,846,6501,848,838,1646,6701,1648,1638,
1237,6600,6602,1239
612,1637,6700,6702,1639,2437,6900,6902,2439,1646,6701,1648,1638,
2446,6901,2448,2438,2037,6800,6802,2039
601,6300,6306,6308,6302,6500,6506,6508,6502,6303,6307,6305,6301,
6503,6507,6505,6501,6400,6406,6408,6402
605.6324.2837.2839.6326.6524.3637.3639.6526.2828.2838.2830.6325.
3628,3638,3630,6525,6424,3237,3239,6426
611,6524,3637,3639,6526,6724,4437,4439,6726,3628,3638,3630,6525,
4428,4438,4430,6725,6624,4037,4039,6626
617,6724,4437,4439,6726,6924,5237,5239,6926,4428,4438,4430,6725,
5228,5238,5230,6925,6824,4837,4839,6826
618.183.6327.6329.181.983.6527.6529.981.174.6328.172.182.974.6528.972.982.
583,6427,6429,581
624.983.6527.6529.981,1783.6727.6729,1781,974,6528,972,982,1774,6728,1772,1782,
1383,6627,6629,1381
630,1783,6727,6729,1781,2583,6927,6929,2581,1774,6728,1772,1782,
2574,6928,2572,2582,2183,6827,6829,2181
619,6327,6333,6335,6329,6527,6533,6535,6529,6330,6334,6332,6328,
6530,6534,6532,6528,6427,6433,6435,6429
623,6351,2983,2981,6353,6551,3783,3781,6553,2992,2982,2990,6352,
3792.3782.3790.6552.6451.3383.3381.6453
629,6551,3783,3781,6553,6751,4583,4581,6753,3792,3782,3790,6552,
4592.4582.4590.6752.6651.4183.4181.6653
635.6751.4583,4581,6753,6951,5383,5381,6953,4592,4582,4590,6752,
5392,5382,5390,6952,6851,4983,4981,6853
*elgen
601,4,6,1,1,1,1,3,200,6
619,4,6,1,1,1,1,3,200,6
*elset.elset=matrix.generate
1,48
```

```
69,72
81,128
149,152
161,208
229,232
241,288
317,320
321,368
397,400
401,448
477,480
*elset,elset=center,generate
481,492
*elset,elset=epil,generate
65,66
75,80
225,226
235,240
145,146
155,160
*elset,elset=epir,generate
307,314
387,394
467,474
*elset,elset=epib,generate
600,617
*elset,elset=epit,generate
618,635
*elset,elset=fibers,generate
49,64
129,144
209,224
*elset,elset=fibersr,generate
289,304
369,384
449,464
*nset,nset=drain,generate
6300,6324,3
6500,6524,3
6700,6724,3
6900,6924,3
6329,6353,3
6529,6553,3
6729,6753,3
6929,6953,3
```

```
181,271,18
1,37,18
981,1071,18
801,837,18
1781,1871,18
1601,1637,18
2581,2671,18
2401,2437,18
2837,2981,18
3637,3781,18
4437,4581,18
5237,5381,18
*nset,nset=topl,generate
2689,2737,1
2409,2688,9
2408,2687,9
2407,2686,9
2406,2685,9
2405,2684,9
2404,2683,9
2403,2682,9
*nset,nset=topright,generate
5489,5537,1
5209,5488,9
5208,5487,9
5207,5486,9
5206,5485,9
5205,5484,9
5204,5483,9
5203,5482,9
*orientation,name=orient1,definition=nodes,system=cylindrical
313,713
1,70
*orientation.name=orientr,definition=nodes,system=cylindrical
3113,3913
1,70
*orientation.name=orientel,definition=nodes,system=cylindrical
313,713
1,-10
*orientation,name=orienter,definition=nodes,system=cylindrical
3113,3913
1,-10
*orientation,name=orienteb,definition=nodes,system=cylindrical
5608,6208
1,-10
```

```
*nset_nset=alln,generate
1,337
401,737
801,1137
1201,1537
1601,1937
2001,2337
2401,2737
2801,3137
3201,3537
3601,3937
4001,4337
4401,4737
4801,5137
5201,5537
5601,5615
5701,5715
5801,5815
5901,5915
6001,6015
6101,6115
6201,6215
6300,6353
6400,6453
6500,6553
6600,6653
6700,6753
6800,6853
6900,6953
*nset,nset=botjoin,generate
5601,5615
*nset,nset=botside,generate
6300,6353
*nset,nset=topall,generate
2401,2737
5201,5537
6201,6215
6900,6953
*nset,nset=hold,generate
253,260
109,116
3053,3060
2909,2916
*elset,elset=leftpress,generate
165,166
```

```
161,161
169,169
164,164
171,171
173,174
187,192
177,178
203,208
193,194
219,224
209,210
235,240
225,226
155,160
145,146
75,80
65,66
1,1
5,6
9,9
11,11
4,4
13,14
27,32
17,18
43,48
33,34
59,64
43,50
75,80
65,66
139,144
129,130
81,81
85,86
89,89
91,91
84,84
93,94
107,112
97,98
123,128
113,114
*initial conditions, type=saturation
alln, 1
```

```
*initial conditions,type=ratio
alln.2.3
**
**material properties for the fibers
*solid section, elset=fibers, material=collagen, orientation=orient1
*material_name=collagen
*elastic.type=engineering constants
3350,6700,3350,.49,0,.49,105,105,
105
*permeability,specific weight=1
5.1e-13
*solid section, elset=fibersr, material=coll, orientation=orientr
*material,name=coll
*elastic.type=engineering constants
3350.6700.3350..49.0..49.105.105.
105
*permeability,specific weight=1
5.1e-13
**
**material properties for the epitenon layer
*solid section, elset=epil, material=sheathl, orientation=orientel
*material.name=sheathl
*elastic,type=engineering constants
3350,6700,3350,.49,0,.49,105,105,
105
**elastic,type=isotropic
**105,.2
*permeability, specific weight=1
5.1e-13
*solid section.elset=epir.material=sheathr.orientation=orienter
*material.name=sheathr
*elastic.type=engineering constants
3350,6700,3350,.49,0,.49,105,105,
105
**elastic,type=isotropic
**105,.2
*permeability,specific weight=1
5.1e-13
*solid section, elset=epib, material=sheathb, orientation=orienteb
*material.name=sheathb
*elastic,type=engineering constants
3350,6700,3350,.49,0,.49,105,105,
105
```

```
**elastic,type=isotropic
**105,.2
*permeability,specific weight=1
5.1e-13
*solid section, elset=epit, material=sheatht, orientation=orienteb
*material,name=sheatht
*elastic,type=engineering constants
3350,6700,3350,.49,0,0.49,105,105,
105
**elastic,type=isotropic
**105,.2
*permeability,specific weight=1
5.1e-13
**
**material properties of the material between
**the fascicles:
**
*solid section, elset=center, material=hard
*material,name=hard
*elastic,type=isotropic
105,.2
*permeability,specific weight=1
5.1e-13
**
**material props. for the "cores"
*solid section,elset=matrix,material=water
*material,name=water
*elastic,type=isotropic
105,.2
*permeability,specific weight=1
5.1e-13
*boundary
bottom,3
bottomr,3
botioin,3
botside,3
5608,2
5608,1
5611,1
5614,1
5605,1
5602,1
5607,2
hold,2
```

drain,8

- \*restart,write,frequency=1
- \*step,nlgeom,inc=200
- \*soils,consolidation,utol=5e5

1e-6,.001

- \*boundary,type=displacement
- topall,3,3,1.5e-6
- \*endstep
- \*step,inc=200
- \*soils,consolidation,utol=5e5,end=ss .001,180,.06,100,.001
- \*endstep

MICHIGAN STATE UNIV. LIBRARIES
31293016826210